Pacific Northwest
NATIONAL LABORATORY

PNNL-37458

Real-time Liquid/Slurry Monitoring (278002) Progress Report Year 1

March 2025

1. Amanda M. Lines
2. Hope E. Lackey
3. Samuel A. Bryan
4. Hari Sivanandan
5. Adan Schafer Medina
6. Kayte Denslow
7. Thomas Serrano
8. Jaehun Chun
9. Rajesh Singh
10. Matt Fountain
11. Carl Enderlin
12. Reid Peterson

U.S. DEPARTMENT OF ENERGY

Prepared for the U.S. Department of Energy
under Contract DE-AC05-76RL01830

DISCLAIMER

PACIFIC NORTHWEST NATIONAL LABORATORY
operated by
BATTELLE
for the
UNITED STATES DEPARTMENT OF ENERGY
under Contract DE-AC05-76RL01830

Printed in the United States of America

Available to DOE and DOE contractors from
the Office of Scientific and Technical Information,
P.O. Box 62, Oak Ridge, TN 37831-0062
www.osti.gov
ph: (865) 576-8401
fox: (865) 576-5728
email: reports@osti.gov

Available to the public from the National Technical Information Service
5301 Shawnee Rd., Alexandria, VA 22312
ph: (800) 553-NTIS (6847)
or (703) 605-6000
email: info@ntis.gov
Online ordering: http://www.ntis.gov

PNNL-37458

Real-time Liquid/Slurry Monitoring (278002) Progress Report Year 1

March 2025

1. Amanda M. Lines
2. Hope E. Lackey
3. Samuel A. Bryan
4. Hari Sivanandan
5. Adan Schafer Medina
6. Kayte Denslow
7. Thomas Serrano
8. Jaehun Chun
9. Rajesh Singh
10. Matt Fountain
11. Carl Enderlin
12. Reid Peterson

Prepared for
the U.S. Department of Energy
under Contract DE-AC05-76RL01830

Pacific Northwest National Laboratory
Richland, Washington 99354

Summary

Integrating on-line monitoring could significantly benefit mission acceleration at the Hanford Site. Utilizing sensors directly on process or transfer lines can provide *in situ* and real-time information on process conditions and can allow for grab sample reduction, avoidance of process upsets or required rework of a campaign, and more informed operation. Ideally a multi-sensor platform capable of providing comprehensive analysis could be leveraged to characterize both chemical composition and solids analysis to meet a variety of site informational needs.

The work discussed here covers the Year 1 (April 2024 – March 2025) progress on the development of a comprehensive on-line monitoring platform. This project is primarily focused on operationalizing sensors already at a high technology readiness level (TRL) to work in concert on a single platform and output data on a single user interface to support simplified operator viewing of information. Notable advancements are anticipated in designing and demonstrating spool pieces that can meet Hanford Site functionality and engineering requirements while conforming to size and material requirements for deployments. Additionally, all sensors will be partnered with automated data analysis tools for real-time translation of data to information. Finally, a user interface will be developed that can allow for simplified read-outs of information to support operator decision making, including allowing for data fusion and cumulative measurements (e.g., total solids) of a given batch or waste processing campaign.

The focus of Year 1 was building an understanding of site informational priorities and engineering requirements through discussions with experts in site chemistry, flowsheets, and engineering. This allowed for a down select to key sensor technologies that would be the focus of this initial platform design. This process was covered in the first deliverable report. Following this task, project focus shifted to procuring and initial testing of equipment. Additional tasks included beginning computational fluid dynamic (CFD) modeling for design support, and initiating user interface design and coding discussions. Details on the selected sensors and high-level progress updates are included in Table 1 below. Overall, the project is meeting target goals and is on track to move into the calibration and spool piece fabrication tasks planned for Year 2.

Table 1. Progress Overview for All Tasks

Sensor/ capability	Information provided	Progress Notes	On schedule
Raman Spectroscopy	Chemical composition (aluminate, phosphate, etc.)	Instrument procurements placed, probes received and successfully tested under flow conditions. Instrument delayed to mid-March	Yes
Laser Induced Breakdown Spectroscopy	Chemical composition (sodium, fluoride, etc.)	Procurements placed, all equipment received and successfully tested	Yes
Flowmeters	Flow, density, etc.	All equipment received and tested.	Yes
Ultrasonic Pulse Echo	Solids settling (supporting critical velocity)	Procurements placed, all equipment received and successfully tested	Yes
SolidsMeter	Solids mass fraction	All equipment received and tested	Yes
Computational Fluid Dynamics	Optimization of spool piece/platform design	Complex model parameters integrated based on literature and SME input	Yes
User Interface Development	Information output	Base plan in place with initial discussions with all sensor SMEs to ensure data compatibility	Yes

Acknowledgments

The authors gratefully acknowledge the support provided by the Laboratory Policy Office (EM-3.2) within the U.S. Department of Energy (DOE) Office of Environmental Management. Pacific Northwest National Laboratory is operated by Battelle for the DOE under contract DE-AC05-76RL01830.

Acronyms and Abbreviations

AC	Alternating Current
AHJ	Authority Having Jurisdiction
BBI	Best Basis Inventory
CCD	Charge coupled device
CFD	Computational fluid dynamics
CFM	Coriolis Flow Meters
COTS	Commercial off the shelf
CTO	Chief Technology Office
DAS	Data Acquisition System
DC	direct current
DFHLW	Direct feed high level waste
DOE	Department of Energy
DST	Double-shell tank
EM	Environmental Management
EMP	Eulerian Multiphase
FIU	Florida International University
FWHM	Full Width Half Maximum
HART	Highway Addressable Remote Transducer
HLW	High level waste
ICCD	Intensified Charge coupled device
ICD	Interface Control Document
IP	Ingress Protection
LAW	low activity waste
LIBS	Laser induced breakdown spectroscopy
LOD	Limit of detection
LPO	Laboratory Policy Office
ML	Machine Learning
MSE	Mean Squared Error
MTEL	Multiphase Transport Evaluation Loop
NCA&T	North Carolina Agriculture and Technology
NPS	Nominal Pipe Size
NRTL	Nationally Recognized Testing Laboratory
PNNL	Pacific Northwest National Laboratory
PSD	Particle Size Distribution
RMSECV	Root mean square error of cross validation
RSD	Remote Sampler Demonstration
RTD	Resistance Temperature Detector
SME	Subject Matter Expert
SRNL	Savannah River National Laboratory
SST	single-shell tank
SVR	Support Vector Regression
TOC	Tank Operations Contractor
TOO	Technology Operations Office
TRL	Technology Readiness Level
UDV	Ultrasonic Doppler Velocimeter
UPE	Ultrasonic pulse echo
WAC	Waste acceptance criteria
WFD	Waste Feed Delivery

WTP	Waste Treatment and Immobilization Plant

Contents

Figures

Tables

1.0 Introduction

On-line monitoring, or the integration of sensors and instrumentation directly onto a process line, can provide unique and valuable insight into process conditions. A wide variety of sensors and tools have been leveraged within many industrial fields to support faster, safer, and more cost-effective process operation.[1-3] Many of these benefits could be realized within legacy waste processing efforts, including the improvement of processing efficiency. Integration of on-line monitoring at the Hanford or other waste processing sites can support mission acceleration in several ways:

- *Grab sample reduction*: Current operational plans at the Hanford Site call for many thousands of samples to be collected and analyzed at the on-site analytical facility, or the 222S facility. This will require 24-hour operation of the analytical facility to support mission timelines. While grab samples must be collected to meet a variety of requirements, many of the planned samples are meant to support process confirmation and could be replaced by on-line monitoring, ultimately reducing the load on the facility and potentially allowing it to operate on more standard shift schedules and avoid potential process delay when waiting for analytical results.
- *Campaign rework or process upset avoidance*: Continuous monitoring of campaign feed production or other key process steps can be used for real-time verification of composition, solids loadings, and other metrics. Thus avoiding situations where off-line sample analysis (completed after process operation) dictates rework. This can prevent potential schedule setbacks.
- *Enhanced feed characterization*: The benefit here is twofold, 1) continuous analysis can allow for better characterization beyond current best basis inventory (BBI) estimates, and 2) on-line monitoring can measure some parameters better than off-line analysis (e.g., critical deposition velocity or solids loading). In either case, better understanding of process feed and operational needs allows operators to process batches more efficiently.

Additional benefits are realized in cost reductions and safety improvements (e.g., reducing the amount of sample handling required). Ultimately, in-line monitoring provides a complimentary tool to grab sample collection that allows the site processing to both meet processing and validation requirements while enabling more informed and efficient waste treatment.

Overall, on-line monitoring comes in many forms and can provide many different types of data and information. To be truly applicable to site operation and mission acceleration for legacy waste processing, on-line monitoring must meet several key needs:

1. Provide *comprehensive* characterization: on-line monitoring must provide a range of information to meet a variety of needs of operators, this includes chemical composition analysis (e.g., amount of dissolved phosphate or sodium) as well as physical property measurement (e.g., solids mass fraction or critical velocity).
2. Output *information* and not data: on-line monitoring must provide simplified output that can easily and immediately be understood and utilized by operators. An example would be expressing a simple solids mass fraction value, as opposed to the raw ultrasonics data used to measure this.
3. Meet site *functional and engineering requirements*: probes and associated spool pieces must be able to fit into site process lines, pits, or systems without introducing additional hazards. This includes being optimized to deal with the hazards associated with process conditions

(e.g., radiation, chemical corrosivity, abrasion from solids, anticipated pressures/pump rates) as well as the connectivity/space requirements.

4. Build trust via *near-term* deployments so tools can be effectively integrated into additional processes in the future: While on-line monitoring tools could be highly valuable in a wide range of processes planned to kick off in about a decade (e.g., the proposed direct feed high level waste [DFHLW]), neglecting to deploy systems as soon as possible will ultimately limit or negate opportunities for future deployments. Historically, site operations need several years to test, deploy, and rely on process tools before they get implemented into high-scrutiny areas such as process steps associated with the proposed DFHLW.

The work completed under this project seeks to support mission acceleration by addressing the needs listed above. Specifically, this project lays the foundation for the engineering and design of deployable on-line monitoring units capable of providing comprehensive real-time information. This will involve building and testing an on-line monitoring platform with integrated real-time data analysis and a user interface for information readout. Work will be conducted over the course of three years, where Year 1 focuses on identification of needed sensing modalities and procurement and initial off-line testing of instruments. Year 2 will focus on engineering sensors and spool pieces for integration into a single on-line monitoring system, building real-time data analysis tools, and the user interface. Year 3 will focus on demonstration of the on-line monitoring platform on representative slurry streams. It should be noted that the on-line monitoring platform that will be completed and demonstrated in Year 3 will also be a lasting capability or testbed that can support future pre-deployment testing or other flowsheet maturation efforts.

This report discusses the progress toward Year 1 goals, where Year 1 tasks included 1) developing an instrumentation plan, 2) procuring and testing chemical composition sensors, and 3) procuring and testing physical property measurement sensors. An overview of the specific sensors that will be leveraged and integrated into the comprehensive on-line monitoring platform can be seen in Table 2, which has been adapted from the project's Instrumentation Plan. Progress on the testing and operationalizing of each sensor will be discussed in individual sections along with high-level overviews of the next steps anticipated in Years 2 and 3. Also included are sections that discuss engagement with stakeholders and collaborations with university partners. In this case, stakeholder engagements are primarily targeted to help ensure the on-line monitoring platform design and demonstration targets are relevant to site needs and requirements and final developments are well positioned for near-term deployment under future efforts. University partnerships are allowing for exploration of novel machine learning tools to predict slurry behavior and allow for better planning and testing of on-line monitoring tools. Overall, the team has met Year 1 goals and is making steady progress towards project goals on the design and demonstration of comprehensive on-line monitoring systems.

Table 2. Overview of sensors selected for integration into the on-line monitoring test platform.

Key information that is needed	Challenges to collecting on-line	Best sensor identified for application	Unique to our approach
Quantification of molecular species that pose processing challenges (e.g., phosphate, aluminate)	Must be hardened to deal with chemical complexity, turbidity, radiation damage, etc.	Raman spectroscopy	Task leaders have long record of advancing both Raman probe and data analysis technologies
Quantification of atomic species that pose processing challenges (e.g., F^-, Hg)	Must be calibrated to overcome turbidity, flowrates, etc.	Laser induced breakdown spectroscopy (LIBS)	Task leaders have track record of LIBS applications to challenging processes
Density/flowrate	Variable solids loading impacts outputs	Multiple types of flow meters	Task leaders have significant engineering experience to inform design
Solids mass fraction	Notoriously difficult to measure where solids loading is not homogeneous	Ultrasonics SolidsMeter	Taking a fresh look at data science for analysis
Critical deposition velocity	Data analysis and defining “settling”	Ultrasonic Pulse Echo (UPE)	Task leaders originally developed this technology

2.0 Completion of Task 1, The Instrumentation Plan; and Stakeholder Engagement

To ensure the final on-line monitoring platform design could meet the needs and requirements of the Hanford site, the first task was to pull together a team of experts to carefully evaluate operator informational needs and site functionality and engineering requirements. This activity ensured that all subsequent project steps were rooted firmly in an understanding of stakeholder needs and targeted at producing an engineering design for a system that can be deployed in the near-term. A team was assembled that included experts in the Hanford process flowsheet, chemistry, and engineering, along with experts in a variety of sensing modalities. The following stepwise process was completed:

1. Identify and prioritize site needs for information, highlighting those pieces of data where on-line monitoring could be most valuable.
2. Build an understanding of functional and engineering requirements by evaluating a range of deployment needs and locations. This not only helped the team understand operational conditions that sensors would have to characterize/operate under but provided insight into near-term and long-term deployment opportunities that could be explored under future efforts.
3. Leverage sensor expertise to down select to those sensors that can provide the prioritized information (from step 1) while being at a high enough technology readiness level (TRL) to meet the functional requirements identified (from step 2)
4. Recommend instrument and probe specifications for selected sensing modalities (from step 3) that can then be procured commercially off the shelf.
5. Communicate findings with stakeholders to validate findings and ensure project is progressing towards a deployable and impactful platform design. *Note*: this is listed as a “final” step here, but stakeholder engagement is a regular function of project work with monthly “small group” check-ins scheduled and twice-yearly “large group” updates planned.

A high-level overview of findings is included here, with more detailed notes regarding demonstration targets and sensor engineering requirements in the subsequent sections highlighting progress on the specific sensing modalities.

2.1 Identifying and prioritizing information needs

Chemical Stability: Understanding the chemical stability (including the content of saturated components) of the slurry is important to preventing challenges such as downstream precipitation that can cause plugging or determining total volume of glass produced. The primary components that can cause downstream precipitation include sodium phosphate, sodium fluoride phosphate salts, sodium oxalate, and aluminate (either as sodium aluminate or gibbsite). Sodium is a key example of a component that impacts final waste form volume.

Slurry Solids Content: Within feed preparation there can be significant uncertainty around the quantity of solids present. The retrieval process can introduce an order of magnitude of uncertainty into the solids concentration that is delivered to the Feed Preparation Tanks. This can impact feed staging or subsequent processing steps, such as transfer to the Hanford Tank Waste Treatment and Immobilization Plant High Level Waste (WTP HLW) Facility which is dependent on knowing the amount of solids present. This will dictate how much liquor to decant and how

much more waste to transfer into the campaign. Ideally, the on-line monitoring platform would provide continuous accounting of the quantity of insoluble solids that are transferred into a Feed Preparation Tank. This could significantly decrease the time required to prepare a campaign feed, as grab samples would be confirmatory as opposed to critical to preparing the campaign.

Slurry mixing and transport properties: Assurance that the slurry mixing and transport properties are appropriate for transport to the WTP is another key need. On-line monitoring could enable intelligent design of a feed campaign, and thus eliminate significant rework if a campaign is found to have unacceptable feed properties after it has been prepared. Key components of this include critical deposition velocity and carrier fluid density/slurry viscosity which can also provide valuable insight into the slurry mixing and transport properties.

2.2 Building an understanding of functional and engineering requirements

The technicalities of anticipated flowrates, pressures, densities, viscosities, and other slurry properties strongly impact performance and required specifications of sensors. Additionally, pipe sizing and spool piece requirements can impact design along with understanding of space limitations in some deployment locations (e.g., pump or valve pits). Further complexities are encountered when understanding hazards certifications and related requirements. The Instrumentation Plan laid out a foundation for continuing discussions with stakeholders on this topic.

2.3 Down selecting sensors and setting instrument/probe specifications

After identifying informational needs, sensors were identified that could provide the specified data. However, not all sensors identified were at a high enough TRL to meet site engineering and functional requirements necessary for near-term deployment. This led to a down select of those key techniques that could meet needs and requirements. These are outlined in Table 1 in the Summary and will be discussed in detail in subsequent sections.

An example of a technique that was not selected is radiometric monitoring. While analysis of radioisotopes would certainly be valuable information in several site applications, only gamma monitoring is at an appropriate TRL of on-line deployment. However, gamma monitoring would generally be saturated (e.g., by cesium) in most locations and would not provide the needed information. Alpha or beta monitoring would be far more useful but are not at a TRL to support deployment. These and other sensors have been noted as opportunities for future sensor advancement R&D.

2.4 Communicating and collaborating with stakeholders

The final step of the Instrumentation Plan process was communicating with stakeholders to validate findings and kick off dialog to optimize approach and target final designs towards the most impactful and deployable configuration. The initial meeting was held on November 25, 2024 and several subsequent meetings and discussions have been held since.

2.5 Communication and stakeholder engagement plans

To ensure project trajectory continues toward supporting deployable on-line monitoring platform designs, regular interaction with stakeholders is included in project schedules. This includes the monthly connection with key individuals in the Hanford Tank Waste Operations and Closure (H2C) Chief Technology Office (CTO) (formerly WRPS) as well as site engineers. This meeting is intended to be highly technical discussions of site requirements and system configurations while also providing a means for sharing regular project updates. In addition to this, a larger group meeting that includes H2C CTO, Flowsheet Integration, and other teams is planned to occur every six months, with the next meeting planned for May of 2025. This meeting is meant to support dissemination of wider project updates and allow for a forum to point out areas of needed R&D or course correction.

3.0 Progress On Raman Sensors

Under Task 1, completing the *Instrumentation Plan*, Raman spectroscopy was identified as a highly valuable sensing modality that can provide chemical composition information on a wide range of chemical targets of value and interest to Hanford process operators. Furthermore, Raman is at a high TRL; instrumentation is commercially available and application to Hanford wastes and process streams has already been well demonstrated under previous Environmental Management (EM) investment. Our past demonstrations and deployments include: developing Raman-based on-line monitoring designed for actual Hanford waste treatment monitoring;[4-11] with highly turbid conditions;[12, 13] under remote in-tank deployments;[14] measurement of pH and poly-oxo ions;[15-17] and waste-form corrosion monitoring.[18, 19] This includes recent Quick Win investment that demonstrated applicability to stream with high solids mass fractions (up to at least 20 wt%) and Technology Operations Office (TOO) investment in designing and testing a spool piece for probe integration into flowing lines.

While Raman can be used to quantify many chemical species (e.g., anions and organics) known to be in wastes, five key targets were identified for demonstration purposes here. These targets, along with references highlighting previous demonstrations of applicability to Hanford samples, are listed in Table 3. Performance on quantifying these targets will be used to demonstrate Raman applicability and accuracy within the on-line monitoring platform. Data science (chemometric modeling) algorithms will be used in conjunction with Raman spectroscopy to quantify these targets. Expansion of models can be considered in future efforts to allow for application to additional chemical species.

Table 3. Identified demonstration species for Raman validation

Species	Site Concerns	Previously demonstrated LOD (M)	Previously demonstrated uncertainty (RMSECV)	Reference(s)	Notes
Phosphate (PO_4^{2-})	Precipitation concern	0.02[20]	0.06[15]	H.E. Lackey et al. 2020, *Anal Chem,* 92(8); H.M. Felmy et al. 2024, PNNL-34721; A.J. Clifford et al. 2021, *Anal Chem,* 93(14).	Up to 10 wt% solids (LOD); 0 wt% solids (RMSECV)
Oxalate ($C_2O_4^{2-}$)	Precipitation concern	0.07[21]	0.003[22]	K.I. Peterson and D.P. Pullman, 2016, *J Chem Ed,* 93(6); H.M. Felmy et al. 2022, *ACS ES&T*, 2(3); A.M. Lines et al. 2019, *Ind & Eng Chem Res,* 58(47).	0 wt% solids (LOD and RMSECV)
Aluminate ($Al(OH_4)^-$)	Precipitation concern, fouling of filters or ion exchange beds	0.09[23]	0.01[22]	A.M. Lines et al. 2019, *Ind & Eng Chem Res*, 58(47); H.M. Felmy et al. 2022, *ACS ES&T*, 2(3); A.M. Lines et al. 2019, *Ind & Eng Chem Res,* 58(47).	0 wt% solids (LOD and RMSECV)
Nitrate (NO_3^-)	Strong signal verification for Raman but also key for totaling with nitrite (not targeted here)	0.03[21]	0.02[22]	A.M. Lines et al. 2019, *Ind & Eng Chem Res,* 58(47); H.M. Felmy et al. 2022, *ACS ES&T*, 2(3); A.M. Lines et al. 2019, *Ind & Eng Chem Res,* 58(47).	Up to 20 wt% solids (LOD); 0 wt% solids (RMSECV)

Species	Site Concerns	Previously demonstrated LOD (M)	Previously demonstrated uncertainty (RMSECV)	Reference(s)	Notes
Hydroxide (OH^-)	Precipitation/ other	0.13[10]	3.2% rel. error[10]	Bryan, S. A. et al. 2005, Acceptance Test Report: S-109 Retrieval. PNNL-15360	measured in S-109 early feed retrieval simulant

In all cases, the team is focusing on quantification of dissolved species. This is a key aspect of demonstration and an essential first step to being able to note differences in composition of solution versus solids. While characterization of solids may also be possible, this is not a listed goal for the Raman system under current scope.

3.1 Instrument, Probe, and Spool Piece Specifications

On-line monitoring of Hanford tank processing includes other challenges in addition to the accurate and timely analysis of extremely complex streams. Tank materials are also radioactive, exhibiting a range of dose rates across the low and high activity waste materials. Exposure to radiation dose will limit the lifetime of any material, although some systems exhibit higher tolerance and robustness than others. The Raman approach is ideal because only robust materials (Raman probe and fibers composed of glass and metal materials) are exposed to the dose while the sensitive equipment and operators can be located hundreds of meters away, connected to the probes by fiber optic cables.

The Raman assembly is designed with the following priorities in mind: (1) safe control by workers, (2) robustness to damage, and (3) spectral signal fidelity in turbid solutions.

3.1.1 Instrument Design

A simplified component diagram of the spectrometer system is shown in Figure 1. Optical interrogation of process solutions occurs in the spool piece. Laser light is delivered to and collected from the process stream via the Raman spectrometer. A computer system is used to control the spectrometer. The Raman spectrometer and accompanying computer system are purchased from SpectraSolutions Inc.

A spool piece is a discrete segment of piping which can be integrated into larger volume flow loops and processing pipelines. The Raman spool piece includes ports through which Raman probes are inserted into the flow stream via a watertight seal. Under deployed applications in the field, this may be a welded connection between the spool piece and probe. Laboratory spool pieces are often integrated into a loop along with sight windows, through which flow and diffuse reflected Raman laser light can be observed.

The spectrometer consists of several key components. Housed in a metal casing are the lasers and the charge coupled device (CCD) array detector. Six lasers are contained in the instrument, with two lasers producing 405 nm light, two lasers producing 532 nm light, and two lasers producing 671nm light. Fiber optic cables are used to transmit light out of the spectrometer housing and into a Raman probe. The Raman probes contain no electrical components. The probes consist of a body containing mirrors and lenses which direct laser light through a stainless-steel barrel containing a focusing lens. The focusing lens produces a focal point 0.5 mm beyond the compression-sealed, watertight, sapphire ceramic window at the end of the probe. Laser light interacts with molecules in the waste to produce the Raman signal, which is scattered in all

directions from the molecules. Light which is scattered 180° from the molecules travels back through the probe and into the collection optical fiber. This optical fiber carries the Raman signal to the CCD detector. The detector is a rectangular grid array, and the signal from each probe is diffracted by optical components such that it interacts with a discrete, narrow region of the CCD array.

The signal from each region of the CCD array is digitized and recorded by the computer system.

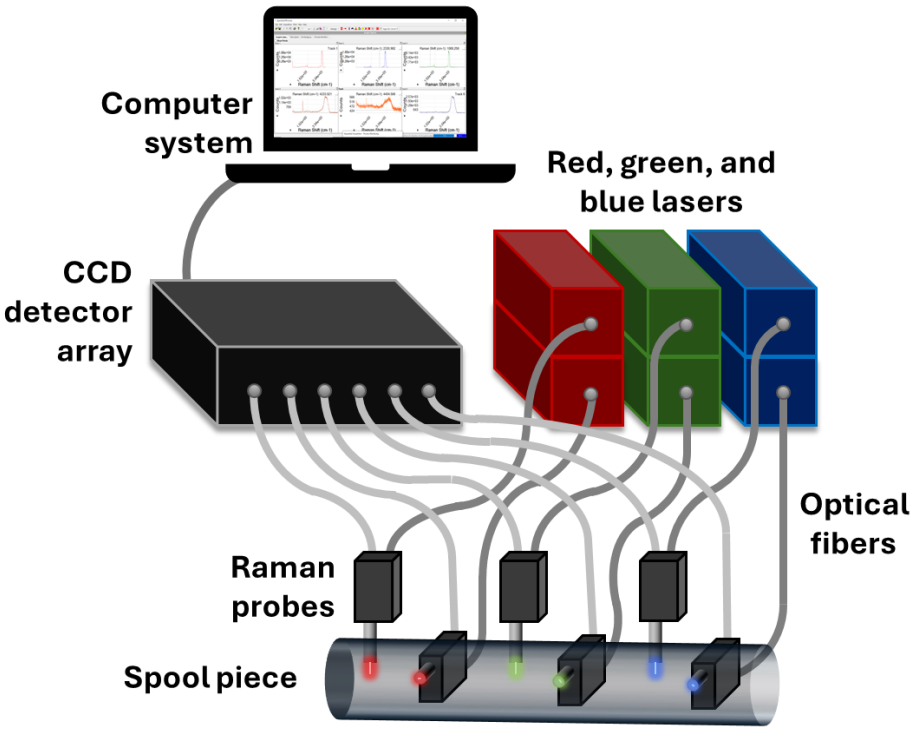

Figure 1. A simplified schematic of the components of the spectrometer system with integration into a flow stream.

Spool piece design will be completed in Year 2, with general schematics to be included in the *Engineering Plan*, which is the first deliverable for Year 2 efforts. Three major modifications will be investigated. First, the positioning of Raman probes will be altered, such that probes providing different laser wavelengths will be spaced along the spool piece to reduce reflection of laser light into the collection ports of other probes. See Section 3.2 for discussion on the impact of laser light reflection during tests with the existing spool piece. The new spool piece, which will feature six probe ports instead of the current four, will have probes of the same excitation wavelength positioned nearby one another, with a greater distance from probes of a different wavelength.

Second, the spool piece diameter will be increased from 1.5 inches to 2 inches in order to better coincide with the pipes expected in the target deployment location. Because the Raman probes are close focus, a change in pipe diameter is not expected to impact Raman performance, and pipes of differing diameters could be utilized in the future for additional applications.

Finally, it is desirable to reduce the required length of the spool piece and thereby the overall spatial footprint of the sensor skid. A flow straightener will be investigated for its ability to shorten

the required distance to achieve and maintain a developed, turbid flow which maintains solid particles in a suspended state. In addition to creating a developed flow in a shorter distance, the flow straightener may have some impact to alleviate bubble formation, which may improve Raman performance, as bubbles catching on the Raman probe lenses causes a large degradation of Raman signal, as discussed in Section 3.2.

3.1.2 Purpose of Design

Safe Control. Due to the hazardous conditions present during tank processing, the ability to control instrumentation from a distance is a key safety feature for sensors on this skid. To collect Raman spectra on process streams, only the Raman probe must be in contact with the process solutions. The optical fibers can be hundreds of meters long, allowing the spectrometer, its computer system, and the computer operator to remain at a substantial distance from the process stream. Each of the six lasers in the system can be individually activated or deactivated using the associated software, allowing any number of lasers to be powered off if a laser safety risk occurs.

Robustness. The Raman system is designed to be robust against incidental damage, degradation over time, and chemical and radiological hazards expected at the deployment location.

The Raman system is highly modular. Each of the six lasers can be replaced individually if they are damaged or if the light intensity degrades over time. Each probe and fiber optic can be replaced individually without affecting any of the other probes or fibers.

Design measures have been taken to reduce the possibility of instrument damage. Optical fibers are stainless steel jacketed, making them resistant to pinching or crushing. In case of damage to the spectrometer box resulting in optical component misalignment, both lasers and detector regions can be manually aligned to restore light transmission and collection.

Additionally, the Raman probes contain no electrical components, and therefore they are very robust against radiation damage, as shown in previous studies. Initial studies of Raman probe lifetime as a function of received radiation dose have been completed by our group.[4] Experiments involved exposing probe and optical window material to gamma doses up to 1.7×10^8 rad, while typical lifetime doses anticipated in Hanford tank processing equipment are estimated to be less than 1×10^8 rad.[24] Materials were dosed in steps to observe how spectral response was affected after different dosing timeframes. The probe and window materials did not fail within the cumulative max dose studied (funding limited the ability to irradiate materials until failure); photos showing window material before and during irradiation are shown in Figure 2(A). Between dosing steps, the irradiated probe and window material were used to measure the Hanford tank AP-105 simulant used as a standard for this purpose. By applying a chemometric model for NO_3^- to this data, the concentration of NO_3^- was accurately measured over all dose ranges, as shown in Figure 2(B), indicating data processing and modeling accurately accounted for spectral intensity and baseline fluctuations.

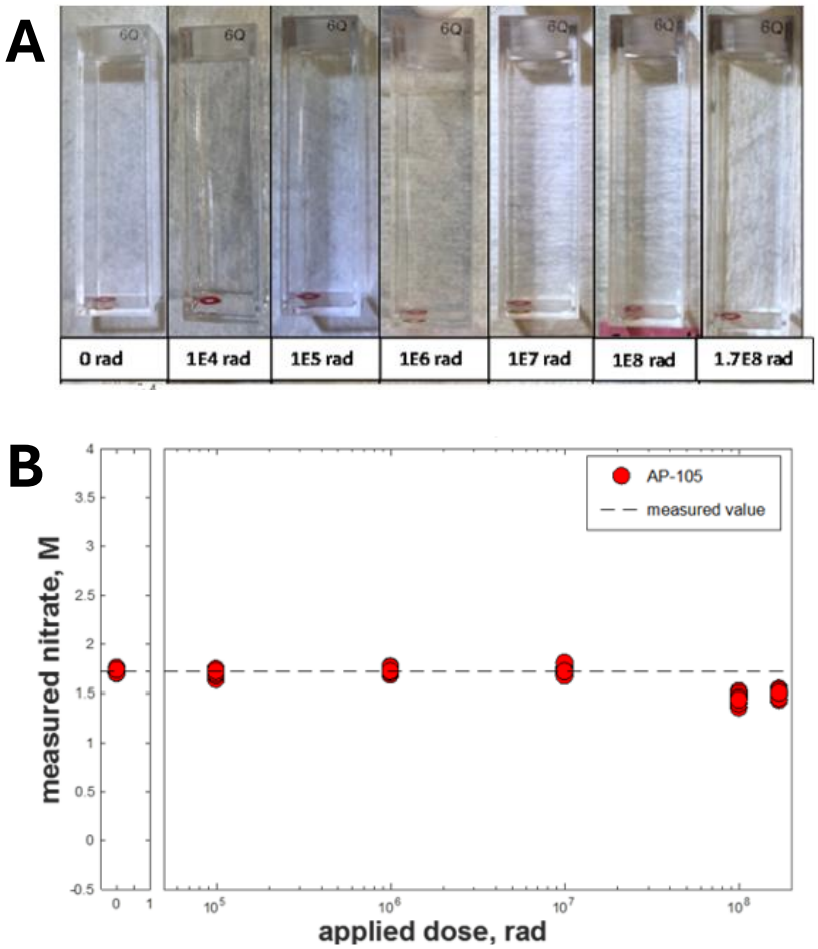

Figure 2. A) Window material before and after complete irradiation; and B) resulting NO_3^- measurements across the dose steps. From previously published work by our team.[4]

Spectral Signal Fidelity. The Raman system is designed to leverage advancements from many previous projects. The most relevant advances are the use of multiple Raman excitation wavelengths and the use of close-focus Raman probes.

Previous work has utilized three separate spectrometers to collect spectral signatures at three Raman excitation wavelengths.[21] Data fusion was conducted, combining the spectral signatures from the three excitation wavelengths for improved quantitation. Here, a single instrument can produce all three excitation wavelengths, allowing for the data fusion approach while maintaining a lower spatial and economic footprint for the Raman system.

Optimization of Raman instrumentation parameters can enhance measurement of low concentration samples. This includes comparing responses for multiple Raman laser excitation wavelengths. A decrease in excitation wavelength generally increases sensitivity, but there is a tradeoff with increasing susceptibility to fluorescence background. Other parameters to be optimized include data collection specifications such as integration time and spectral averaging. In addition, various modeling approaches can be explored, including multiblock, or simultaneous characterization of data from multiple Raman systems. In our recent work, different modeling approaches produced varying degrees of uncertainty in outputs, with multiblock approaches showing good reduction of uncertainty, or improved confidence in the accuracy of quantifying low

concentration samples. In actual Hanford waste samples, improved sensitivity was observed at lower excitation wavelengths but higher fluorescence from the Hanford tank processing samples was also observed. Chemometric models utilizing multiblock approaches, simultaneously using data from three Raman excitation systems (405, 532, and 671 nm) performed well and provided improved robustness in the face of fluorescence or spectral interferences.

The Raman probes utilized here are close-focus probes, producing a laser focal point 0.5 mm from the probe's terminating window. The focal point produces the strongest Raman signal from the laser beam. The window is sapphire ceramic, which is resistant to caustic and acidic conditions and has a high hardness, reducing the abrasion rate due to solid particles in the slurry passing over the window. The 316L stainless-steel alloy of the barrel is also resistant to the expected chemical conditions in the process stream.

The concept of using close-focus Raman probes for the interrogation of turbid solutions has been evaluated by our group. Several close-focus Raman probes with variable focal length were tested in turbid solutions to determine the ability for the probes to function under these conditions. The probes used included two close-focus probes with a 1 mm and 0.5 mm focal length, schematically shown in Figure 3(A), and a ball lens probe, shown in Figure 3(B), which focuses light at the surface of the lens. By using close-focus probe design, the laser excitation light interacts with the sample solution in contact just beyond the probe's window, and the Raman signal is not scattered (and lost) by solid particles deeper within the turbid sample solution. Preprocessing techniques can then be employed to overcome the challenges of signal loss with increasing turbidity in solutions of variable turbidity.

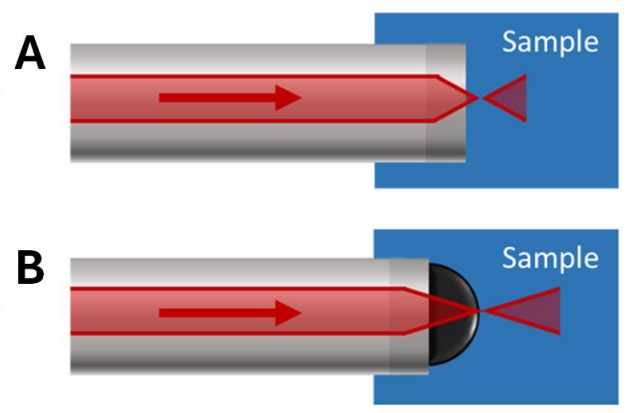

Figure 3. Schematic of A) close focus Raman probe, and B) ball lens probe.

3.2 Testing Probes in Flow Loop

Immersion probes with a close focus were procured for the Raman system setup. Under previous Quick Win work, it was demonstrated that close-focus Raman probes could be successfully used for qualitative characterization of solutions up to 20 wt% solids. After receiving probes, they were tested first to verify focal length, as shown in Figure 4. The F probe is a prototype close focus probe, acquired during Quick Win work, and the B1, B2, and B3 probes were recently made according to the specifications of the F probe.

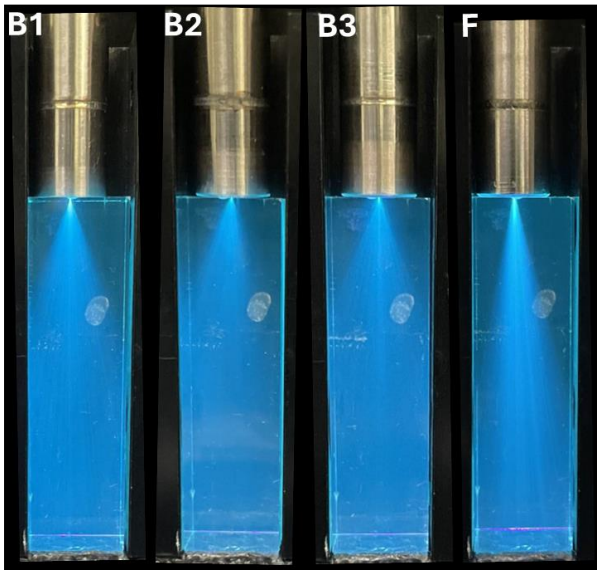

Figure 4. The beam profiles of newly acquired (B1, B2, and B3) Raman barrels with close focus (0.5 mm) lenses and the prototype Raman barrel (F).

Raman probes were then tested against samples of sodium nitrate at three different solids loadings to verify performance under different solids loadings (Figure 5). Probes performed as expected with minor variations between probes, the greatest variation occurring between the F probes and the three B probes.

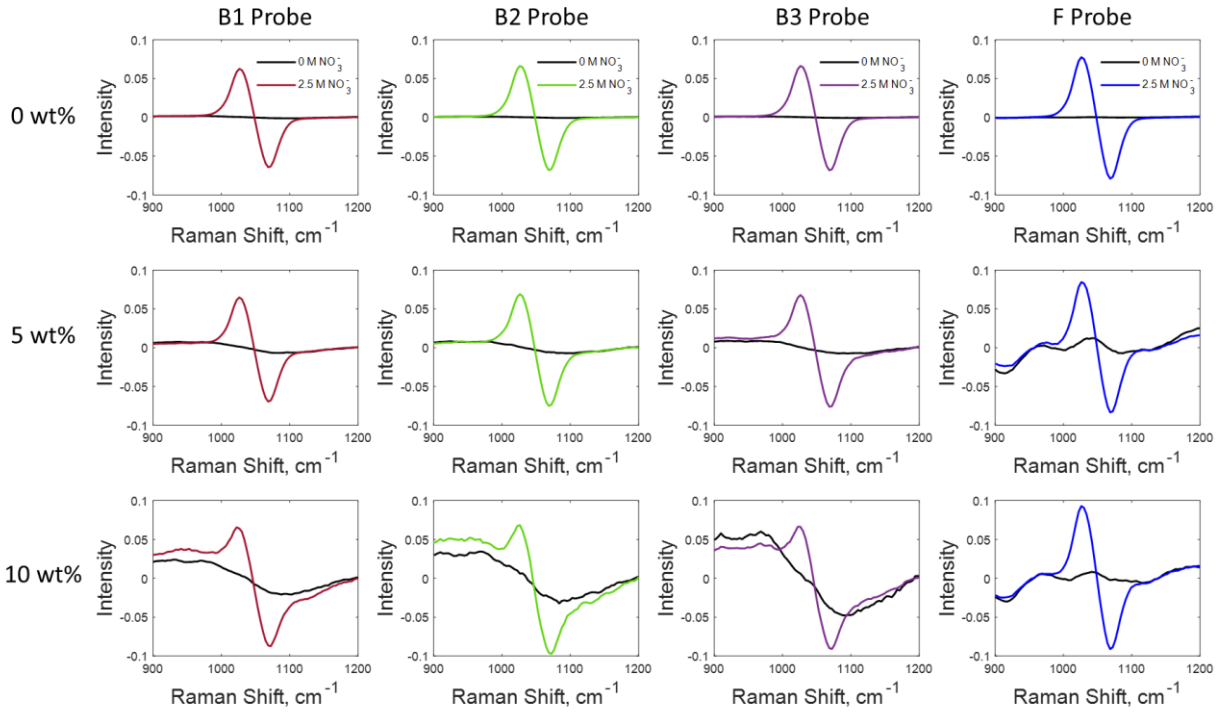

Figure 5. Raman signal of nitrate on four close-focus probe barrels at three weight percents of iron oxide solids.

Probes were integrated into a bench scale flow loop using a Raman spool piece designed and fabricated under a recent TOO project.[25] This allowed for performance testing under variable flow conditions and results can be seen in Figure 6. The spool piece was run under a turbulent flow regime with a volume of 12 L and a flow rate of 18 gallons per minute. Probes were positioned straight (90°) and angled (65°) relative to the flow path. Probes were also positioned either flush to the side of the spool piece pipe or set within the center of the pipe.

Generally, probes performed as expected, and ongoing challenges were identified and explored. The tests provided useful information for finalizing the spool piece design in Year 2 in order to optimize data output. Note, design for LPO funded work will need to be different from previous TOO funded work to accommodate additional probes, providing a more comprehensive Raman characterization of the process stream. Specifically, under TOO work, it was found that using three Raman excitations provided the most robust response to variable conditions, hence the Raman system design highlighted in Section 3.1.

When using the original spool piece design from recent TOO work, the 671 nm and 532 nm spectrometers detected stray light from neighboring probes, in both the straight and angled positions. Internal reflection of laser light in the metal spool piece tube and bubbles caused light scattering. The intensity of lines will be reduced in highly turbid solutions. Further, these lines do not overlap any of the primary bands of the analytes of interest. In future spool, the straight and angled probes which neighbor each other will be the same color, with greater distance between probes of different colors. Preprocessing can accommodate the laser lines via wavenumber selection, excluding the affected, non-analyte region, though spool piece design finalization in Year 2 will include modifications to reduce this effect.

Sharp lines of a single pixel width, noted in Figure 6(A), are cosmic ray lines and typically have no significant effect on chemometric model accuracy or precision.

Bubbles within the flow stream caused reduction in Raman signal, as expected. The water bands, centered around 3200 cm^{-1}, show variation in Figure 6(A, B, and D). Smaller reductions in intensity are caused by laser power fluctuations, while the significant reductions can be caused by bubbles forming on the Raman probe windows, which scatters excitation and response light. The angle of probes did not seem to affect bubble impacts, as shown by the large variation in Figure 6(B; 90°) and (D; 75°). Rather, the positioning of the probes flush to the pipe appears to be the most significant factor in bubble impacts, with Figure 6(B and D) showing the probes which were flush to the pipe and Figure 6(A and C) showing the probes which were centered in the flow stream. Chemometric methods with robust error statistics facilitate the exclusion of such anomalous spectra. For example, Q-residual errors provide a measure of deviance of a spectrum from the profiles contained in the calibration spectral set, and they have been successfully used to eliminate spectra affected by bubbles within irradiated aqueous systems.[26]

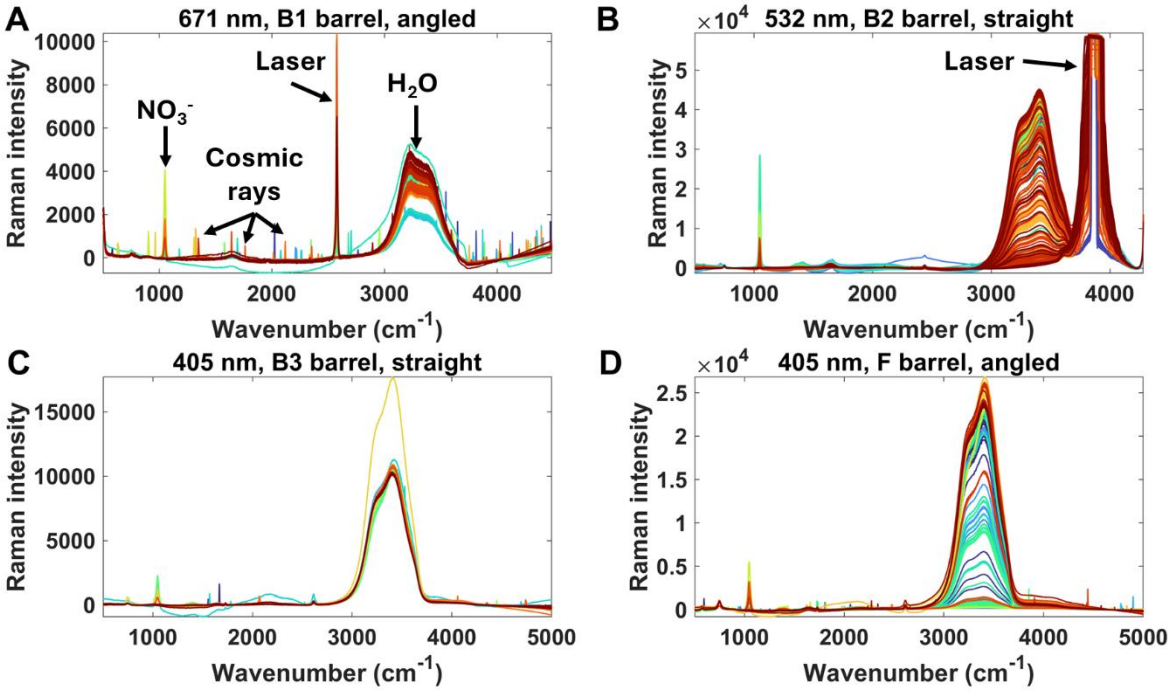

Figure 6. Flow loop spectra preprocessed with second order baseline.

3.3 Testing Raman Instrument

The Raman instrument faced several delays due to supply chain issues. While probes could be effectively tested and integrated into spool piece design optimization work, the Raman instrument testing schedule was pushed out. The spectrometer is anticipated to arrive mid-March, which will leave enough time for targeted Year 1 testing, but unfortunately is too late to include results in this report. Discussion below highlights planned testing for the Raman spectrometer.

Detector Testing. Each laser is assigned a region of the CCD detector, called a track. Each track must be characterized and calibrated to reduce the differences in signal between the six tracks. Firstly, the frequency of response (wavenumbers, cm^{-1}) must be calibrated to the pixel of the detector which receives each frequency. Off the shelf, each track varies slightly in which of its pixels pick up each frequency of light, due to small differences in the optical components of each track. Therefore, a naphthalene standard, which has known frequencies of Raman response, is measured on each track. The pixel of response for each peak is recorded and interpolated to produce a calibrated frequency axis.

Secondly, the intensity of response across the frequency axis must be characterized. A series of ten nitrate dilutions (non-turbid) can be used to measure the signal-to-noise ratio and the linear response range for each track. To reveal any differences between probe barrel performance, each track will be used to measure a subset of five non-turbid nitrate dilutions and five turbid nitrate samples of the same concentration using each of the six close-focus Raman barrels.

Probe Integration. Verification of consistency of response across probes on various tracks will be completed.

Sensitivity to Analytes. The sensitivity of each track to the Raman analytes of interest will be assessed through collection of the training set, which is predominantly covered in Year 2 tasking.

3.4 Training Set Design

An initial training set of 116 samples will be utilized to: (1) determine the sensitivity, selectivity, and errors of quantitation for each Raman analyte on each track of the Raman spectrometer, (2) determine the error of quantitation for each LIBS analyte, and (3) provide a dataset for the development of Raman and LIBS data fusion. Fusion of spectral datasets has previously been shown to reduce errors for analytes with complex or low optical signatures.[21, 27]

The training set is designed to encompass concentration range and concentration ratio variance for a range of Raman and LIBS analytical targets. The concentration ranges for Raman active analytes are shown in Table 4 and for LIBS in

Table 5. These ranges span those identified in the *Instrumentation Plan*.

This training set contains simple and simulant-based samples. Simple compositions were chosen for 46 of the samples to (1) provide pure Raman and LIBS spectral signatures for each component and (2) investigate the spectral overlap of signals from the components as solutions containing an increasing number of components. This is particularly valuable for LIBS calibration of sodium concentration, as there are nine chemical sources of sodium ions in the simulant solutions, and the matrix in which an analyte is dissolved can affect the LIBS signal for the analyte. Simple solutions contain 2.0 M NaOH and up to four other Raman and/or LIBS analytes.

The simulant-based samples are based on high- and low-sodium simulants from Russell et al.[1] The concentrations of components with low solubility are lowered in some cases to avoid precipitation, which would cause unaccounted for turbidity in the solutions. The chemical components used in the simulants are sodium salts of the anionic analytes listed in Table 4 and

Table 5, except for chloride, which is introduced as sodium chloride and potassium chloride, and aluminate, which is introduced as aluminum nitrate. Each simulant type sample contains at minimum eight chemical components.

Series of simulant-based samples are made. The first sample of each series excludes one to three of the chemical components utilized in the full simulant. In the following samples in the series, the excluded chemicals are introduced at varying concentration levels, up to the maximum concentrations listed in Table 4 and

Table 5. The weight percent of solids is varied across the series. This type of variation provides a range of concentrations for each analyte while in the presence of many other analytes which may produce overlapping spectral responses.

The variety of sample compositions included in the training set is visualized in Figure 7. Figure 7 (A, B, and C) show variation in four of the Raman primary analytes as well as weight percent of solids. Figure 7(D) shows the variation in the three LIBS analytes and weight percent solids. The spread of datapoints across the analytical space demonstrates the variety of samples which will be incorporated into chemometric, multivariate spectral models. Incorporating such a variety of samples helps to create a more robust model which captures matrix- and concentration-dependent effects on spectral signatures.

Training set samples will be collected in scintillation vials under stirring, ensuring that solids are suspended in solution. Each close-focus barrel will be used with each laser color to collect a calibration transfer set, allowing any track to be measured at any position in the flow loop. The calibration transfer set is a subset of the training set, and it is used to create transformation vectors which can transform data collected on one track and barrel into data identical to what would be collected on a different track and barrel. Calibration transfer allows for an extensive training set to be collected on one set of probes and then be applied to a different instrumental configuration. This ensures that should probes and track assignments need to be altered during instrument deployment, the workload to facilitate the alteration is minimal.

Table 4. Raman active molecule concentration ranges.

Chemical	Maximum Concentration	Analyte Type
Phosphate	0.20 M	Primary
Oxalate	0.15 M	Primary
Aluminate	0.40 M	Primary
Nitrate	4.0 M	Primary
Hydroxide	9.0 M	Primary
Nitrite	1.5 M	Stretch goal
Sulfate	0.10 M	Simulant component
Carbonate	0.70 M	Simulant component
Fe-rich sludge	22 wt%	Suspended solids

Table 5. LIBS active analyte concentration ranges.

Chemical	Maximum Concentration	Analyte Type
Sodium	0.20 M	Primary
Fluoride	0.20 M	Primary
Chloride	0.33 M	Stretch goal
Fe-rich sludge	22 wt%	Suspended solids

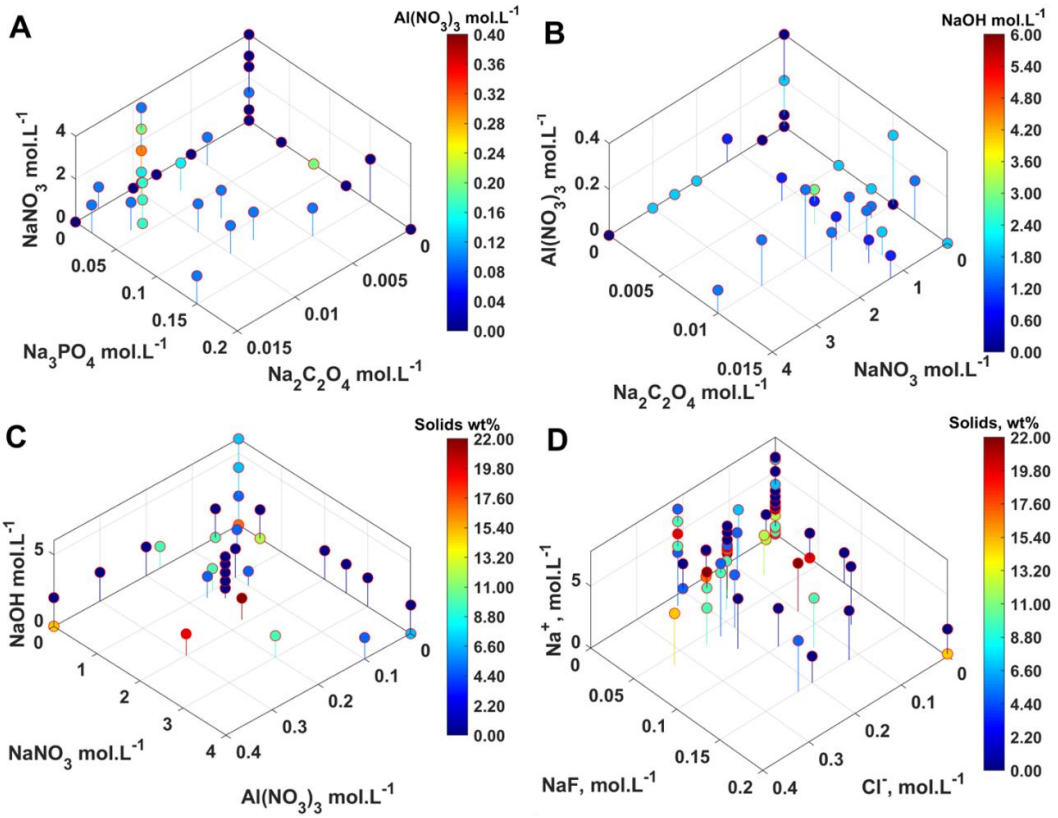

Figure 7. Concentration profiles of the training set showing combinations of (A), (B), and (C) primary Raman analytes and (D) LIBS analytes.

3.5 Next Steps and Opportunities

Following completion of testing in Year 1, the team is well positioned to move into Year 2 which will focus on preparing the Raman system for integration onto the full on-line monitoring platform. Year 2 tasks include calibrating the Raman system and building the chemometric modeling tools used to translate Raman data (spectra) into information (concentrations of the five target species). Many of the approaches to developing robust chemometric models have been previously developed and demonstrated and will be leveraged here.[4-12] In this case, that will not include directly using previously developed models but rather building models according to mathematical operators shown to be highly successful under past work. This rebuild is necessary to support data fusion efforts with the other sensing modalities including LIBS and flow meters.

Additional Year 2 tasking includes completing the design and fabrication of the spool piece (based on design developed under recent TOO work). Here modifications will be implemented to take advantage of findings from TOO work. Flow testing at bench scale will be completed and will be leveraged to provide initial validation of chemometric model operation as well as test approaches to data fusion with flow meter data.

Support of tasking to complete the engineering design plan for the on-line monitoring platform will be included along with potentially integrating Computational Fluid Dynamics (CFD) modeling to ensure full system design can be effectively fielded without impacting downstream sensors.

4.0 Progress on LIBS Sensors

LIBS was identified as a crucial sensor technology to provide key operational information. LIBS is highly complementary to Raman spectroscopy and is uniquely capable of supplying atomic information for a vast array of potential targets relevant to waste treatment applications, while also supporting on-line sensor configurations.

In this project, the demonstration targets are primarily focused on sodium and fluoride, with additional potential stretch goals including chloride and mercury. These targets, along with several examples that illustrate the broad applicability of the LIBS technique, are outlined in Table 6.

Table 6. Selected demonstration species for LIBS validation, from Instrumentation Plan.

Element	Wavelength of lines used	LOD	Reference
Targets of interest to this work			
Na	588.9 nm	0.006 ppm 0.014 ppm (liquid)	Radziemski and Cremers[28]
F	685.604 nm	20 ppm (gas)	Dudragne[29]
Cl (stretch goal)	837.594 nm	90 ppm (gas)	Dudragne[29]
Hg (stretch goal)	253.65 nm	0.5 ppm (aerosol) 0.005 ppm (gas) 84 ppm (solid) 2 ppm (liquid)	Radziemski and Cremers[28] Schmidt and Goode[30]
Examples of other challenging targets (not a focus of this work)			
Fe	567.9 nm	10 ppm (liquid)	Gondal and Hussein[31]
U	367.007 nm	18.5 ppm (liquid)	Sarkar et al.[32]

It is important to note that although LIBS has been extensively demonstrated across various applications, its TRL for analyzing flowing slurries remains relatively low. This is primarily due to challenges in the design of flow cells (spool pieces) and the complexities involved in data analysis.

In the area of data analysis, a significant challenge lies in distinguishing between dissolved content and suspended solids. To effectively understand precipitation or other process concerns, it is essential to differentiate between dissolved species and solids. Our team is actively exploring and considering different data science approaches to address this challenge.

4.1 Instrument and Probe Specifications

In this project, we will develop a LIBS system for the on-line monitoring of slurry. The experimental setup for LIBS is relatively straightforward for the analysis of condensed matter. LIBS utilizes a pulsed laser to ablate or vaporize the material of interest, and by analyzing the self-emissions from the resulting plasma, both qualitative and quantitative elemental information can be obtained.[33]

The main components of the LIBS system include a pulsed laser, optics for laser focusing and light collection, a spectrometer, and a detector. Each component plays a significant role in the

system's operation. The properties of the laser (e.g., energy, wavelength, and pulse duration) are critical parameters that influence plasma evolution and consequently the LIBS signal. A high-resolution spectrograph is necessary to resolve complex and crowded spectral features, while an intensified CCD (ICCD) is typically used as a detector to provide gated detection and high sensitivity. Figure 8shows the typical LIBS schematic.

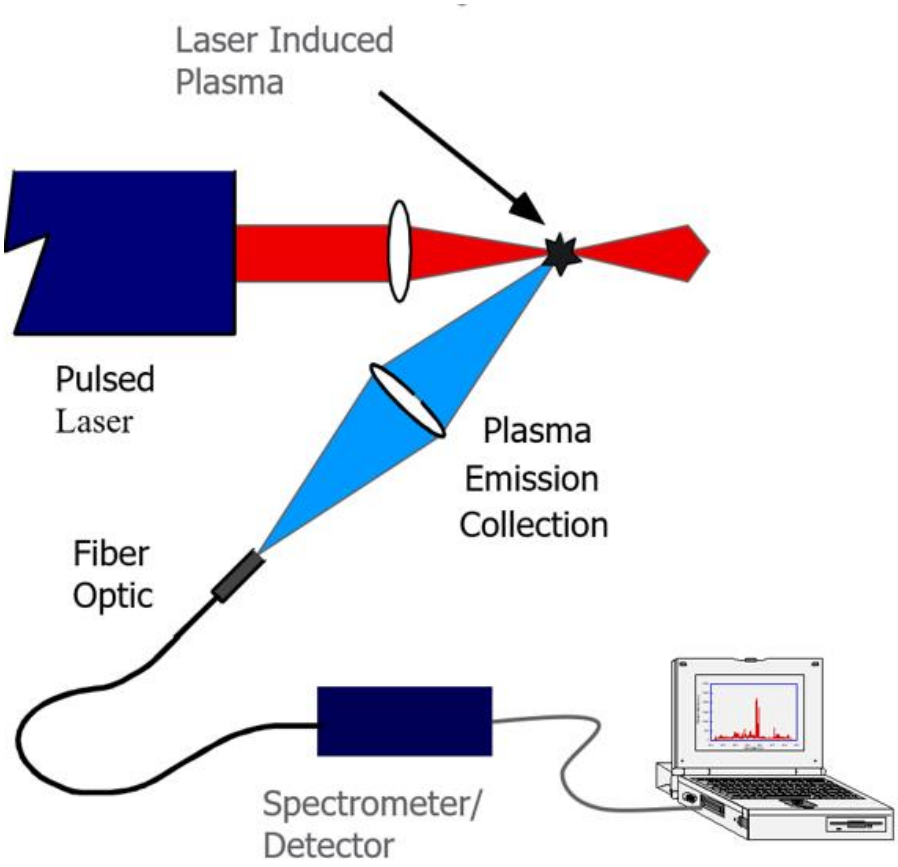

Figure 8. Schematic of the typical LIBS set up.

For the skid platform development, we selected an Nd:YAG laser operating at 1064 nm with a pulse duration of approximately 6 nanoseconds for plasma production. This choice was made due to the laser's cost-effectiveness and compact size. The laser can be operated at its harmonics wavelength (532 nm and 266 nm). The selection of plasma production laser wavelength can influence the laser-target coupling, which is a critical consideration for slurry analysis. Given the complex chemical composition of slurry, which includes both low-Z and high-Z elements, we anticipate that the LIBS spectral features will be densely packed. Consequently, high spectral resolution is essential for obtaining accurate LIBS measurements. Photographs of the LIBS system set-up is given in Figure 9.

Table 7 lists the specifications of the laser and spectrograph procured for the on-line skid platform development. Additionally, the detection system covers a broad wavelength region, which is useful for selecting and detecting emission features of targeted element which appears at wide spectral region.

Table 7. Specifications of instrument procured for LIBS set up.

Instrumentation	Specifications	Rationale for instrumentation selection
Nd: YAG laser	Wavelength: 1064 nm, 532 nm and 266 nm Pulse duration ~ 6 ns FWHM Beam divergence < 0.5 mrad Maximum energy @ 1064 nm ~ 700 mJ; @ 532 nm ~350 nm; and @266 nm ~ 150 mJ	Cost effective and small footprint, Multiple wavelengths to control the laser-target coupling, higher beam energies may be required for brighter plasma generation.
DEMON spectrograph with ICCD detector	Echelle spectrometer with pre-monochromator and active wavelength stabilization in Littrow-configuration, Spectral resolution 5–12 pm, wavelength range 190–900 nm, Gated detection down to a few ns, Light coupling using fiber cable	High spectral resolution may be required for selecting emission from specific species in the complex spectrum. Gated system will be required for differentiating the emission from continuum, excited atoms, and molecules.

Figure 9. (left) Schematic of the LIBS set-up developed for slurry analysis. (right) photograph of the set up.

The developed LIBS setup utilizes polarization optics to attenuate the laser beam energy at the target. Light emitted from the plasma is collected using a fiber and transported to the spectrograph. To enhance light collection efficiency, additional modifications will be made using dichroic optics. The DEMON spectrograph, known for its very high spectral resolution, will be employed for detailed analysis. Additionally, a low-resolution spectrograph will be added to capture broadband spectral features with low spectral resolution.

4.2 Designing the Spool Piece, Modeling and Functional Requirements

A LIBS flow cell or spool piece could take several forms. Several design options are already under consideration with plans to finalize design in Year 2. Activities will involve planning discussions between site flow sheet/engineering experts and LIBS experts to define pathways that can 1) allow for successful collection of data and 2) meet site functionality and engineering requirements.

Additionally, CFD modeling is being considered to help support optimization of design and validation of integration approach into the comprehensive on-line monitoring platform.

The current LIBS system is designed for solid targets, and it will be expanded to perform experiments using liquid samples. Several challenges exist in using LIBS for liquid analysis.[34, 35] These include splashings, surface turbulence, and large shot to shot variation. In Year 2, a LIBS scheme for analyzing liquids/slurry will be developed. A schematic of the potential LIBS online monitoring slurry is shown in Figure 10.

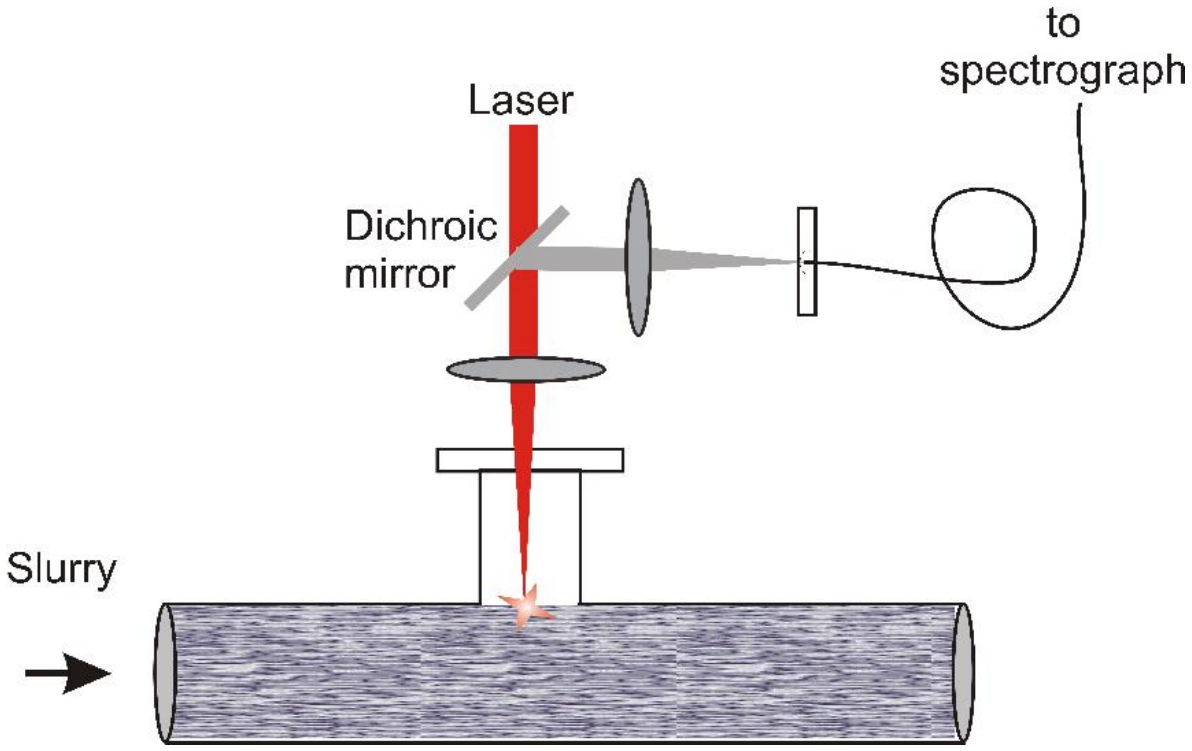

Figure 10. Schematic of the LIBS set up for monitoring liquid/slurry targets.

4.3 Testing LIBS Instrument

Identification of the spectral lines of targeted materials (Na, F, and Cl) has been carried out, and initial measurements were undertaken using condensed salt targets. The selected spectral lines are as follows: for sodium (Na I) at 589.0 and 589.5 nm; for chlorine (Cl I) at 837.6 nm; and for fluorine (F I) at 685.6 nm. The preliminary recorded profiles from these species in salt targets are presented in Figure 11.

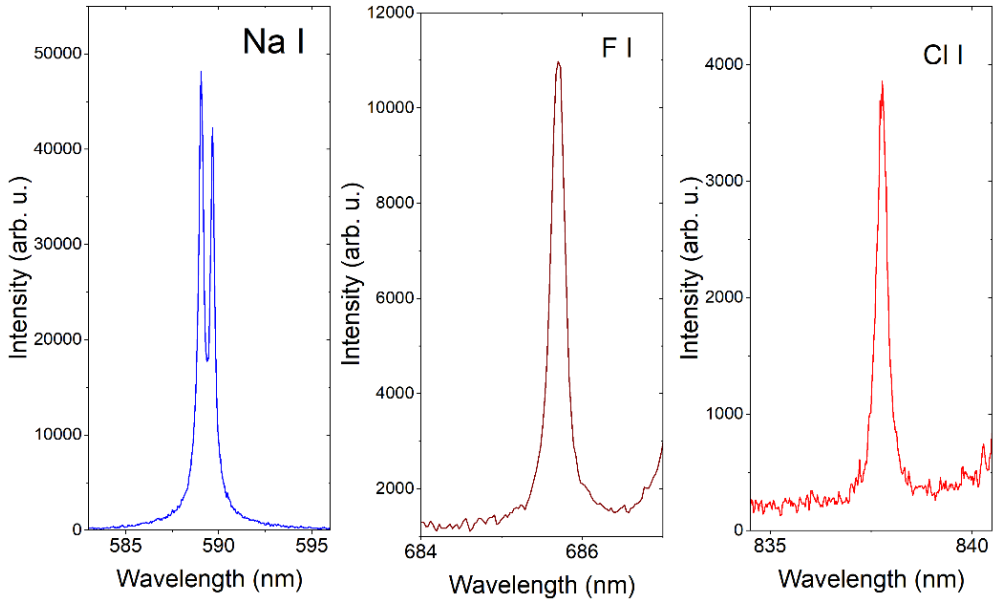

Figure 11. The emission spectral lines from Na, F and Cl. The measurements were taken using salt targets.

Continuation of calibration, testing, and operationalizing of the LIBS sensors system will continue into Year 2. System performance has met Year 1 testing goals.

4.4 Training Set Design

Calibration of the LIBS system will have several steps. Initial testing can essentially be seen as instrumentation checks and building team familiarity with operation. The more complex data collection campaigns will involve collecting optical libraries, or training sets, to build chemometric models for data analysis. This will be done in conjunction with Raman data collection where the training set described in Section 3.4 will be collected on the LIBS system as well.

4.5 Next Steps and Opportunities

With the completion of Year 1 testing, the team is well positioned to kick off spool piece design and data handling/translation tools in Year 2. Spool piece design and engineering tasks will be completed in concert with CFD modeling as well as input from Hanford flowsheet and engineering experts. This may be one of the more complex spool pieces that will be integrated into the test platform for a variety of reasons and will represent a notable and novel achievement by the team. In addition to this, chemical data science optical training sets will be collected in collaboration with the Raman task. This will allow for robust and novel data fusion approaches that could help overcome several of the data analysis challenges anticipated form both Raman and LIBS.

A new post doc will be joining the team in Year 2 to support these efforts and will work closely across the Raman and LIBS efforts to support instrument calibration and data science model building.

Much like the Raman task, the LIBS task team will support completion of the engineering design plan for the on-line monitoring platform where CFD modeling will be leveraged to ensure full system design can be effectively fielded without impacting downstream sensors.

5.0 Progress on Flow Meters

Measurements of flow, density, temperature, etc. are essential to confirm process transfer targets are being met, support cumulative mass measurements in conjunction with other sensor data, and monitor operational parameters to avoid and mitigate upset conditions. During the first task of project work, flow meters were identified as a key component to a comprehensive and widely applicable on-line monitoring platform.

Obtaining accurate flow and density measurements within a flowing stream exhibiting highly variable solids loadings and chemical compositions is challenging. To mitigate for this challenge, two types of flow meters were identified and procured to be used in tandem and will be evaluated for their ability to provide accurate measurements. Specifically, a Coriolis meter and an electromagnetic flow meter were obtained. Details on the specifications of each will be included in the below sections. Note, these items are at a high enough TRL that they can be bought commercially off the shelf, built using appropriate materials to withstand the operational environment anticipated at Hanford (e.g., corrosive and radioactive streams) and configured and calibrated for specified process flow rates and densities. The key points of operationalizing under this work will include validating acceptable flow conditions and measurement accuracy under complex and variable process conditions and utilizing data fusion to connect data streams to support cumulative mass measurements within the user interface.

5.1 Approach

The system engineering approach is being employed to integrate measurement needs, instrumentation, and data acquisition and control. A preliminary concept of operations (ConOps) was used for developing the Gen II test loop. The ConOps is being expanded to incorporate application of real time monitoring measurements output to process operations. A functional architecture is being refined and used to compile component and system requirements associated with both testing and needs for field deployment. The functional architecture will address functionality for instrumentation, waste and flow stream properties, and the hazardous environment. The compiled functions and requirements (F&Rs) will be used to conduct design reviews and develop specifications for the Gen III test loop. Updates to the F&Rs will be made based on test results to allow an initial set of F&Rs to accompany the final test assessment.

The initial use of systems engineering has been applied for the evaluation and down selection to obtain the preliminary components for flow and density measurements discussed in Section 2. The approach is being expanded to encompass the full real time monitoring system and associated system interfaces, inputs, and outputs.

5.2 Consideration and Down Selection

A broad sweep of slurry flow technologies and the experience of subject matter experts was relied upon for down selecting technologies. Non-invasive techniques such as ultrasonic flow technologies, which can be applied to the outside of existing pipe, seem promising for the waste application. However, the impact of temperature variations and high solids concentrations make them unreliable for flow rate and density measurements. In addition, the complexity of the technology applied to flow measurements can result in greater service needs to maintain the instrument, which is undesirable for the radioactive environment. Industrial applications for ultrasonic flow meters tend to be for applications with known solid densities (e.g., sewage treatment, dredging).

The abrasive nature of the process material and the radioactive environment make mechanical means of flow monitoring, such as vanes, undesirable. Development of the monitoring application is focused on avoiding the addition of any flow impeding hardware. Thermal mass flow meters tend to be used primarily for gas applications, and the Hanford waste would create significant fouling issues for any known technologies.

In the face of these challenging scenarios, the Coriolis technique stands out for its ability to handle highly variable flow properties of slurries and provide direct measurements of both mass flow rate and density. For providing a secondary measurement of volumetric flow rate, the electromagnetic flow meter was identified as the preferred solution. The electromagnetic meter can also provide a measurement of slurry conductivity that can be used to verify the validity of the Coriolis measurements. Their principles of operations are described below and recommendations for application of the two technologies in tandem are provided in Section 5.3.

5.3 Sensor Specifications

Design and testing of the deployable skid technology will be done across multiple flow loop iterations. A first-generation flow loop (Gen I) is a benchtop installation that will span testing up to a 1.5 in line size. Thereafter, a second generation (Gen II) loop will be designed and commissioned to test 2 in line sizes, followed by modification to a third-generation loop (Gen III) as needed to accommodate larger (3 in) line sizes and sensor installations, as needed. The flow meters discussed below will be deployed to handle the requirements for the Gen II and Gen III loops. Ideally, the Gen III loop will be the Multiphase Transport Evaluation Loop (MTEL) testbed housed at PNNL.

The objective of the real-time monitoring system is to measure the process flow rate and slurry density within transfer lines. Accurate monitoring of these parameters is crucial for assessing pipeline transport velocities and to mitigate the risks of particle settling and potential plugging.

To be able to detect flow conditions beyond the specified process flow conditions and still provide good resolution within the process operating range, the upper limits for the instrument meter ranges were targeted to be approximately 1.15 to 1.35 times that of the upper bounds for the process conditions presented in PNNL-36598 These yields target upper bound parameter values for the Coriolis and Electromagnetic meters of:

- Density – 1800 kg/m3
- Mass flow rate – 1200 kg/min (~180 gal/min)
- Velocity – 6 m/s (accounting for upper bound in a 2-inch line)
- Up to 22% wt pct solids.

5.3.1 Coriolis Meter – Principles of Operation

The following description for the operation of Coriolis flow meters (CFM) has been modified from the description presented in Onishi et al.[36]

CFM measure both mass flow rate and density directly with the parameters of mass, time, and length as the bases of all measurements. Mass flow rate measurements with a CFM are accurate under conditions of changing viscosity, conductivity, density, and temperature of the flowing fluid. The principle of operation is based on Newton’s second law.

The sensor contains a flow tube that has a symmetrical flow path lying in a single plane. Earlier configurations of flow tubes have included D- and U-shaped geometries. Improvements in sensor technology and electronics now allow measurements to be obtained from straight flow tubes. The flow tube is vibrated at the natural frequency of the filled tube using a feedback circuit and drive coil. The vibration is induced at the midpoint of the flow tube such that the resulting motion (i.e., oscillation) of the tube is perpendicular to the plane of the flow tube.

As fluid enters the flow tube, it takes on the lateral momentum of the vibrating tube. As the fluid is accelerated in the lateral direction; a force is applied to the wall of the flow tube. As the fluid approaches the exit of the tube; it resists having its lateral motion decreased. The resulting force applied to the tube wall at the downstream side of the flow tube is opposite in direction to that imposed on the upstream half of the tube. These forces cause the flow tube to twist or bend. The forces applied to the flow tube switch direction with each half cycle.

The amount of twist or bend in the flow tube is directly proportional to the mass flow rate of material through the tube. The lateral velocities, of both the upstream and downstream sides of the flow tube, are measured. The time difference between the velocity detector signals appears as a phase shift and indicates the twist of the flow tube. The phase shift, between the velocity signals, indicates a mass flow rate. If no flow exists, then no twist is created in the flow tube, and the measured velocities are in phase.

The density of the material in the flow tube is obtained from measuring the natural frequency of the system. The total mass of the tube and internal material is related to the natural frequency through the following relationship:

$$m_{Total} = \frac{k}{f^2 4\pi^2} \qquad \text{(Eqn 5-1)}$$

Where k is the factory-determined spring constant and f is the natural frequency of oscillation. The bulk density of the flow stream can then be obtained by subtracting the known mass of the tube and dividing by the internal volume of the flow tube such that

$$\rho_{Bulk} = \frac{(m_{Total} - m_{Tube})}{V_{Tube}} \qquad \text{(Eqn 5-2)}$$

Where ρ_{Bulk} is the bulk density of the material within the Coriolis meter tube, m_{Tube} is the mass of the Coriolis meter tube, and V_{Tube} is the internal volume of the Coriolis meter tube.

Importantly, CFM are not designed to obtain an average value over the length of the Coriolis meter tube. The fluid properties over the length of the tube are assumed constant. High-frequency transients such as slug flow or rapidly fluctuating slurry concentrations result in inaccurate measurements. Length scales associated with the non-homogeneity of the fluid must be significantly greater than the length of the flow meter sensor tube.

Applied to slurries, significant deviations from vendor specifications for accuracy have been observed at flow rates less than 20% of the meter range. Figure 12 plots meter accuracy and percent of meter full-scale flow rate. The vendor-specified accuracy is presented along with two plots that have been obtained from experimental testing at PNNL.[36] The experimental testing utilized Micro Motion Elite Series Meters. The operating ranges of the CMF200 and CMF300 models were 0 to 3200 lb/min and 0 to 10000 lb/min, respectively.

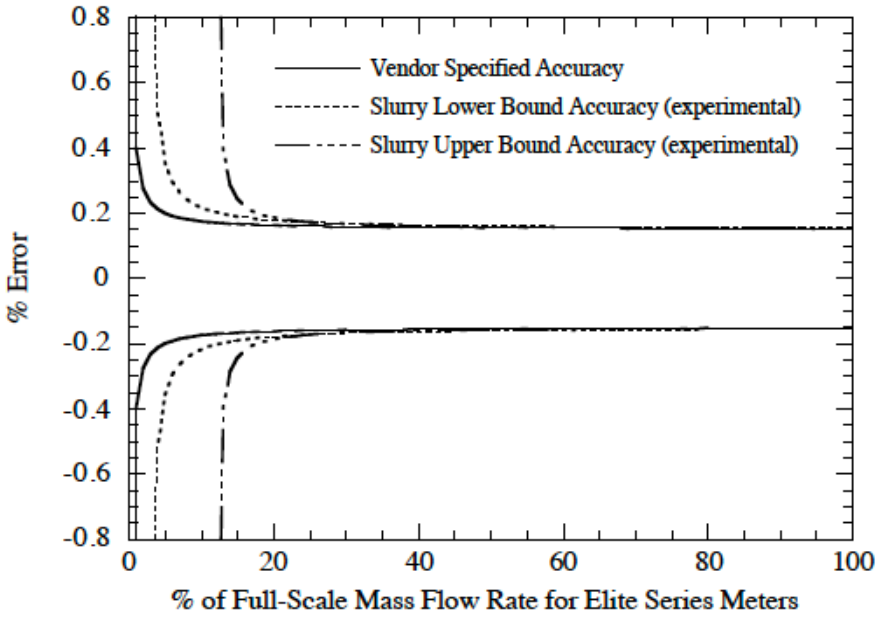

Figure 12. Percent error as function of the percent of full-scale mass flow rate for elite Series Micro Motion Flow Meters based on vendor specification and experimental results with slurry.

The two plots of experimental data shown in Figure 36 represent the upper and lower bounds of meter accuracy that have been observed during tests with suspended slurries. Testing was conducted with slurries containing granular material such as zeolite and silica sand and cohesive material such as kaolin clay. The carrier fluids consisted of water and mixtures of water, sugar, and salt. The specific gravities of the slurries ranged from 1 to approximately 1.5. The bounding results presented are based on experimental work conducted at PNNL.[37]

An additional complication for Coriolis measurements experienced during operations is the introduction of gas coming out of solution within a pumped test loop. The gas tends to come out of solution much faster than it is absorbed. This effect has been observed in water tests, depending on the location of the CFM within the test loop. In a slurry, the microbubbles will adhere to the particulate, reducing the rate at which they dissolve back into solution. This complication is reduced when dealing with salt solutions of high ionic strength. The problem can be mitigated by applying a positive cover pressure to the test loop using a pressurized surge/bladder tank.

CFM are not affected by upstream piping configurations other than geometries that may allow gas to accumulate, which can result in periodic releases of bubbles, introducing noise in the measurements.

The recommended separate sensor and remote transmitter configuration involves separate considerations for installation. For slurry media, manufacturers recommend that sensors be oriented in a vertical pipe run with flow upward. This orientation allows for media drainage when shut down and reduces the potential for particle accumulation.

Typical piping connections for the sensor unit include standard pipe flanges, and tubing connections such as standard Swagelok, Swagelok VCO, or Sanitary Tri-Clamp. Pipe flange connections may require the most change-out time and complexity because of the time involved in manipulating the multitude of small parts, including bolts, nuts, and gaskets. Piping connections via sanitary tri-clamp fittings may be the simplest and least time-consuming method.

Manipulation of the tri-clamp gaskets can be avoided by bonding them onto the sensor side of the tri-clamps.

If possible, mounting the sensor at the high point in the process line should be avoided to minimize gas accumulation in the meter. The installation should ensure that the CFM will not be subjected to mechanical vibration. Mounting multiple CFM in proximity to one another should be reviewed to eliminate the potential for vibration crosstalk between sensors.

The transmitter should be mounted to a structure at a convenient elevation and orientation for personnel to remove and reinstall covers and access electrical terminals and test points. Depending on the manufacturer and model, the sensor may be up to 1000 ft (cable run) from the transmitter. The transmitter and sensor are interconnected by a special electric cable provided by the manufacturer.

The introduction of electrical noise to the CFM units should be minimized by:

- Powering the units using isolated circuits
- Following the manufacturer's recommendations for electrical connections and proper grounding
- Routing signal cables separately from sources of electrical noise
- Ensuring that neither the sensor nor the transmitter is installed close to generators of electrical noise, such as variable frequency drives.

Maintainability of CFM is enhanced with separate sensors and transmitters. This configuration is also desirable in an application where the sensor will be handling high-level radioactive slurries. The transmitter electronics should be located some distance from the source of radiation. This allows transmitter reconfiguration and change-out with minimal radiation exposure to workers.

Most CFM are available with some form of communication capability, either standard or optional, other than the industry standard 4~20mA analog current loop signal outputs. Perhaps the most common implementation, and the one used most during PNNL test efforts, is the Highway Addressable Remote Transducer (HART) Protocol. The HART Protocol is an industry standard promulgated by the HART Foundation. HART Protocol provides a means of full-duplex communication with an instrumentation transmitter using existing 4~20mA loop wiring. This is accomplished by inserting Bell standard 202 frequency-shift-keyed digital data "on top" of the 4~20mA signal. Some CFM transmitters use HART Protocol to transmit sensed data. For example, most CFM sense mass flow, density, and temperature (via a Resistance Temperature Detector [RTD] in the sensor) while the volumetric flow rate is calculated by the transmitter from the measured mass flow rate and density.

Routine maintenance activities mostly consist of periodic (flow) re-zeroing of the transmitter for conditions that ensure that the sensor is full of media fluid and that no flow exists. Fouling or wear of the sensor tube can be a cause of zero shift. Depending on process fluids, flushing to periodically mitigate fouling can be another maintenance consideration.

Both the sensor and transmitter unit can be replaced individually. The remote location of the transmitter eliminates the potential for the transmitter to be contaminated. Sensor replacement in a nuclear environment poses unique problems not encountered with other process materials. The system design needs to account for sensor replacement after the unit has been contaminated and a calibration check (performance check) performed on the installed replacement unit. Usually, calibration facilities with uncertainties as low as the factory's calibration system are not available for in-field applications. It may be desirable to provide a means of functionality checking and rough calibration in a field installation. Such a capability could be built into a system using remote control valves to divert process water from a supply tank mounted on a weigh system through the flow sensor. The functional check could be performed during line-flushing operations or other normal process activities using process water, thus requiring no additional water (and no increase in waste volume).

Deployed configurations often allow the functional check to be performed with water flowing through the meter in either direction, allowing the existing process pipe configuration to be used. A reasonable functionality check and rough field calibration (performance check) can be made by monitoring and comparing the CFM-indicated flow rate to the weight accumulation rate on the scale. If the installed orientation of the CFM allows the meter to be fully drained, a two-point check of the meter density can be made using air and process water.

Past applications of CFM operated in radioactive environments have occurred. In addition to reviewing past operational experiences, the radiation hardness of a CFM is possible through operation in a controlled radioactive test environment. PNNL possesses a gamma irradiation facility within the 318 Building. Under future efforts, it would be a straightforward process to conduct a radiation exposure test of a CFM system in this facility. Two CFM sensors would be connected in series in a test loop. One sensor, the unit being tested would be placed in a test tube in the facility, where it receives a known dose rate. Because of size limitations of the test tubes in the gamma irradiation facility, the sensor would be a specially configured version of a small, standard sensor. The reconfiguration would allow it to fit in the test tube but would not involve any change in construction materials or operation. A baseline sensor would be located outside the gamma facility, receiving no radiation dose above normal background levels. A pump would be used to periodically circulate water through the test loop, and both sensors would experience the same flow rate of the same fluid. Both transmitters would be located outside of the irradiation facility and configured to output mass flow, density, and temperature. A PC-based data acquisition system monitors the transmitters' analog outputs. The output indications would be regularly monitored and checked for divergence as a function of dose/service time.

5.3.2 Coriolis Flow Meter Selection

PNNL-36598 identified the process conditions to target when choosing the flow meters and is summarized in Section 5.3. Sizing of the Coriolis sensor is primarily based on needs for measurement of mass flow rate. Line size is secondary and is based on allowable pressure drop or potential line clearances required for process stream. This often results in the line size of the Coriolis meter to be reduced from that of the process pipeline. To this end, the Proline Promass I 500 2-inch full bore Coriolis flow meter manufactured by Endress & Hauser was selected to serve as the flow meter in the Gen II and Gen III flow loop designs. This CFM has a maximum

measurement range of 180,000 kg/h with an accuracy of ±0.1% of mass flow rate reading and an accuracy of 0.00025 g/cm3 for density.

The CFM has been sized to the smallest measurement range that would cover the process parameters identified in section 5.1. For example, the meter can measure flow velocities of 47 ft/s and 21 ft/s in 2 in and 3 in lines respectively for the target density.

5.3.3 Electromagnetic Flow Meters

The following description for the operation of Electromagnetic (EM) flow meters has been modified from the description presented in Onishi et al.[36] EM flow meters apply Faraday's Law for electromagnetic induction to obtain the velocity of a conductive fluid. As a conductive fluid passes through a magnetic field, a voltage is produced. The magnitude of the voltage is directly proportional to the fluid velocity, the magnetic field strength, and the pipe diameter. For in-line meters, the magnetic field and the measured fluid velocity are perpendicular; therefore, the velocity can be described by

$$U = \frac{V}{KBD} \qquad \text{(Eqn 3)}$$

where U is the average fluid velocity, V is the induced voltage, K is the proportionality constant, B is the magnetic field strength, and D is the internal pipe diameter.

EM meters are not affected by changes in the fluid density or viscosity (direct-current meters have been susceptible to noise resulting from high-viscosity fluids) and result in negligible pressure drop because their flow channel is a short section of straight pipe. Both direct current (DC) and alternating current (AC) EM meters exist. Pulsed-DC systems operate at low frequencies (4 to 7 Hz), which allows the electronics to be re-zeroed between the pulses. However, the low sampling frequency of the meters makes them susceptible to noise from the flow of slurries, electrochemical reactions, and high viscosities.

AC EM meters reverse polarity at 60 Hz and are less susceptible to the noise from the flow of slurries. However, the AC meters do experience zero drift. A dual-frequency EM meter intended to allow for continual re-zeroing while maintaining immunity to noise created by flowing slurries was manufactured by Yokogawa. The Yokogawa instrument had a carrier frequency of 7 Hz with a low pass filter and a 72-Hz superimposed high-frequency waveform. The resulting accuracy of the Yokogawa EM meters was rated at 0.5% volume flow rate for a flow rate range of 20% of the span and higher.

The accuracy of an EM meter depends on a uniform conductivity over the cross-section of the pipe. Variations in conductivity can occur with incomplete mixing of an added fluid such as in water dilution or stratification of a slurry flow. The stratification of slurries often results in reduced accuracy at higher percentages of the flow range than that specified by the manufacturer. Therefore, a vertical orientation is recommended for slurry applications with an upward flow through the meter. A length of 5 to 10 pipe diameters of straight pipe is required to exist immediately upstream of the installed EM meter, depending on the upstream pipeline configuration and components.

5.3.4 Electromagnetic Flow Meter Selection

The Promag P 500 3-inch electromagnetic flow meter manufactured by Endress & Hauser was selected to serve as the verification flow meter in the Gen II and Gen III flow loop designs. This EM meter has a recommended measurement range of 25 gal/min to 800 gal/min with an accuracy of ±0.5% of the flow rate reading. The EM meter can measure flow velocities of 86 ft/s and 38 ft/s in 2 in and 3 in lines respectively.

5.3.5 Proposed configuration

The primary measurements that will be used for data fusion are anticipated to be those obtained from the Coriolis meter. The primary purpose anticipated for the EM meter will be to measure the conductivity of the process stream and to monitor changes in conductivity. For accuracy of measurements, the CFM requires a uniform mixture relative to the length scale of the sensor. The EM meter provides a measurement method of checking that the time scale/frequency of changes in the process mixture are not significantly shorter than that associated with the length of the CFM.

The configuration for using these meters in tandem will ideally consist of upward vertical flow through the meters with the EM meter upstream of the CFM. This configuration allows upstream pipeline configuration required for the EM meter to be configured and the CFM to be installed close to the EM meter as the CFM has minimal upstream requirements for pipe configuration. The vertical orientation mitigates stratification of multiphase flow and the accumulation of gas or solids within the sensor tube.

Testing will be conducted with this vertical orientation for system integration. However, if requirements determine that field deployment in a horizontal orientation may be needed, testing could accommodate getting comparative measurements and associated limits of operation.

5.4 Testing Sensors

Preliminary testing of spool piece components and flow meters will be accomplished on a benchtop flow loop referred to as the Gen I flow loop (Figure 13). This loop consists of 1.5 in reinforced flexible tubing, 1.5 in stainless steel pipe, and 1.5 in sanitary tubing driven by a MFM Inc non-metallic centrifugal pump. Gen 1 loop was used to perform benchtop testing, model collection, and instrument testing of flow loop components that will inform the design of the larger scale Gen II loop. The following section describes the use of the Gen I loop in the initial validation testing of the flow meters.

Figure 13. Mentoring of junior staff members in the operation and maintenance of the Gen I flow loop.

5.4.1 Functional Testing of Flow Meters

The difference in working principle between the CFM and EM meters require some specialized testing upon receipt (Figure 14). In brief, the CFM should have a density calibration check, the EM meter should have a coating and fouling check (although the CFM would benefit from this as well), and both should have a data acquisition check and a zero-flow condition check. The testing methodology is as follows:

Density Calibration Check: The CFM's measurement of the density of air at zero flow should be compared with standard values. This will be followed by a check of water density during zero flow. Finally, the meter will be drained and the consistency and accuracy of the values confirmed. This test will identify issues with density signal drift as the loop is filled and emptied. The EM does not measure density, so this check is not useful.

Coating and Fouling assessment: The CFM and EM meters can both be affected by coating and fouling. This can be checked by comparing the meters' responses to measuring the flow of plain (i.e., tap) water before and after a liquid media that may deposit thin coatings/foulings such as iron oxide. The measurements before and after the presence of iron oxide can be used to determine if a fouling correction will need to be made. This can be combined with a zero flow condition check, where the meter is isolated from the flow loop and the measurement analyzed for deviations that would track interferences such as electrical line disturbances.

Data Acquisition and signal check: Lastly, a data acquisition check will be performed. The meters were ordered with the capability to communicate via the HART protocol. This allows for dynamic range adjustment to demonstrate the meter's value and accuracy across varying operational parameters.

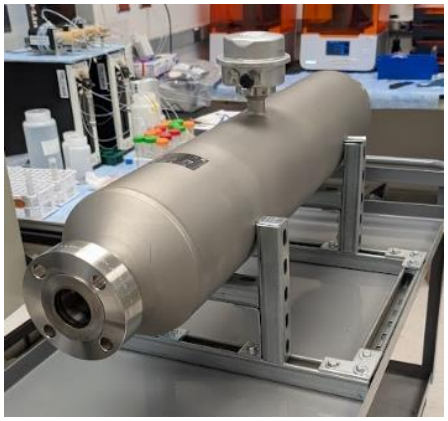

Figure 14. Coriolis and Mag flow meters during functional testing

During operational testing, the following factors can be evaluated:

- the impact of re-zeroing to compensate for fouling
- the impact of line flushing to clear fouling/mitigate zero-shift
- the impact of operational issues and mitigation associated with gas coming out of solution; greatest concern for zero-flow check with process fluid.

5.5 Data Handling and Initial Notes About Connection to User Interface

We are initiating the development of statistical models to calculate cumulative measurement error. This will initially start with Raman data but will be extended to quantify the error introduced when integrating Raman spectroscopy with flow data. Historical data from different chemical processes is being leveraged to build a base case in the near term, but this will be adapted to the new data to be collected on project sensors in Year 2. Ultimately this approach will be extended across the entire suite of sensors in the test platform, enabling a comprehensive analysis of combined measurement systems over time.

Additionally, we have selected a technology stack that enables the development of robust front-end interfaces while leveraging the speed and efficiency of the Rust programming language alongside the versatility of the Python programming language, ensuring both performance and functionality.

5.6 Next Steps and Opportunities

With the completion of receipt and testing of the flow meters, the team is ready to kick off Year 2 activities. These will include integrating flow meters into a series of loops to test accuracy under variable process conditions, including variable solids loading and chemical composition. These efforts will be partnered with testing and calibrating other sensors to support data collection and development of data handling and data fusion tools to complete cumulative mass measurements.

Efforts will integrate additional team members, including a new post-bachelors engineering intern. Additionally, support in completing the engineering plan as well as providing needed support and data for CFD and other modeling aspects will be key tasks.

6.0 Progress on Ultrasonic Pulse Echo System for Critical Velocity Detection

Slurry mixing and transport properties in horizontal slurry transfer piping are essential information for Hanford site operation and waste treatment. Metrics such as critical velocity are widely recognized as needed information and are used to allow operators to avoid suboptimal or upset/off-normal flow conditions (e.g., solids settling, accumulation, and plugging). In the case of critical velocity, operators need to understand the flow velocity at which solids in the slurry will settle before transporting slurry in pipes. This is a metric that cannot be measured off-line as settling is unique to process flow conditions, pipe configurations, and slurry properties.

The Ultrasonic Pulse Echo (UPE) system was first developed at PNNL between 2010–2012 and was successfully demonstrated and validated.[38-44] It leverages commercial off the shelf equipment partnered with proprietary data analysis approaches to accurately detect solids settling. Project work here is being leveraged to modernize the UPE system and expand applications to include both 3 in and 2 in pipe diameters. Additionally, exploration of system modifications and optimizations to support field deployment and in-concert measurements with other sensors is being completed.

CFD modeling has been initiated to support spool piece design efforts on this task. See Section 8.0 for details.

6.1 Technical Basis for Modernizing the Ultrasonic PulseEcho System

The critical velocity of a slurry in horizontal transfer piping is the superficial fluid transfer velocity at which solid particles deposit or settle at the bottom of the pipe. Simplified illustrations of examples of solid particle behavior in a slurry pipe under different flow conditions are provided in Figure 15. The straight portion of the curve between Points A and C encompasses the flow velocity range at which the solid particles are suspended in the carrying liquid. However, as the flow velocity is decreased from Point A, the uniformity of suspension gradually decreases. This decrease continues until Point C, where a portion of the solids are being conveyed along the bottom of the pipe. At Point D, a stationary bed of solids has formed. The so-called critical velocity, below which the bed of solids begins to form, lies between Points C and D. **The exact location depends on which definition of critical velocity is used.**[45]

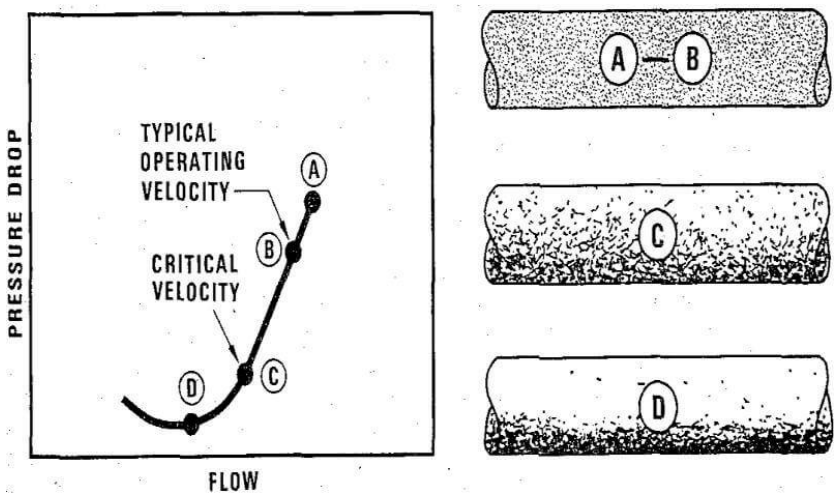

Figure 15. Example of a pressure drop vs. flow velocity plot for slurry in a horizontal pipe with an example of how critical velocity might be defined. Right: Corresponding illustrations of vertical distribution of solid particles in the slurry pipe at different pressure drop and flow velocity conditions.[45]

The standard method for recognizing and declaring that critical velocity conditions have been reached in a pipe—finding the inflection point in a pressure drop vs. flow velocity plot (like Point D in Figure 15)—has been rendered ineffective when used with non-Newtonian slurries like Hanford HLW simulants because the inflection point typically doesn't exist.[46]

Calculating critical velocity may seem more straightforward than measuring it, but critical velocity can only be reliably calculated for slurries whose physical properties (e.g., particle size and distribution) are accurately characterized and fall within the limits established for currently available critical velocity correlations, such as the popular Oroskar-Turian correlation.[47] Slurries with constituents that fall far outside the correlation limits, fail to meet their underlying assumptions, or are difficult to accurately sample and characterize require testing to empirically determine their critical velocity. The broad and complex constituents of many Hanford HLW slurries fall within this category.[46, 48] A modified Oroskar-Turian equation or other correlation that accurately or at least consistently calculates a conservative critical velocity for Hanford HLW slurries has yet to be developed.[49] Even if a perfect equation for predicting critical velocity existed, only small design margins exist between Hanford WTP slurry handling capability and the waste acceptance criteria (WAC), so errors associated with slurry sampling and offline analysis to satisfy equation inputs such as particle size distribution (PSD) would need to either be very low or known to favor conservatism. Unfortunately, based on sampling challenges, that may not be reasonable to expect.

The UPE system was first developed at PNNL between 2010–2012 to detect the primary symptom of critical velocity—particle settling at the bottom of a horizontal slurry pipe (or mixing vessel)—and was successfully demonstrated and validated on 3 in pipe diameters.[38-44] The UPE is composed of commercial off-the-shelf equipment partnered with PNNL proprietary data analysis algorithms to accurately detect solids settling. However, the last year the prototype UPE system was matured and tested was 2012. Modernization of the UPE system's hardware and software were necessary to prepare it for testing under this project.

Project work here is being leveraged to modernize the 11–15-year-old UPE hardware and software, demonstrate its application to 2 in piping as well as 3 in piping, scale up from a single transducer (single monitoring location) to multiple transducers, and address lessons learned from 2010–2012 testing. Additionally, exploration of system modifications and optimizations to support field deployment and in-concert measurements with other sensors is being completed.

A UPE system is composed of ultrasonic transducer(s), which are installed on the outside surface of the pipe or vessel to be monitored, and an electronic data acquisition system (DAS) to which the UPE transducer(s) are connected via signal/power cable(s). The first prototype UPE system is shown in Figure 16.

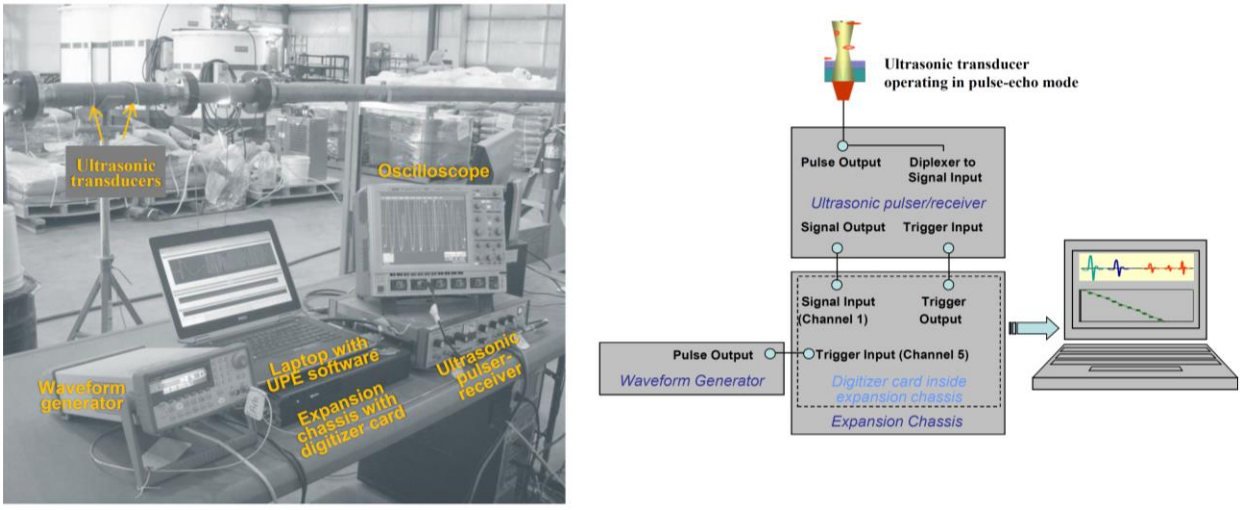

Figure 16: Photograph (left) and diagram (right) of the first UPE system (transducers and DAS electronics) used for testing in 2010-2012.

6.2 Ultrasonic PulseEcho Transducer Requirements and Specifications

The commercial UPE transducer(s) are just one part/sub-system of a UPE system but they will be exposed to the harshest conditions in an operational environment. The transducer(s) are also key to the system's sensitivity to particle settling (along with low-jitter digitizer and analysis algorithm).

UPE transducer design specifications (materials, sizes, heat/radiation tolerance, etc.) and operating specifications (ultrasonic frequency, bandwidth, and wave mode) are driven by:

- known or estimated physical properties of the HLW slurries *inside the pipe* whose critical velocities need to be characterized
- the characteristics *of the pipe* onto which the UPE transducers must be installed
- the environmental conditions immediately *at/around the pipe* at UPE transducer installation locations
- the safety and logistical requirements of the *greater operating environment*.

The physical properties of the HLW slurries whose critical velocities need to be characterized; the pipe characteristics of HLW slurry transfer lines; the anticipated environmental conditions; and

the anticipated safety and logistical requirements are summarized in Section 6.2.1 for Hanford tank farm and WTP applications.

The UPE transducer specifications that were developed and selected for this task, based on the requirements in Section 6.2.1, are provided in Section 6.2.2.

6.2.1 UPE Transducer Requirements

Transducer Requirements Driven by HLW Slurry Physical Properties: Nuclear waste slurries stored in underground tanks in the Hanford Site's tank farms are complex mixtures of salt solutions and multi-component undissolved solid particles (Figure 17). In general, HLW slurries have broad PSDs with pseudo-homogeneous carrier fluids containing a heterogeneous settling portion, where solids have a wide range of particle size, density, and chemical characteristics. Particle sizes range from sub-micron to millimeters and are interacting, non-spherical, and non-uniform.[46, 50] As shown in Table 8, solids concentrations in slurries could reach 30 percent by volume (vol%). Depending on the solids concentration, the slurries may exhibit a Newtonian or non-Newtonian rheology.

Figure 17. Photo of Hanford waste in a storage tank.[51]

Table 8. Slurry properties used to develop specifications for cross-site transfer line piping and booster pumps, with flow velocity targets of 4.5-6.0 feet/second.[52, 53]

Fluid Property	Achievable Design Velocity (ft/s)	
	4.5	6.0
Specific gravity (mixture)	1.5	1.25
Viscosity (centipoises)	30	10
Miller number	<100	<100
Minimum pH	11.0	11.0
Fluid temperature (°F)	35 to 200	35 to 100
Solid content (volume %)	30	20
Particle size (μm)	0.5 to 4,000	0.5 to 4,000
0 to 50 μm, % of total	≈ 95	≈ 95
50 to 500 μm, % of total	<5	<5
500 to 4000 μm, % of total	<1	<1
Friction factor	0.404 (non-Newtonian)	Newtonian flow

Therefore, the UPE transducer(s) shall be capable of detecting the onset of particle settling in Newtonian and non-Newtonian slurries with solids concentrations up to at least 30 vol%.

Specific physical characteristics of the solids fraction and liquid fraction of waste in Hanford tank farms have been reviewed by the Hanford tank operations contractor (TOC) and their subcontractors to serve as inputs for the calculation of waste feed delivery (WFD) system capabilities, for example waste transfer system capabilities. The physical characteristics of the carrier fluids and solids for HLW slurries are provided in reports such as RPP-RPT-51652, *One System Evaluation of Waste Transferred to the Waste Treatment Plant*[49] and PNNL-20646, *Hanford Waste Physical and Rheological Properties: Data and Gaps*.[54] More recent analyses may be available from over the past 13 year; however, they have yet to be captured in comprehensive review documents.

Unless otherwise noted, the requirements provided in this section are based on liquid, particle, and solid-liquid mixture (slurry) properties in RPP-RPT-51652, *One System Evaluation of Waste Transferred to the Waste Treatment Plant*, which references and incorporates work from PNNL-20646, *Hanford Waste Physical and Rheological Properties: Data and Gaps*.

Undissolved Particle Sizes and Densities: The PSDs of multiple different sludge and saltcake samples from different Hanford waste tanks are provided in Figure 18. PSD traces for sludge and saltcake tank waste samples analyzed using three different PSD measurement methods.[54]. The results for the sludge and saltcake samples are presented for three different PSD analysis methods. It helps to view the PSDs of separate samples analyzed using different PSD methods to understand the extreme/bounding PSD cases.

PSD Summary: Sludge, Flowing Sonicated

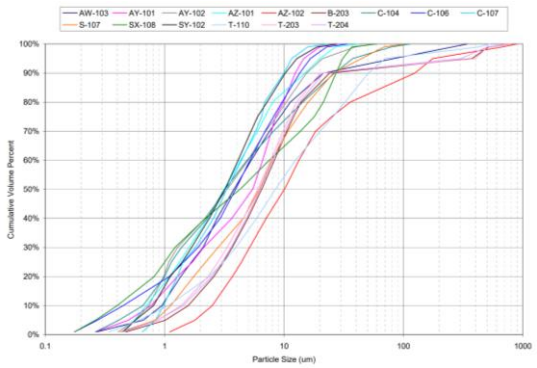

PSD Summary: Sludge, Flowing Unsonicated

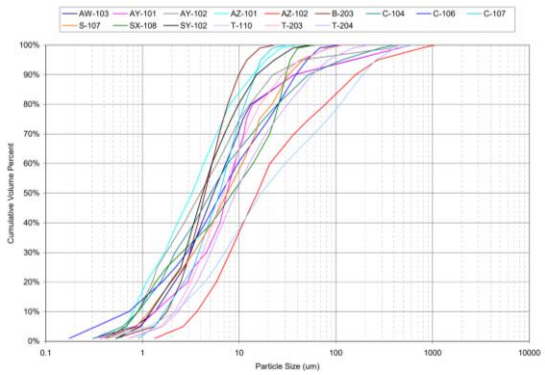

PSD Summary: Sludge, No-flow Unsonicated

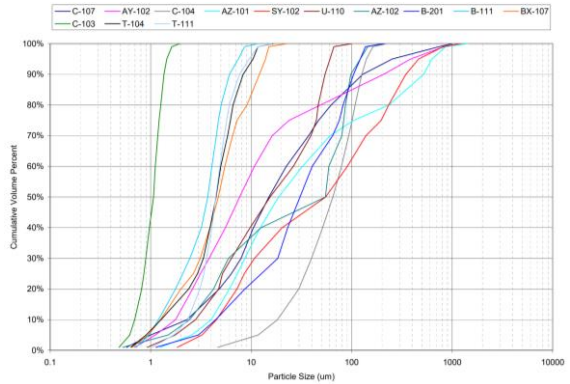

PSD Summary: Saltcake, Flowing Sonicated

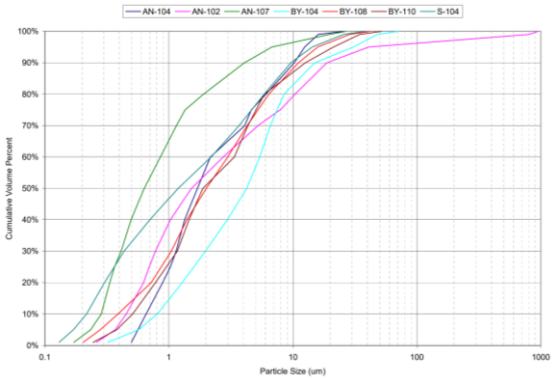

PSD Summary: Saltcake, Flowing Unsonicated

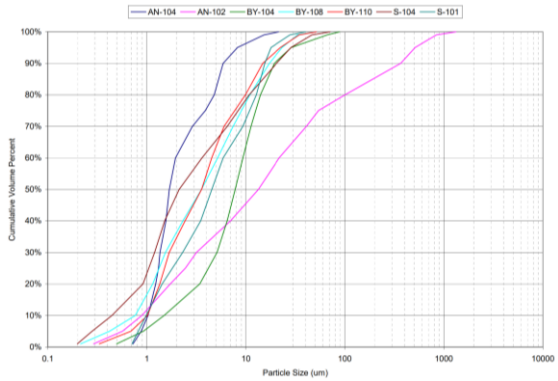

PSD Summary: Saltcake, No-Flow Unsonicated

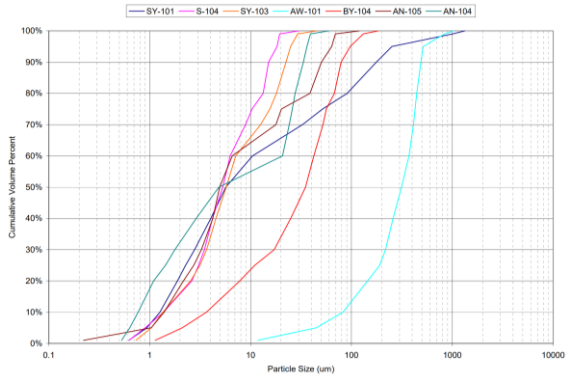

Figure 18. PSD traces for sludge and saltcake tank waste samples analyzed using three different PSD measurement methods.[54]

Overall, Figure 18. PSD traces for sludge and saltcake tank waste samples analyzed using three different PSD measurement methods.[54] shows that particle sizes generally range from approximately 0.20 micrometers (µm), or microns, to about 1000 µm. The lower bound particle size information provided in Figure 18. PSD traces for sludge and saltcake tank waste samples analyzed using three different PSD measurement methods.[54] is similar to the lower bound particle size in Table 8; however, the upper bound particle size in Table 8 (4,000 µm) is approximately four times the size of the upper bound particle size in Figure 18. PSD traces for sludge and saltcake tank waste samples analyzed using three different PSD measurement methods.[54]. The difference can likely be attributed to the fact that design margins are placed on slurry properties used in the development of equipment design specifications like those in Table 8. In cases where values from RPP-RPT-51652, *One System Evaluation of Waste Transferred to the Waste Treatment Plant*[49] are significantly different from the values from (Table 8),[52, 53] the more conservative value, as it applies to the UPE (e.g., smaller particle size), shall be included in the range of values (e.g., upper and lower bound particle sizes) that is used as the basis for a UPE requirement.

Therefore, the UPE transducer(s) shall be capable of detecting the onset of particle settling in slurries with solid particle sizes of 0.2 µm to at least 1,000 µm with the PSDs shown in and Figure 18. PSD traces for sludge and saltcake tank waste samples analyzed using three different PSD measurement methods.[54]**. The UPE transducer(s) shall be capable of the same for slurries with the 4,000 µm value presented in Table 8. Note: Agglomerations of particles are also possible at sizes estimated to be as large as 9,525 µm (see Table 9).**

Table 9. Particle size and density combinations for use in limits of WFD technology calculations.

Particle	Diameter (µm)	Density (g/mL)
Most dense primary particle (Pu)	100	19
Largest primary particle observed by SEM (gibbsite)	200	2.4
Largest Particle hypothetically combined with highest density (Bi_2O_3) in AY-102	1,268	8.9
Agglomerate based on PSD limit (gibbsite)	1,441	1.6
Largest Particle hypothetically combined with highest density (Ag_2O) in AZ-101	1,441	7.14
Largest agglomerate based on pump screen mesh (gibbsite)	9,525*	1.43

Notes: *9,525 µm = ⅜-inch.

The density values for the primary particles in slurries reported in RPP-RPT-51652 range from 1.8 grams/milliliter (g/mL) (aluminum phosphates) to 19 g/mL (plutonium metal). The relative frequences of particle density values based on the number of tanks in which various primary particles have been observed is provided in Figure 19.

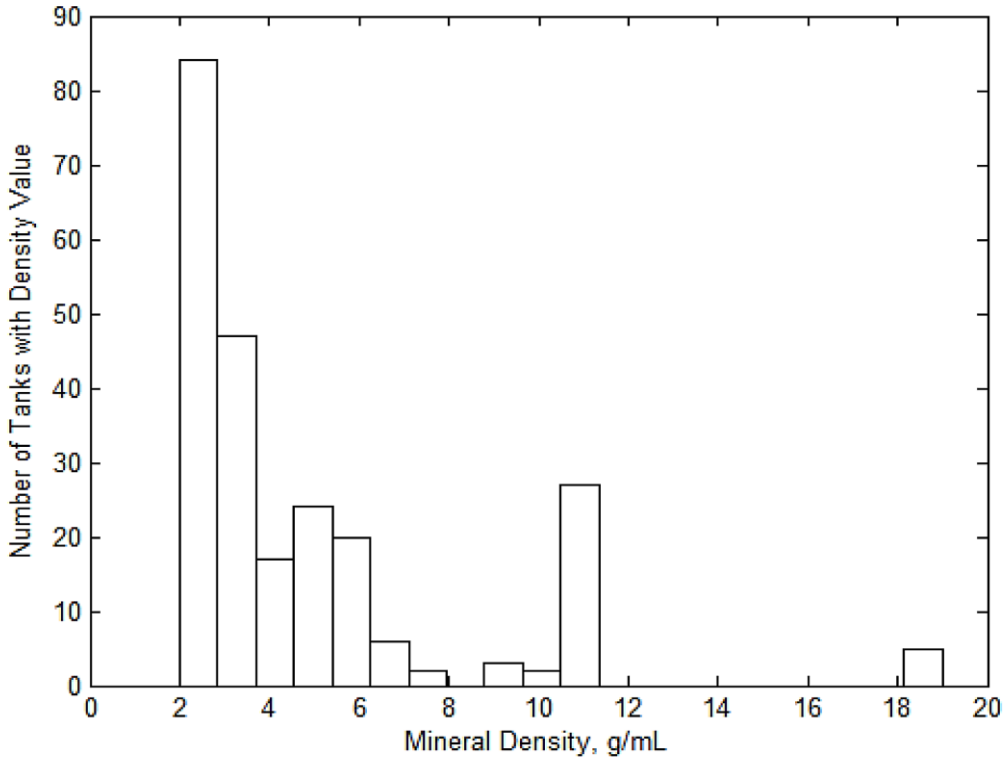

Figure 19. Density histogram of particles with the frequency of a given primary particle with a given density (determined by the number of tanks in which the primary particle was observed).

The densest plutonium metal particles are hypothesized to be as large as 100 µm. The largest undissolved solids waste particle that might hypothetically be transferred in waste feed is 9,525 µm (3/8 in) and would most likely have a density of an agglomerate of gibbsite (1.43 g/mL). Large agglomerates have been found in single-shell tank (SST) heel samples and some large particles will likely be in the HLW feed double-shell tanks (DSTs).

Therefore, the UPE transducer(s) shall be capable of detecting the onset of particle settling in HLW slurries with solid particle densities of 1.8 to 19 g/mL, where the largest size of the highest density particle may only be as large as 100 µm. The UPE transducer(s) shall be capable of the same when agglomerates with densities of 1.43 g/mL (see Table 9) are present in the slurry.

Liquid Waste Density and Viscosity: The available data, models, and model predictions for physical properties of the liquid phase of Hanford tank wastes have also been examined by the Hanford TOC and their subcontractors. Model-predicted values ranged from 1.14 to 1.37 kg/L for liquid density and 2.44 to 8.00 centipoise (cP) for liquid viscosity. Accounting for model uncertainties, the ranges are 1.08–1.47 kg/L for liquid density and 0.80–13.54 cP for liquid viscosity (before end-of-mission activities) of the Baseline Case in ORP-11242 *River Protection Project System Plan, Rev. 6*. The relative frequences of liquid viscosity values is provided in Figure 20Figure 19. Cumulative distribution functions for the lower and upper limits of the 95% confidence interval on liquid viscosities for HLW feed baches is provided in Figure 21.

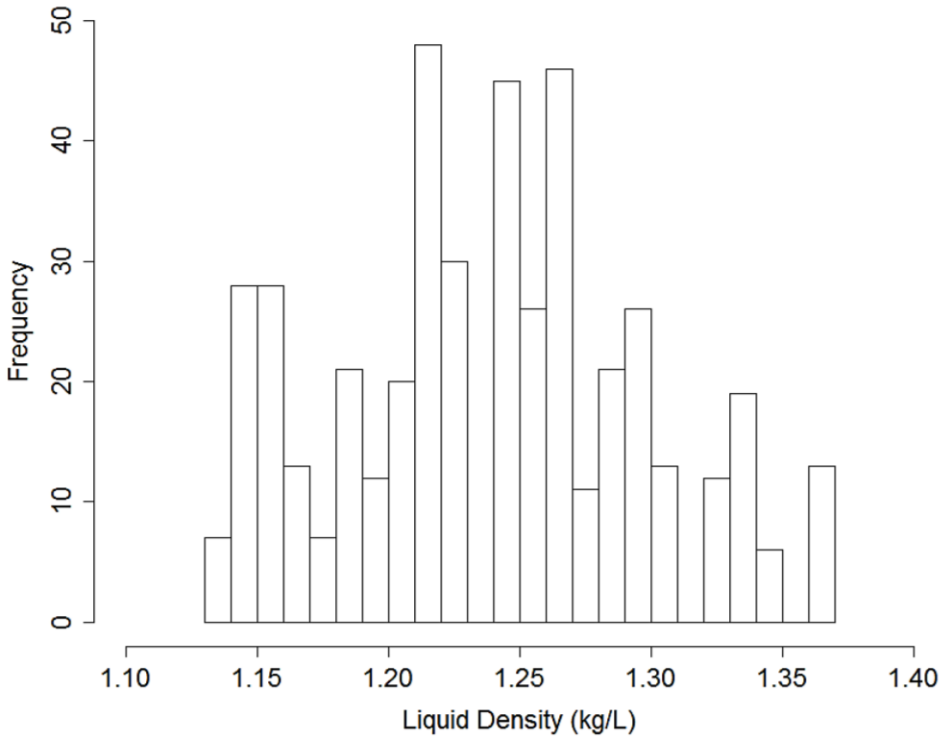

Figure 20. Histogram of model-predicted liquid densities for HLW feed batches (before end-of-mission) for the Baseline Case of *System Plan* Rev. 6.

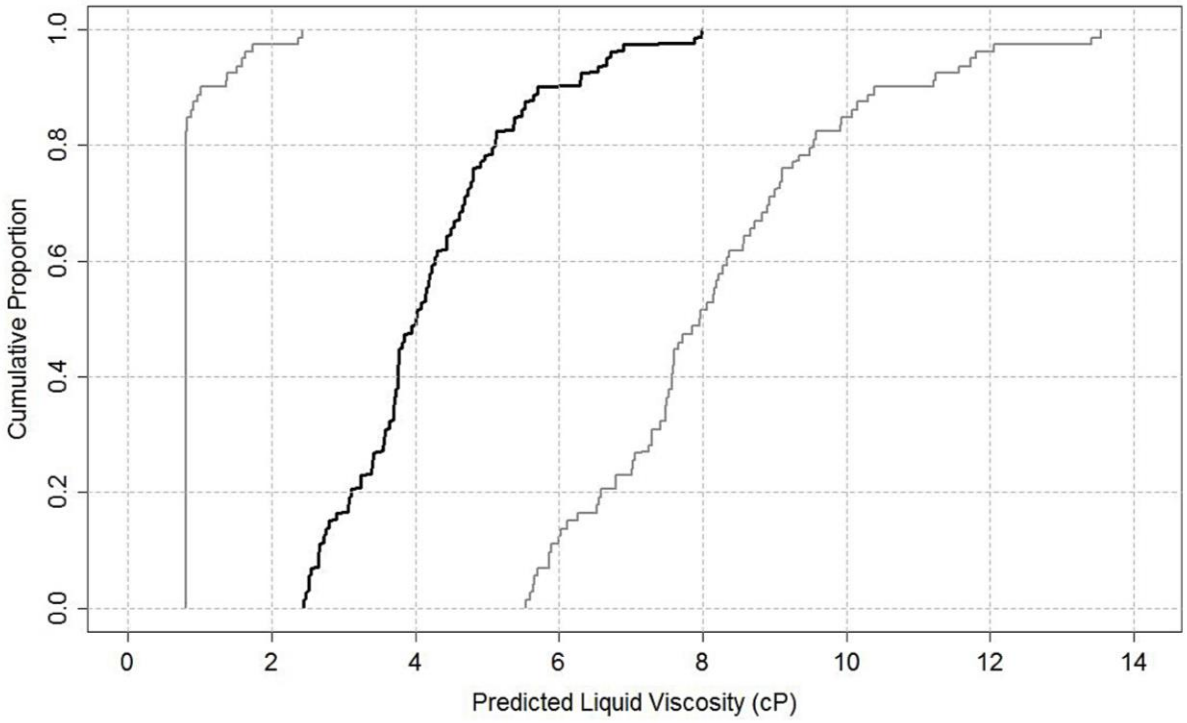

Figure 21. Cumulative distribution functions of predicted liquid viscosities (black line) and lower and upper limits of 95% confidence intervals (gray lines) for HLW feed batches (before end-of-mission) for the Baseline Case in *System Plan* Rev. 6.

Therefore, the UPE transducer(s) shall be capable of detecting the onset of particle settling in HLW slurries with liquid fraction densities as low as 1 kg/L up to at least 1.5 kg/L and liquid viscosities as low as 0.8 cP up to at least 14 cP.

Slurry Solids Concentration: Several tank waste samples have been analyzed to characterize, among other properties, solids concentration. Values of approximately 6, 9, 12, 15, 19, 29, 30, and 37 wt% have been measured, before blending/mixing. The 6 wt% value was for AY-102, which is no longer in service; its waste was transferred to other DST(s). The solids concentrations by weight listed here would result in smaller values for concentrations by volume since particle material densities fall between 1.8 and 19 g/mL. Therefore, the vol% values in Table 8 represent upper bound values, which is logical when they are used to drive design specifications.

Therefore, the UPE transducer(s) shall be capable of detecting the onset of particle settling in HLW slurries with solids concentrations of approximately 9 wt% up to at least 37 wt%.

Transducer Requirements Driven by Slurry Transfer Line Pipe Characteristics: The currently envisioned application space is the Hanford WFD system that will transport liquid/slurry wastes among the six DST farms (AN, AP, AW, AY, AZ, SY) in preparation for transport of batches of the waste out of the DST system as feed to WTP. A simplified representation of the Hanford WFD system is provided in Figure 22. The potential installations point(s) within the WFD in the Hanford tank farms are on the piping of: HLW slurry transfer line(s), DST valve/jumper pit(s), or the piping of the waste feed acceptance flow loop with remote sampler.

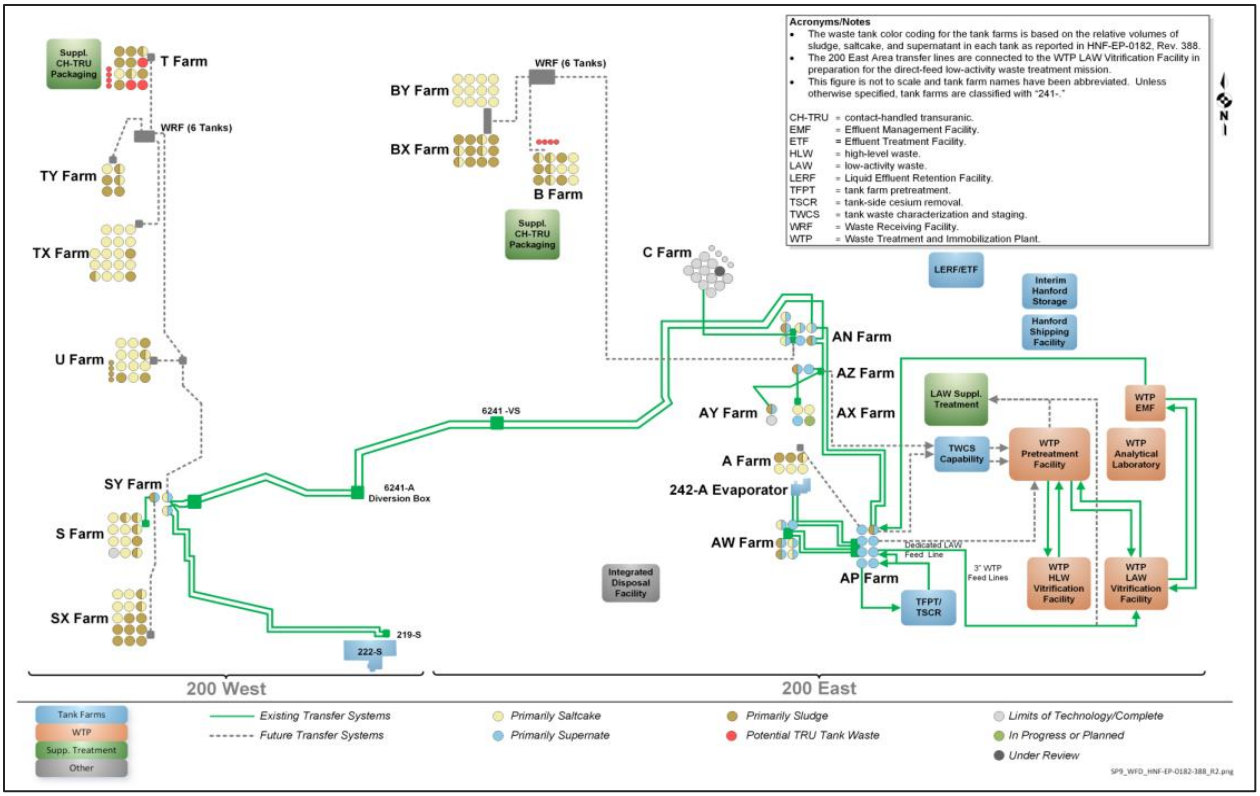

Figure 22. Simplified representation of the Hanford WFD system[55]

Slurry Transfer Line Piping Materials, Diameters, Schedule, and Configurations: All of the 200 Area DSTs generally use buried supernatant and slurry transfer lines to transfer waste from tank farm to tank farm. All the DST transfer lines are of double-wall construction, with the innermost waste-carrying pipe encased within a larger outer pipe that provides the secondary containment barrier. Typically, the supernatant transfer lines are 3 in nominal pipe size (NPS) with 6 in NPS encasements (see Figure 23) and the slurry transfer lines are 2 in NPS with 4 in NPS encasements. The AN, AP, and AW tank farms have transfer lines that are made entirely out of carbon steel with one exception: the supernatant transfer line SN-274 in the AW tank farm uses 304L stainless steel (S/S) for the inner pipe. All the transfer lines within the AY and AZ tank farms are virtually identical to SN-274 with schedule 40 (Sch40), 304L S/S inner pipe and carbon steel encasements. Four refurbished and four new transfer lines with Sch40, 304L S/S inner pipe and carbon steel encasements were installed in the SY tank farm; however, the SL-178 and SL-179 slurry transfer lines are still made entirely out of carbon steel.[49]

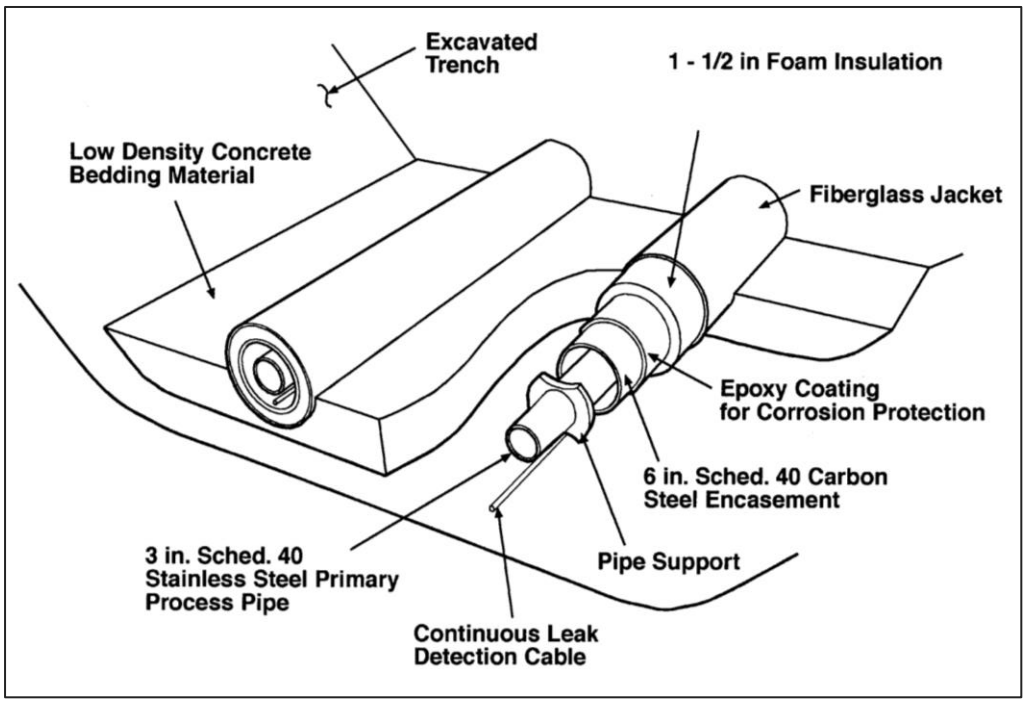

Figure 23. Simplified representation of a pipe-in-pipe waste transfer line in the Hanford WFD system.[52]

Examples can be found in historical documents, including the three transfer lines at WTP, two for HLW and one for LAW, are all 304L S/S, Sch40, 3 in NPS transfer lines with a carbon steel encasement that is 6 in NPS. The outside of the encasement of pipe-in-pipe transfer lines is epoxy coated for corrosion protection and provided with closed-cell insulation and an exterior fiber-reinforced jacket as shown in Figure 23.[52, 56]

Therefore, the UPE transducer(s) shall be capable of detecting the onset of particle settling in HLW slurries in 2 in NPS Sch40 piping that is made of carbon steel piping or 304L S/S. The UPE transducer(s) shall be capable of the same in 3 in NPS Sch40 S/S piping. The UPE transducer(s) shall also be compatible with piping that is of double-wall construction (4 in NPS around 2 in NPS and 6 in NPS around 3 in NPS), with annular pipe supports as shown in Figure 23, and with epoxy/insulation/jacketing on the outside of the outer encasement.

Slurry Transfer Line Piping Pressures: In general, the lowest pressure rated lines (275 pounds per square inch gauge or “psig”) exist within the inter-farm pipelines and higher-pressure-rated lines (400 psig) connect the farms together and to the WTP.[49, 56] The outer containment pipe is currently non-pressurized.[49]

Therefore, UPE transducer(s) shall be capable of detecting the onset of particle settling in HLW slurry piping operating at pressures as low as 275 psig up to at least 400 psig.

Transducer Requirements Driven by Slurry Transfer Line Immediate Operating Environment: Though the UPE system that is matured/modernized under this project will only be installed on a test flow loop under the current project scope, requirements for a field-installed UPE system are taken into consideration during the development/selection of transducer specifications for this project because it is valuable to demonstrate transducer technology that reflects the types/models appropriate for field deployment.

Slurry Transfer Line Piping Temperatures: The assumed temperature of the slurries in Hanford tank farms is 30°C, though tank waste slurries have been characterized at temperatures up to 65 °C, which is the near the maximum allowable waste feed temperature of 66°C at WTP per the Interface Control Document (ICD) limits.[49, 54] However, the operating temperature design specification for DST submersible mixer pumps that will be in direct contact with the waste is 10–88°C.[49] The maximum temperature listed in Table 10 is 200°F (93°C). Even during warm summer months when the ground temperature is at its maximum, the surface temperature of the insulated steel slurry transfer lines should not be greater than the temperature of the slurry inside the transfer line piping.

Therefore, UPE transducer(s) shall be compatible with, and be capable of detecting the onset of particle settling in HLW slurries in, piping at temperatures of up to at least 93°C.

Slurry Transfer Line Radiation Type and Dose Rate: The primary dose-contributing radionuclides presently encountered in many Hanford work environments are cesum-137 (137Cs), which is predominantly in LAW, and strontium-90/yttrium90 (90Sr/90Y) in secular equilibrium, which is predominantly in HLW.[49] These nuclides are most often encountered in tank waste characterization and remediation work, and often in association with large dose rates and dose gradients.[57] Therefore, gamma radiation is the dominant type of radiation from Hanford waste.

The radiation dose rate design specification for transfer piping and DST submersible mixer pumps that will be in direct contact with the waste is 1,000 rads per hour (R/hr).[49, 58] 3D geometries such as pipes and valves tend to selectively shield low-energy beta radiation but not gamma radiation.[57] Therefore, gamma radiation can be expected to be the dominant type of radiation from Hanford waste on the surface of a pipe; however, information on the measured or modeled gamma dose rates at contact on a waste slurry transfer pipe is not publicly available. Documents such as W058-P-041 *Buried Transfer Piping Expected Dose Rates during Transfer* and PRC-STP-00718 Rev. 2 *Preliminary Documented Safety Analysis for the Sludge Treatment Project Engineered Container Retrieval and Transfer System* may contain such information and attempts are being made to obtain copies; however, those copies had yet to be obtained at the time this report was written.

Estimates of contact dose rates by Hanford TOC subject matter experts are up to 300 R/hr. The 300 R/hr dose rate will be used as a placeholder value to support UPE transducer specification development until a design basis document or other document with a stated dose rate at contact with a slurry transfer line is located.

Therefore, UPE transducer(s) shall not degrade from exposure to gamma dose rates of at least 300 R/hr. At a minimum, the transducer(s) shall be tolerant to this dose rate for a period of at least 10 years to avoid the need for higher replacement frequencies that may be deemed impractical by Hanford contractor(s).

Transducer Requirements Driven by Slurry Transfer Line Greater Operating Environment: UPE transducer(s) and cable(s) may be installed in valve/jumper pit boxes and/or in non-climate-controlled Connex style containers within the Hanford WFD system. Cables extending beyond such containers/enclosures will be in conduit. Transducer(s) and cable(s) will not be directly exposed to wind, precipitation, or sunlight; however, they will be exposed to temperatures similar to outdoor temperatures, as well as dust/dirt/sand and moisture from condensation and/or precipitation that enter through small gaps or openings in an enclosure (e.g., vents, door/panel seams, conduit openings). The outside ambient temperature design specification that has been used for DST submersible mixer pumps is -32 to +46°C.[49]

Therefore, UPE transducer(s) and associated signal/power cable(s) shall be able to operate in an environment immediately around the transducer(s) where the air temperature may range from -32 to +46°C at atmospheric pressures. The UPE transducer(s) shall also be able to operate with dust/dirt/sand in the environment. UPE transducer(s) and cable(s) should have Ingress Protection (IP) ratings of at least 52 (see the IP rating chart in Figure 24).

Submersion of UPE transducer(s) in standing water is not expected, nor is the accumulation of ice, snow, or dust/dirt/sand over the transducer(s). The UPE transducers will not be exposed to water jets, scrubbing action, or cleaning/de-icing chemicals. However, incidental bumping/jarring of UPE transducer(s) may occur in the operating environment during installation, maintenance, or replacement of other sensors, materials, or equipment near the transducer(s).

Therefore, UPE transducer(s) and cable(s) shall be physically protected from incidental bumping by workers and impact from small falling objects like tools, if not already in a double-wall spool piece. Buried cable conduit and/or above-grade conduit shall protect the transducer cable(s) from being cut or crushed by workers, machinery, and vehicles.

Figure 24. IP rating chart[59]

6.2.2 UPE Transducer Specification Development

The collective set of transducer requirements described in Section 6.2.1 provided the technical bases for developing the UPE transducer specifications described in this section.

Transducer Specifications Driven by HLW Slurry Physical Properties: The condensed subset of requirements from Section 6.2.1 that pertain to slurry properties are the following.

UPE transducer(s) shall be capable of detecting the onset of particle settling in HLW slurries that:

1. **are Newtonian and non-Newtonian**
2. **have solids concentrations up to at least 30 vol%**
3. **have solids concentrations of approximately 9 wt% up to at least 37 wt%**
4. **contain solid particle sizes of 0.2 µm to at least 1,000 µm with the PSDs shown in Figure 18.** PSD traces for sludge and saltcake tank waste samples analyzed using three different PSD measurement methods.[54]**, and potentially up to 4,000 µm listed in Table 8**
5. **contain particle agglomerations of sizes estimated to be as large as 9,525 µm shown in Table 9**
6. **contain solid particle with material densities of 1.8 to 19 g/mL, where the largest size of the highest density particle may only be as large as 100 µm, and potentially contain agglomerations with material densities of approximately 1.43 g/mL**
7. **have liquid fraction densities as low as 1 kg/L up to at least 1.5 kg/L**
8. **have liquid viscosities as low as 0.8 cP up to at least 14 cP.**

Ultrasonic energy scattering from particles in a slurry underpins the UPE methodology. The UPE methodology and signal analysis algorithm utilize incoherent ultrasonic backscatter energy from an ensemble of sound-scattering particles (“scatterers”) to determine whether particles near the bottom of a pipe are moving or settling.

Scattering converts the energy of a coherent, collimated beam from an ultrasonic transducer into incoherent, divergent waves as a result of wave interaction with inhomogeneities in a material (particle scatterers in slurry). A conceptual illustration of an incident wave scattered by particles is provided in Figure 25.

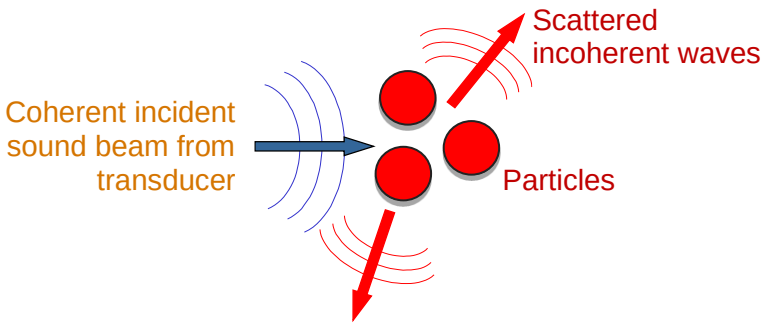

Figure 25. Conceptual illustration of ultrasonic scattering.

The scattered energy is not entirely lost, as a portion of it scattered back in the direction of the incident sound beam and detected by the same ultrasonic transducer used to transmit the coherent beam. The portion of energy returned to the transducer is called “backscatter.” The UPE instrument uses ultrasonic backscatter received by its transducer to assess particle motion in pipes and vessels.

For scattering to arise in a slurry, the following conditions must all be met:

1. Particle scatterers must have **acoustic impedances** different from that of the surrounding fluid in the slurry.
2. A **minimum particle inventory** must also exist in the transducer sound field volume to generate sufficient backscatter for reliable measurements.
3. The **ultrasonic wavenumbers** in the slurries that are on the order of at least a portion of the particle sizes in the slurries for sufficiently strong backscattering to arise and lend the slurry to monitoring by the UPE system.

Acoustic Impedance: Acoustic impedance (Z) is a material property defined as the product of the material’s density ρ and speed of sound value c. Energy reflection or scattering results when a transmitted ultrasonic wave impinges an acoustic impedance interface formed by two adjacent materials (particles and carrier fluid) of dissimilar Z. The fraction of the incident wave intensity reflected at the interface, known as the reflection coefficient R, is calculated by (Equation 6-1), where Z_2 and Z_1 represent the acoustic impedances of the two materials on either side of the interface. Multiplying R by 100 yields the relative percentage of the original energy reflected or scattered. Strong reflections or scattering occur with higher values of R.

$$R = \left(\frac{Z_2 - Z_1}{Z_2 + Z_1}\right)^2 = \left(\frac{\rho_2 c_2 - \rho_1 c_1}{\rho_2 c_2 + \rho_1 c_1}\right)^2 \qquad \text{(Equation 6-1)}$$

The Z values of the solid particles that result when the lower and upper bound particle material density values of 1.8 to 19 g/mL (for aluminum phosphate and plutonium, respectively) are multiplied by the longitudinal speed of sound (cL) values for these materials (approximately 5570 meters per second [m/s] and approximately 2415 m/s, respectively),[60, 61] the resulting Z values are at least four times the Z values of the liquid fraction, which are calculated by multiplying the lower and upper bound liquid density values of 1–1.5 kg/L (1–1.5 g/mL) by their cL values (estimated to be 1500–1700 m/s). Therefore, ultrasonic energy in the slurries will result in an R of at least 60% from particles, which is significant and will allow ultrasonic measurements and, by extension, the UPE transducer(s) to meet SLURRY REQUIREMENTS 6 and 7 on particle density and liquid fraction density.

Minimum Particle Inventory in Transducer Sound Field: The UPE methodology is built on a basic assumption that a slurry contains solid particles, and those particles are present in a sufficient concentration to satisfy a minimum required inventory of particle scatterers in the transducer sound field(s) to support reliable measurements at all slurry flow velocities. The concept of ultrasonic backscatter from particles in a transducer’s sound field propagating in a slurry is illustrated in Figure 26.

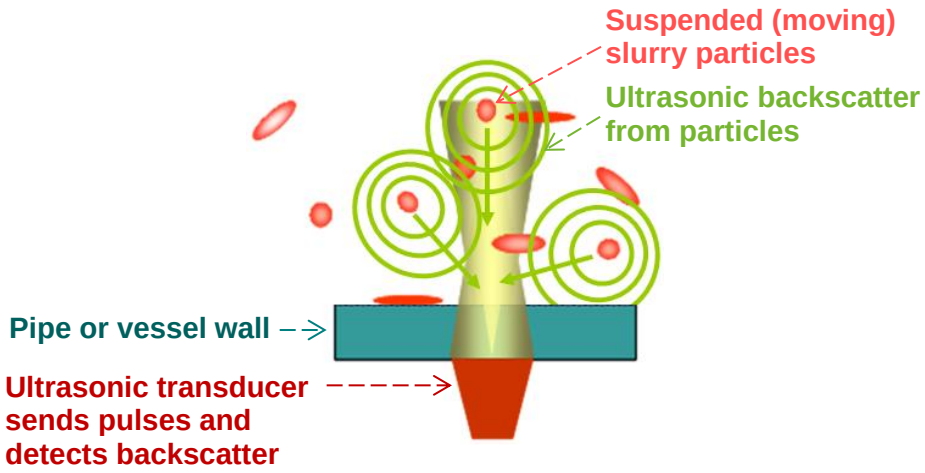

Figure 26. Conceptual illustration of the detection of ultrasonic backscatter from slurry particles by a UPE transducer.

Theoretical models exist to estimate the minimum inventory, which can then be used to calculate minimum particle concentration; however, the outcome of the calculations have more uncertainty than empirical data from testing. Flow loop testing was conducted in 2011 with the first UPE system to quantify the lower bound concentration limits (i.e., the minimum solids concentration that must be present in a slurry to facilitate the UPE methodology). Flow loop testing with slurries that contained glass and S/S particles in water-based, kaolin-based, gibbsite-based, or iron oxide-based carrier fluids showed that 0.02–0.29 vol% of UPE-detectable particle sizes need to be present in a slurry to facilitate the UPE methodology, depending on the carrier fluid attenuation.[43] The detectable particle sizes will be discussed in the next sub-section on ultrasonic wavenumbers.

The expected solids concentration of particles in HLW slurries is at least 9 wt%. Therefore, the UPE transducer(s) can meet SLURRY REQUIREMENT 2 and 3 on solids concentration provided (1) the solids fraction contains a fraction of particle sizes that are detectable by the UPE transducer(s) and (2) the concentration of that detectable fraction is, conservatively, 1 vol% or greater. Higher solids concentrations in slurries generate more scattering and are more conducive to the UPE methodology, so higher concentrations are not a concern.

Ultrasonic Wavenumbers: The scattering strength for wavelength-particle combinations is indicated by the non-dimensional wavenumber ka, which is the ratio of particle radius to ultrasonic wavelength in the slurry. The ka value is calculated using (Equation 6-2.

$$ka = \omega a/c = 2\pi fa/c = 2\pi a/\lambda, \qquad \text{Equation 6-2)}$$

where k is wavenumber ($2\pi/\lambda$), a is particle radius, ω is ultrasonic angular frequency, c is speed of sound, f is ultrasonic frequency, and λ is wavelength.[62,63] A modified version of this equation that substitutes particle diameter d for $2a$ is shown in (Equation 6-3.

$$ka = \pi d/\lambda \qquad \text{Equation 6-3)}$$

Wavelength λ is that which results in the bulk slurry and is calculated using (Equation 6-4. Table 10 provides a summary of the λ sizes relative to a for three different ka regions.

$$\lambda = c/f, \qquad \text{Equation 6-4)}$$

Table 10. A summary of wave propagation regimes defined by particle-wavelength relationships.

***ka* Region**	**λ Region**	**Wave Propagation Regime**
$ka << 1$	$\lambda >> a$	Long-wavelength (Rayleigh scattering)
$ka \sim 1$	$\lambda \sim a$	Intermediate-wavelength (Mie scattering)
$ka >> 1$	$\lambda << a$	Short-wavelength (Geometric scattering)

As a general guide, scattering begins to arise for relatively large ka values in the intermediate-wavelength regime and increases significantly in the short-wavelength regime. The attenuation increases with increasing ka value but obeys a different scaling for each of the three wave propagation regimes. Attenuation initially scales with the square of the frequency in the long-wavelength regime, but as ka increases in this regime, attenuation scales with the square root of the frequency.[64,65] Scattering dominates the other types of interactions in the intermediate-wavelength regime and there is a complicated dependence on frequency and particle size. As the particle size increases relative to the wavelength, the attenuation coefficient increases until it reaches a maximum when $a \sim \lambda$; above this value, the attenuation coefficient decreases, and at high ratios of a to λ it becomes negligible.[66] Finally, attenuation scales with frequency to the fourth power in the short-wavelength regime.[64,65]

This knowledge is sufficient to select one or more appropriate UPE ultrasonic transducer frequencies that give rise to ultrasonic scattering but mitigate the extent of attenuation by scattering and absorption, which reduce the strength of an ultrasonic field from a transducer and limit the range or distance over which it can propagate. This balance is achieved by selecting transducer frequencies that result in ka values that do not far exceed a value of approximately one. This range of ka values corresponds with the intermediate-wavelength regime where $a \sim \lambda$.

UPE transducers are commercially available transducers that are available in incremental nominal/center frequencies, two of which are 5 megahertz (MHz) and 10 MHz. The 5 MHz and 10 MHz transducers have ka values in slurries such that the largest particle sizes from which backscattering occurs to facilitate the UPE methodology are approximately 30 μm at 5 MHz and 15 μm at 10 MHz. The previously mentioned 2011 flow loop testing evaluated these two transducer frequencies. The test results showed that at least 0.07 vol% of 15+ μm solids need to be present to facilitate the UPE methodology for 10 MHz UPE transducer(s) and approximately 0.02 vol% of 30+ μm solids need to be present in a slurry to facilitate the UPE methodology for 5 MHz UPE transducer(s). Highly attenuative carrier fluids like the iron oxide-based slurry require higher vol% concentrations but no more than approximately 0.3 vol%. **It is therefore sufficiently**

conservative to say that at least 1 vol% of UPE-detectable particle sizes should be present in a HLW slurry to facilitate the UPE methodology.

The 10 MHz frequency is the highest practical UPE transducer frequency to use because anything higher is overly attenuated by highly attenuative slurry carrier fluids like iron oxide-based fluids. It is the optimal UPE transducer frequency to use when all or more than, conservatively, 95% of the particles in a slurry are below the 30 µm cut-off particle size for 5 MHz. If, conservatively, at least 1 vol% of the particles in the slurries is expected to be 30+ µm, then 5 MHz is a more optimal frequency since it is less vulnerable to attenuation by the carrier fluid than the 10 MHz. When there is a high degree of uncertainty about the PSDs of slurries, then both frequencies can be used.

A review of the PSDs for sludge samples and saltcake samples in Figure 18. PSD traces for sludge and saltcake tank waste samples analyzed using three different PSD measurement methods.[54] shows that at least some small fraction of each PSD trace includes 15 µm particles, except for the sludge no-flow, unsonicated case. It is assumed the PSD traces for *flowing* (sonicated or unsonicated) are the best representations of the PSDs of slurries *flowing* through a slurry transfer line pipe. Backscatter signals only become stronger with increasing particle size, which is conducive to the UPE methodology. **Therefore, at least a 10 MHz UPE transducer frequency can meet SLURRY REQUIREMENT 4 and 5 on particle size ranges. Both the 5 MHz and 10 MHz transducer frequencies will be included in UPE testing on this project**.

The first UPE system that was tested in 2010–2012 was demonstrated on a range of test slurries that simulated one or more aspects of Hanford HLW slurries, from particle properties and concentrations to carrier fluid rheology, viscosity, and density. The test slurries included Newtonian and non-Newtonian slurries, different viscosities, and different shear strengths. **Therefore, the UPE transducer(s) can meet SLURRY REQUIREMENT 1 and 8 on liquid phase viscosity and Newtonian and non-Newtonian slurries.**

The only transducer specification driven by the slurry properties is: Transducer Operating Frequencies of 10 MHz and 5 MHz; all other specifications are driven by pipe characteristics.

Transducer Specifications Driven by Pipe Characteristics: The condensed subset of requirements from Section 6.2.1 that pertain to pipe characteristics are the following.

UPE transducer(s) shall be compatible with, and be capable of detecting the onset of particle settling in, HLW slurry transfer piping that is:

1. **2 in NPS, Sch40 carbon steel or 304L S/S piping**
2. **3 in NPS, Sch40, 304L stainless steel**
3. **at 275-400 psig**
4. **potentially constructed of double-wall piping (4 in NPS around 2 in NPS, 6 in NPS around 3 in NPS), contains annular pipe supports and has epoxy/insulation/jacketing on the outside of the outer encasement.**

Note: Should configurations change to require Sch80 piping or other major modifications, recalibration of sensors and modification of sensor connections/specifications will be required.

The UPE system requires at least one ultrasonic transducer to be installed on the underside of horizontal piping on the outer surface of the pipe. UPE transducer specifications that must be considered when selecting transducers for installation on piping are:

1. Internal damping/bandwidth to minimize the time duration of the “ring down” signal after the transducer is pulsed so that near-surface resolution is possible at the pipe wall/slurry interface where particle settling occurs.
2. Size and shape, so that they are compatible with access limitations and pipe diameter and so that the insonified region is as small as possible, and therefore as sensitive as possible to the onset of particle settling.
3. Acoustic impedance (Z) matching to the pipe material to maximize energy transfer from the transducer(s) to the pipe.
4. Ultrasonic wave mode generated by the transducer, such that it propagates through pipe *and* the Newtonian and non-Newtonian slurries.
5. Whether it is designed for pulse-echo operation, where the same transducer transmits and receives signals.
6. Number of ultrasonic elements per transducer, so that the backscatter signals from slurry particles are as strong as possible.
7. Ultrasonic element material responsible for the electromechanical conversion of electrical energy to ultrasonic energy and vice versa.

Damping/Bandwidth: The wall thickness of 2 in NPS Sch40 pipe is only 0.154 in. (3.9 mm) and the wall thickness of 3 in NPS Sch40 pipe is only 0.216 in. (5.5 mm). Therefore, the “near surface” resolution of the transducer(s) is very important if the pipe wall/slurry interface is to be monitored for particle settling. Highly damped transducers with bandwidths that are as close to 100% as possible, and that even exceed 100%, have the shortest “ring-down” times and therefore allow near-surface signals to be resolved at the pipe wall/slurry interface. **Therefore, UPE transducers are specified to have bandwidths of 100% (-10/+50%).** Such transducers are referred to as wide-bandwidth or broadband.

Size and Shape: Transducer shape and dimensions are selected so that they are compatible with the installation constraints (access and pipe diameter) and create an insonified area at the pipe wall/slurry interface that is as small as possible. The smaller the insonified area, the more sensitive the transducer(s) are to the onset of particle settling.

Round transducers of the smallest diameters available (e.g., 6.35 mm) are selected instead of square or rectangular transducers because they create insonified “spots” or points at the pipe wall/slurry interface that are slightly smaller than the diameter of the transducer(s). Flat-face transducers are selected instead of curved-face transducers that match the outer radius of the pipe. The primary reason is the use of flat-faced transducer avoids the need for custom-made transducers from specialty manufacturers that may not remain in business for the remainder of the Hanford mission. Round, flat-faced transducers have been commercial-of-the-shelf (COTS) products for decades and will continue to be, making it easier to obtain UPE transducers from multiple commercial vendors in the future.

To maximize the sensitivity of the flat-faced, round UPE transducer(s) to the onset of particle settling in piping, the face(s) of the transducer(s) get centered with the bottommost point(s) along the underside of the pipe (6 o’clock position) so that the direction of the ultrasonic beam(s) are orthogonal to the direction of the pipe/flow. The only contact area between the transducer face

and outer pipe wall would be a thin strip across the face of the transducer unless provisions are made to maximize the contact area and thereby the transfer of ultrasonic energy to the pipe wall. The contact area(s) between the transducer face(s) and the pipe wall get maximized by installing the transducer(s) on small flat areas machined into the pipe wall. The UPE transducer installation approach is satisfied by installing the transducer(s) on a spool piece that is then installed in-line with the system to be monitored.

The smallest COTS round transducers are 0.125 in. (3.18 mm) and 0.250 in. (6.35 mm). **For 2 in NPS Sch40 pipe, the 3.18-mmtransducers have been selected for this project because the transducer spot size needs to be as small as possible to monitor the bottommost point(s) along pipes with such a tight radius of curvature.** The 3.18-mm or 6.35-mm transducers can be used on 3 in NPS Sch40 pipe. **On this project, both diameters will be tested because (1) the 6.35-mm transducers have already been proven effective during 2010–2012 testing and (2) it would be valuable to compare the sensitivity of the two transducer diameters on 3 in NPS Sch40 to ensure the most sensitive/effective one is used in the future.**

An example of UPE transducers installed on the outside surface of the underside of a pipe in a test flow loop in 2012 is provided in Figure 27. The transducers were installed on a spool piece that was then installed in-line with the 3 in NPS Sch40 304L S/S flow loop piping. The UPE spool piece section was made of thick wall 304L S/S tubing so that the minimum required pipe wall thickness (Sch40) would be preserved when small 1 in x 1 in flat areas were machined into the outside surface of the pipe where transducers were installed. The flat areas were used to facilitate installation of flat-face transducers onto the pipe. They also ensured the ultrasonic beam directions were orthogonal to the pipe direction and provided 100% contact between the transducer faces and the pipe wall.

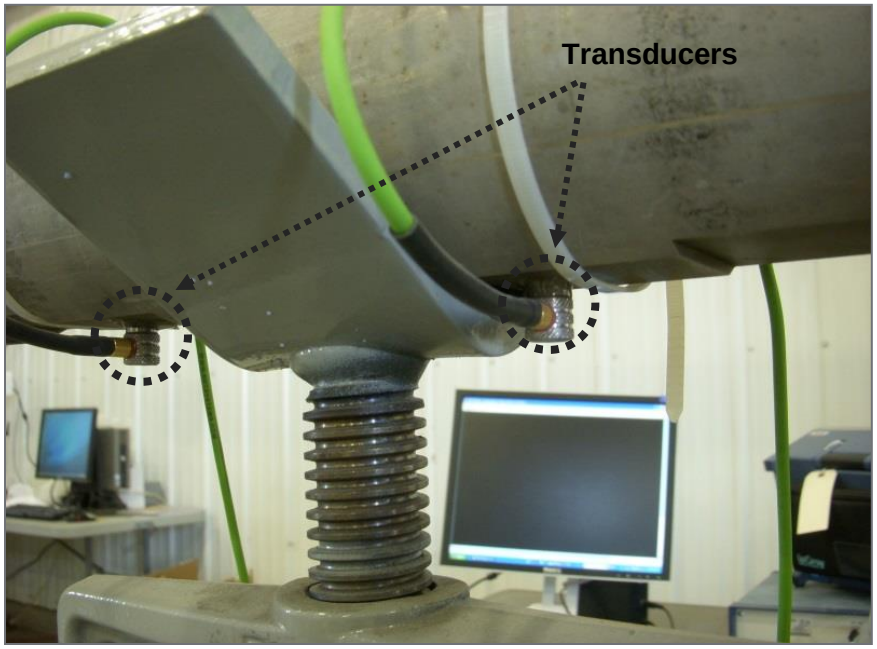

Figure 27. Photograph of 6-mm-dia. UPE ultrasonic transducers installed on the underside of a 3 in dia. S/S pipe spool piece.[44]

Z-matching: All transducers have a protective face to prevent damage to the ultrasonic elements, which are responsible for converting electrical energy to mechanical (ultrasonic) energy and vice

versa. Transducers with face plates that are ¼-wavelength thick and made of a material with a Z value close to that of steel (as opposed to plastic or glass) will be used for this project, which is appropriate for both S/S and carbon steel since they have nearly the same density, speed of sound, and thus Z values.

Ultrasonic Wave Mode: Longitudinal (compression) wave mode transducers designed to propagate through solids and liquids. Shear (transverse) wave mode transducers are available; however, they are only useful for solids and liquids that can support a shear wave; they would not be applicable to non-Newtonian fluids, which some HLW slurries may be. **Therefore, longitudinal mode transducers will be used for this project.**

Operating Mode and Number of Elements: Single-element ultrasonic transducers designed for pulse-echo operation are specified for UPE systems. Dual-element transducers, where one element transmits and the other receives, have been tested in the past to determine if the ring-down signals inherent to single-element transducers could be eliminated while preserving sensitivity to backscatter signals from particles. The test results showed single-element transducers were superior to dual-element transducers in terms of sensitivity. **Therefore, single-element transducers will be used for this project.**

Ultrasonic Element Material: Transducer elements for the generation and detection of ultrasonic energy from electrical energy can be piezoelectric or electromagnetic/magnetostrictive. Electromagnetic/magnetostrictive elements rarely require couplants/bonding agents but have a low electromechanical conversion efficiency and are only compatible with ferromagnetic materials. Piezoelectric elements are over 90% efficient at electromechanical conversion, are compatible with all solid materials, regardless of ferroelectricity. **Therefore, piezoelectric materials, specifically piezoceramics, will be used as the ultrasonic element material for UPE transducers on this project.**

The condensed set of transducer specifications *driven by the pipe characteristics* are:

1. Ultrasonic bandwidth of 100% (-10/+50%).
2. 3.18-mm to 6.35-mm transducers.
3. Transducer face plates that are ¼-wavelength thick and aluminum oxide (Z-matched for steel).
4. Ultrasonic longitudinal (compression) wave mode.
5. Single ultrasonic element designed for the pulse-echo operating mode.
6. Ultrasonic piezoelectric element material.

During 2010–2012 UPE system performance testing on 3 in NPS, Sch40, 304L S/S piping utilized COTS 6.25-mm, single-element ultrasonic piezoelectric contact transducers that generated longitudinal/compression waves, had face plates Z-matched for steel, and had bandwidths that were close to 100%. **Therefore, PIPING REQUIREMENT 2 related to compatibility with, and detecting particle settling in, 3 in NPS Sch40 S/S piping can be met.**

However, the compatibility of UPE transducer(s) with, and ability to detect particle setting in, 2 in NPS Sch40 piping has not been demonstrated. **Therefore, it is not yet known if PIPING REQUIREMENT 1 can be met. An objective of this project is to demonstrate whether UPE transducer(s) can meet detect particle settling in 2 in NPS Sch40 304L S/S pipe (i.e., whether PIPING REQUIREMENT 1 can be met, during testing on the PNNL MTEL).** A stretch goal is to demonstrate the UPE transducer(s) on 3 in NPS 304L S/S piping again, especially if

slurry simulants that will be used during testing on this project are different from those used during testing in 2010–2012. The difference in ultrasonic properties between S/S and carbon steel are inconsequential to the ultrasonic transducers and their measurements. Therefore, there is no need to demonstrate UPE functionality on both carbon steel and 304L S/S piping; demonstration on one of the materials (304L S/S) in the PNNL MTEL will be sufficient to represent performance for both materials.

The ultrasonic velocity through water, the base liquid for HLW slurries, changes as a function of temperature and pressure. The sound velocity sharply increases in the range of 275–400 psig. The net effect would be beneficial as it would increase the amount of ultrasonic energy transferred into the slurry. The Z of the slurry will increase with increasing pressure so that it is more closely matched to that of steel, which lowers R at the pipe wall/slurry interface, allowing a larger fraction of energy to pass from the pipe wall to the slurry and vice versa. The attenuation and speed of sound of a liquid do not change with increasing pressure and, therefore, nor does its acoustic impedance. **Therefore, PIPING REQUIREMENT 3 related to slurry pressure can be met by the UPE transducer(s).**

Double-wall spool piece construction has not yet been tested with UPE transducers, though transducer function or performance would not be affected by an outer encasement. The transducer(s) would be mounted on the primary pipe and surrounded by air in the annulus, just as it would on a single-wall spool piece. The 3.18-mm and 6.25-mm UPE transducer(s) have maximum heights of 14 mm and are equipped with side-mounted connectors for signal/power cables, so the connectors would not add to the 14-mm transducer heights. A 2 in NPS Sch40 pipe in a 4 in NPS Sch40 pipe encasement has a 21.0-mm-wide annular gap while a 3 in NPS Sch40 pipe in a 6 in NPS Sch40 encasement has a 32.6-mm-wide gap. The UPE transducer(s) would easily fit in the annular gap of a double-wall pipe in the Hanford WFD system. **Therefore, UPE transducers would meet PIPING REQUIRMENT 4 related to double-wall construction.**

However, for the ease of UPE transducer access during testing on this project, single-wall pipe construction will be used in the spool pieces installed in the MTEL at PNNL. Fixtures may be added around the transducer(s) to aid in transducer centering during installation; provide protection from impact/bumping by staff working near the spool piece(s); and provide strain relief for the transducer signal/power cables.

Whether UPE spool piece(s) would be required to have double-wall construction in the Hanford WFD may depend on where the spool piece(s) would be installed and whether the Hanford TOC/WTP safety engineers require it. If double-wall construction is required, then one or more cable feed-through ports in the outer encasement of each UPE spool piece will be required. Each UPE spool piece may also need to be equipped with its own leak detection system as the UPE spool piece(s) would be isolated from the rest of the piping of the line being monitored.

Transducer Specifications Driven by Slurry Transfer Line Immediate Operating Environment: The condensed subset of requirements from Section 6.2.1 that pertain to the immediate operating environment around a slurry transfer line are the following.

UPE transducer(s) shall:

1. **be compatible with, and be capable of detecting the onset of particle settling in HLW slurries in piping, at temperatures of up to at least 93°C, and**
2. **not degrade from exposure to gamma dose rates of at least 300 R/hr for a period of at least 10 years.**

Piezoelectric materials are rated for temperatures that are conservatively half the Curie temperature of the material (approximately 300°C). However, the coefficients of thermal expansion of the other materials used in the construction of transducers dictate the overall temperature rating of a transducer. The COTS UPE transducers are rated for continuous use on materials up to 50°C. Use at higher temperatures is permitted per the manufacturers, but only for 10 seconds at a time with a 1-minute cool time in between. The use of a “delay line” or “buffer rod” between the transducer and pipe is also required.

The use of extra materials between the UPE transducer(s) and pipe would introduce extra material interfaces and therefore energy reflections that would reduce the overall energy that can enter the pipe for slurry monitoring. Using a thicker wall primary pipe in the UPE spool piece(s) would be preferred over the use of delay line(s) or buffer rod(s). PNNL will continue to work with the Hanford contractor(s) with the TOC or WTP to understand the top-end of the expected temperature ranges of the HLW slurries once the location(s) for UPE spool installation have been identified to determine (1) whether the temperature will exceed 50°C and (2) if so, how to design the internal steel pipe/tube of the UPE spool piece(s) such that the temperature at the transducer is managed at 50°C or lower. **Therefore, the UPE transducers may meet IMMEDIATE ENVIRONMENT REQUIRMENT 1 related to temperature; however, more information on the temperature of the would-be installation location(s) is needed before a final determination can be made.** PNNL may opt to include the use of a UPE spool piece primary pipe wall thickness that would reduce the temperature of the transducer(s) to 50°C or lower if the slurry was 93°C.

The dose limit of conventional ultrasonic contact transducers, which the UPE transducers are, is 1–2 megagray (MGy), where 1 MGy = 100,000,000 rad.[67] At a dose rate of 300 R/hr, continuously, **the UPE transducers would be able to safely meet IMMEDIATE ENVIRONMENT REQUIREMENT 2 related to dose rate and minimum lifetime at that dose rate.**

However, a very thin (<< 1 mm thick) bonding agent needs to be applied between each UPE transducer face and the outer surface of the spool piece to serve as an ultrasonic couplant that (1) displaces all air gaps at the transducer/pipe interface(s) that may be caused by pipe surface texture/roughness and (2) maximizes the transmission of ultrasonic energy into and out of the pipe. Basic non-radiation-resistant epoxy was used to bond/secure the UPE transducers to the spool piece flat areas during 2010–2012 testing (e.g., the example shown in Figure 27) since the flow loops used were non-nuclear test platforms and each test campaign lasted less than a year.

A radiation-resistant epoxy that is chemically compatible with carbon steel and S/S will be explored when the UPE transducer(s) are bonded to spool pieces integrated with the MTEL loop at PNNL during testing on this project. The same epoxy that was applied to the outside of transfer piping encasements in the Hanford WFD system to provide corrosion protection will be considered for UPE transducer bonding since the epoxy has already been accepted for chemical/corrosion compatibility for field use. Assuming it is available and not overly attenuative, it may be the most practical way to avoid chemical/corrosion compatibility studies of other epoxies.

Finally, transducer signal/power cables will be selected that are compatible with the transducers that are either radiation tolerant or can be placed in conduit that shields the cables.

Transducer Specifications Driven by Slurry Transfer Line Greater Operating Environment: The condensed subset of requirements from Section 6.2.1 that pertain to the greater operating environment around a slurry transfer line are the following.

UPE transducer(s) and associated signal/power cable(s) shall:

1. **be able to operate in an environment immediately around the transducer(s) where the air temperature may range from -32 to +46°C at atmospheric pressures**
2. **be able to operate with dust/dirt/sand in the environment**
3. **have IP ratings of at least 52**
4. **be physically protected from incidental bumping by workers and impact form small falling objects like tools, if not already in a double-wall spool piece**
5. **have buried cable conduit and/or above-grate conduit to protect the transducer cable(s) from being cut or crushed by workers, machinery, and vehicles.**

The UPE transducers are designed for use in rugged industrial environments with dust/dirt and for use with liquid couplants. **Therefore, the UPE transducer(s) can meet GREATER OPERATING ENVIRONMENT REQUIREMENTS 1–3.**

If UPE spool piece(s) are required to have double-wall construction, then greater environment requirement 4 would be satisfied. Otherwise, a protective fixture will be designed and installed over each UPE transducer to protect it from bumping/impact. **Therefore, the UPE transducer(s) would be able to meet GREATER OPERATING ENVIRONMENT REQUIREMENT 4.**

The UPE transducer(s) can be used with long, low-attenuation coaxial signal/power cables to render them compatible with long-distance cables. The cable(s) would be placed inside above-grade and/or buried conduit that is strong enough to avoid cable crushing under the weight of staff and vehicles. **Therefore, the UPE transducer(s) would be able to meet GREATER OPERATING ENVIRONMENT REQUIREMENT 5.**

6.2.3 UPE Transducers and Bench-scale Functional Tests

The full set of transducer specifications that were developed in Section 6.2.2 and driven by the requirements in Section 6.2.1 are:

- Transducer Operating Frequencies: 10 MHz and 5 MHz.
- Ultrasonic bandwidth of 100% (-10/+50%).
- 3.18-mm to 6.35-mm transducers.
- Transducer face plates that are ¼-wavelength thick and aluminum oxide (Z-matched for steel).
- Ultrasonic longitudinal (compression) wave mode.
- Single ultrasonic element designed for the pulse-echo operating mode.
- Ultrasonic piezoelectric element material.

Transducers of these specifications were ordered/used for the project and their functionality was demonstrated during bench-scale testing in February 2025. Transducer suppliers were NDT Systems and Evident Scientific. Photos of the 5-MHz UPE transducer(s) on a mock test liquid during bench-scale functional testing are shown in Figure 28.

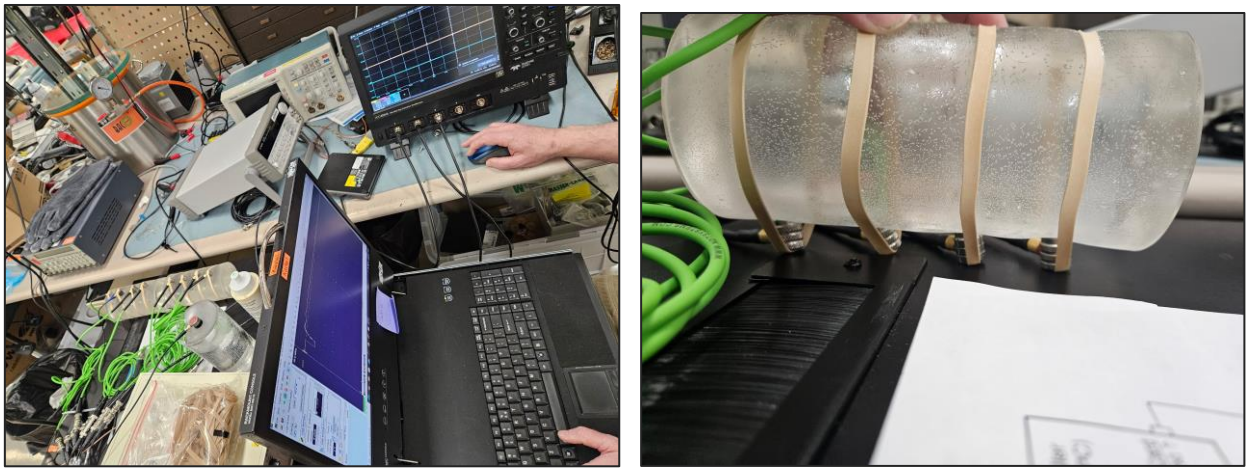

Figure 28. Photograph of UPE transducers during bench-scale testing in February 2025. Left: Multiple UPE transducers (with green cables) on mock slurries. Right: Close-up of 6.35-mm-dia. UPE ultrasonic transducers on the underside of a 3” dia. mock test liquid (gel matrix).

A short-duration, high-energy, “spike” pulser/receiver unit is used as part of the UPE DAS to pulse the UPE transducers, detect the backscattered signals, and amplify and frequency-filter them. The short duration pulse supports near-surface resolution at the pipe wall/slurry interface, which is essential for the UPE methodology. Low-time jitter from the digitizer is also essential for the UPE methodology. Low-jitter signals were obtained when the new DAS electronics were connected during bench-scale testing. A set of 177 individual time-series signals were collected and co-plotted to demonstrate signal stability. The results are provided in Figure 29.

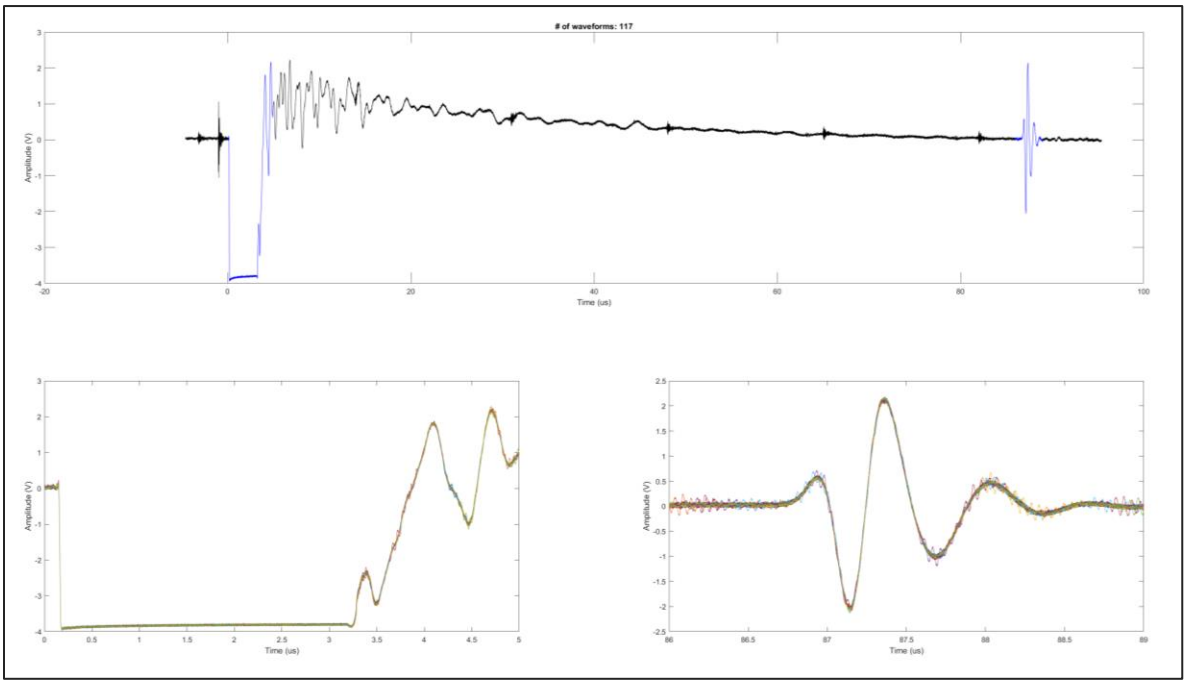

Figure 29. A set of 177 signals from a UPE transducer that were digitized, saved, and co-plotted to demonstrate low-jitter stable time-series signals. Top panel: 100

microsecond long signals. Bottom-left panel: Zoomed-in signal detail at 0–5 microseconds. Bottom-right: Zoomed in signal detail from 86–89 microseconds.

Ultrasonic signals from a 5-MHz UPE transducer that were successfully generated by the pulser/receiver and transducer, which were digitized and displayed on the monitor of the UPE DAS, is provided in Figure 30.

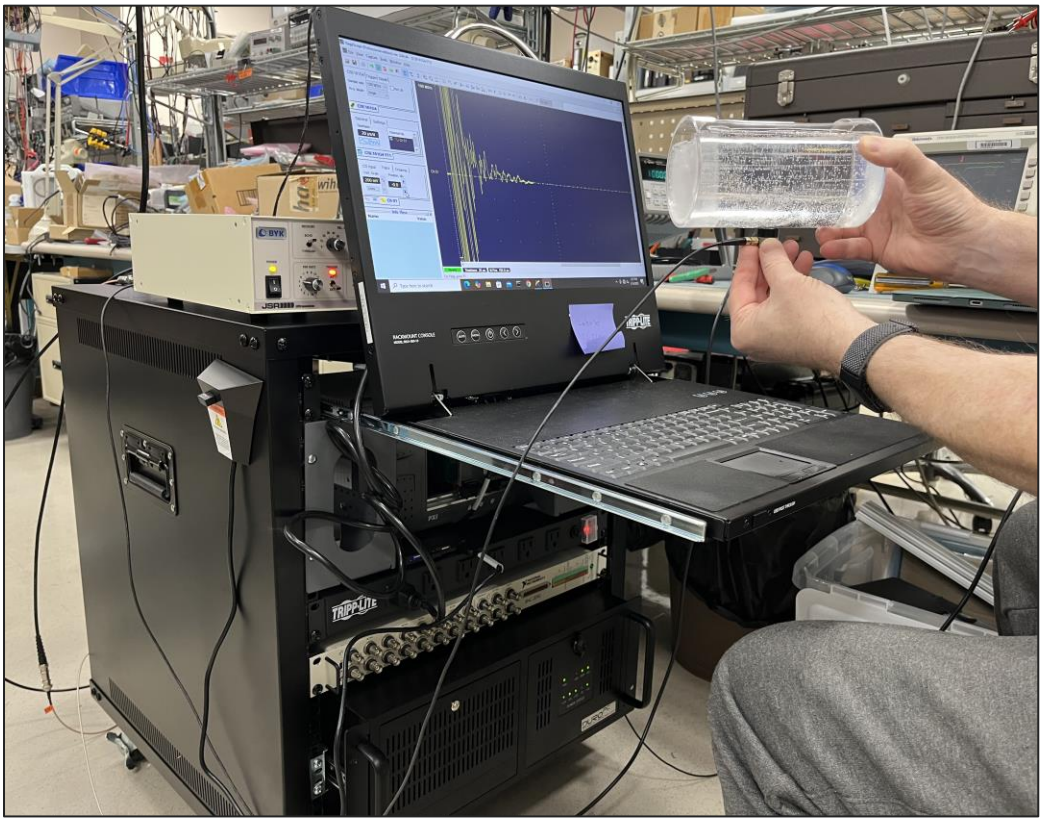

Figure 30. Photograph of a UPE transducer signals displayed on the UPE DAS during bench-scale functional testing in February 2025.

The DAS electronics to which the UPE transducers are connected via signal/power cables are responsible for digitization of the analog transducer signals to convert them to digital signals with 500 samples per second greater. The DAS also displays the signals in real-time and will apply the UPE algorithm to distinguish between moving and settled particles in front of the transducers. A connection diagram of the UPE DAS is provided in Figure 31.

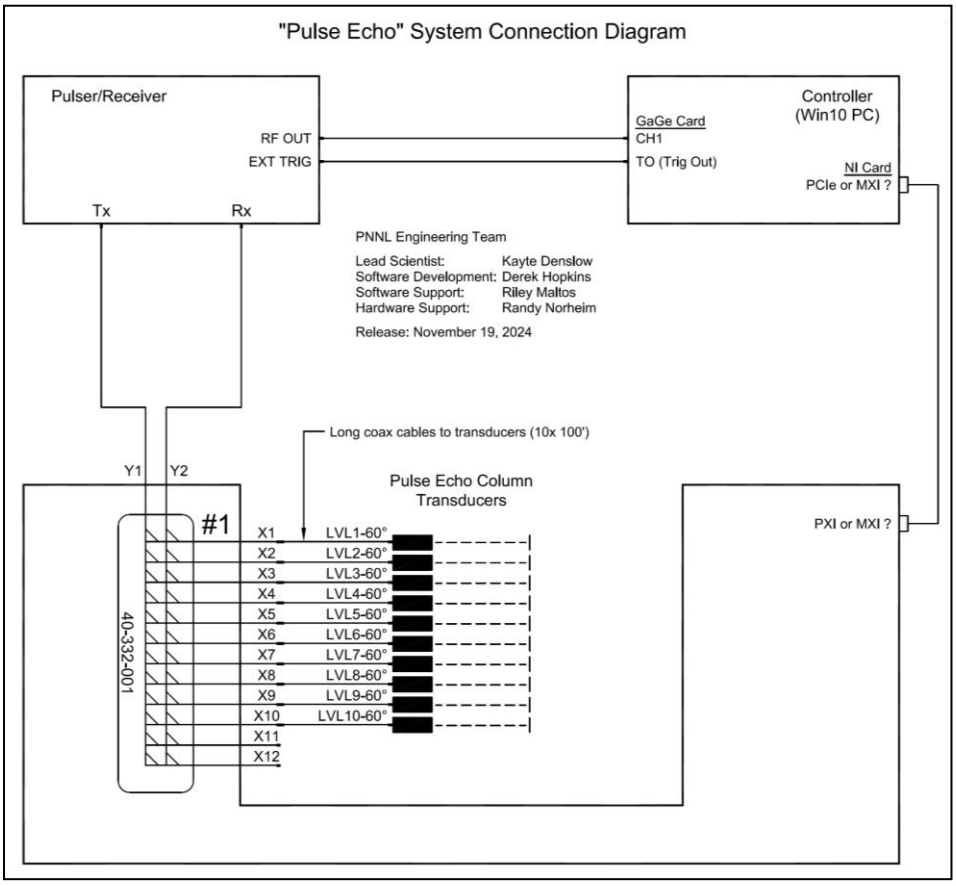

Figure 31. Connection diagram for the UPE DAS shown in Figure 30.

COTS electronics compose the UPE DAS that are either already rated by a Nationally Recognized Testing Laboratory (NRTL) or approved by an electrical authority having jurisdiction (AHJ). The UPE DAS electronics are not outdoor rated. It is assumed that the UPE system electronics to which the transducer(s) interface via cables/connectors will always be indoors in climate-controlled work trailer/portables.

The UPE DAS upgrades that were made in 2024–2025, to improve upon the original prototype UPE system used in 2010–2012 testing, are:

- Digital ultrasonic pulser/receiver instead of an analog pulser/receiver, which will allow software-controlled pulser settings to be sent to each transducer, and software-controlled receiver signal conditioning settings to be applied to each transducer automatically.
- High-speed, high-resolution 16-bit digitizer card that is be more sensitive to signal modulation than the 12-bit card used in 2010–2012 testing.
- The addition of matrix switching cards that allows for data acquisition with up to 10 UPE transducers, which allow a UPE spool piece to be monitored for settling at up to 10 different locations (instead of just one location or manual connection/disconnection between transducers at different locations).

The primary reason to monitor multiple locations along a UPE spool piece is to address uncertainty in where settling will occur first.

Installation Location(s) for Representative Critical Velocity Characterization: Each UPE transducer monitors the slurry passing by a discrete location along a pipe where the transducer is installed. UPE system will report whether settling is occurring or not in front of a transducer regardless of where the transducer is installed along a pipe. It is the user's responsibility to select installation locations along the pipe where flow conditions exist that represent the conditions in the rest of the horizontal piping, or where flow conditions exist where particle settling is a concern. For example, particle settling may not occur just after a pipe elbow, but rather tens of pipe diameters worth of pipe length downstream of an elbow. If only one UPE transducer is installed and the installation location is not one that represents flow conditions/flow velocity in the rest of the piping, then the UPE readings will be misleading even if they are correct. It is customary for engineers to install UPE transducer(s) a distance equal to at least 40 pipe diameters away from a flow disturbance (e.g., pipe elbows or weld protrusions).[38, 39, 44] The UPE spool piece installations in the flow loops shown in Figure 32 are located such that the UPE transducers are 60–70 pipe diameters down from flow disturbances.

CFD modeling has been initiated for 2 in piping to support the selection of transducer installation location(s) along the MTEL flow loop that will be used to support testing of the UPE system under this task. See Section 8.0 for details.

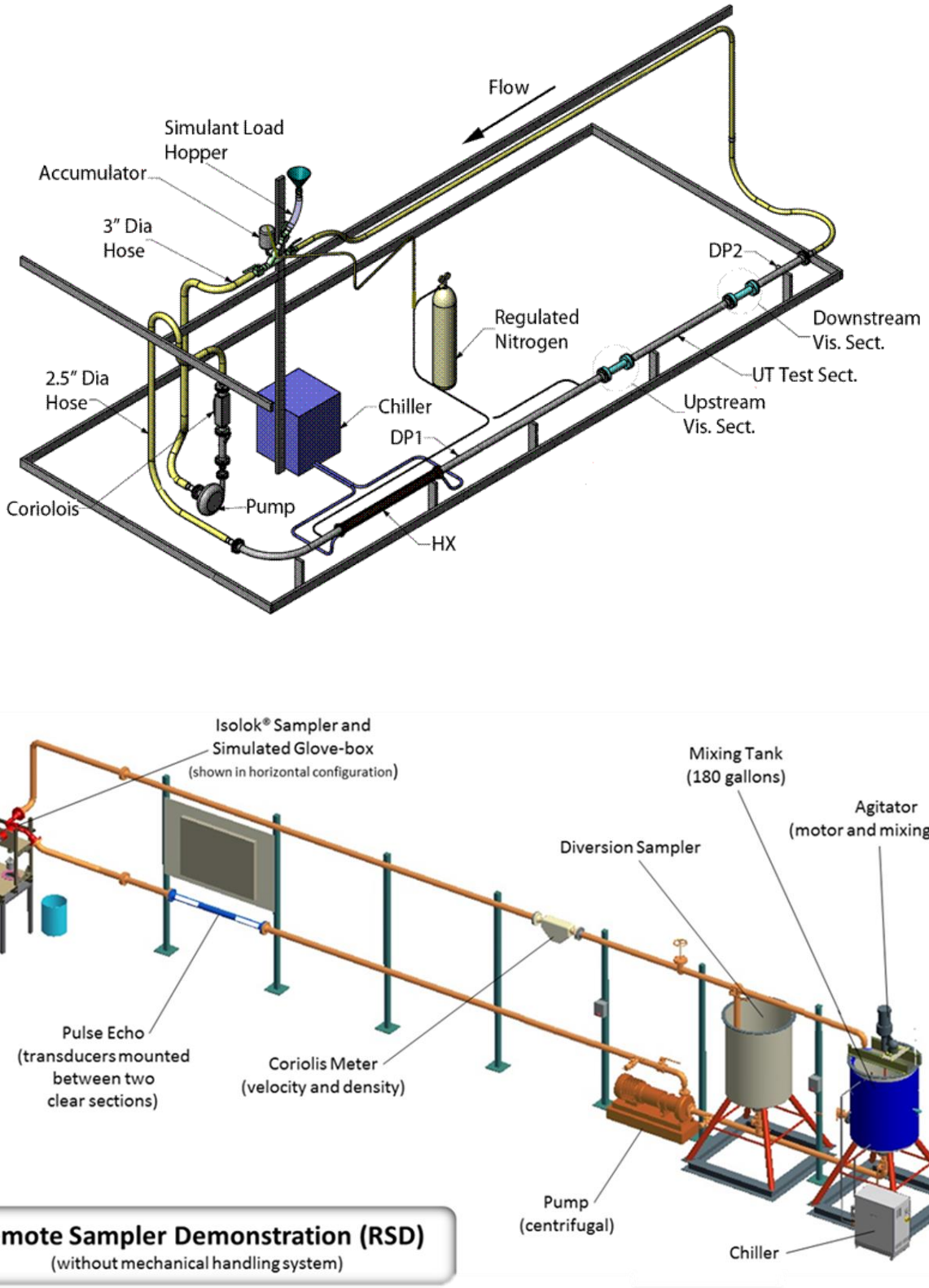

Figure 32. Illustrations of the test flow loops used during UPE test campaigns. Top: MTEL at PNNL (the UPE spool piece is labeled as 'UT Test Sect.' Bottom: Remote Sampler Demonstration (RSD) at Monarch Machine Shop.

6.3 Data Handling and Initial Notes About Connection to User Interface

Data handling between the UPE system and single user interface is being discussed with a general strategy that will allow each controller to communicate with the interface. This can allow for more efficient steps where the data handler can react to new data being ingested and trigger the necessary data processing jobs. Data will be passed using an open-source messaging library. These publishers will be written in Rust and will be customized to interface with the instrument operator's preferred data acquisition method. Initial plans include leveraging a lightweight graphical user interface provided for operators to configure behavior at the beginning of their work.

6.4 Next Steps and Opportunities

With the completion of Year 1 tests, the team is prepared to kick off Year 2 testing and calibration. Tasks will include spool piece fabrication, test matrix design, full scale testing on the MTEL system at PNNL, and updating of software/data handling tools. For example, adding a data visualization feature in the UPE software that provides a binary yes/no indication of whether particle setting is occurring at each transducer location.

Because UPE represents a recognized need by various stakeholders to collaborate on other flow sheet maturation goals may be identified and supported as testing allows. These mutually beneficial tests could allow for more thorough testing and operationalizing of the UPE technology while enabling stakeholders to better understand utility and deployability of this technology.

7.0 Progress on Ultrasonic SolidsMeter System for Solids Mass Fraction Measurement

Solids content, or solids mass fraction, within a slurry is also a key piece of information needed by operators to improve efficiency of tank waste staging and treatment. This represents another key area where laboratory analysis is difficult to apply, as it may be difficult to collect representative samples at various process points.

Ultrasonics is a promising technology that could be applied on-line and in real-time to measure solids mass fraction. These sensors have been applied to solids content measurements in other contexts, but application to tank waste slurries with highly variable solids properties and contents will be a key step forward for the technology. Much of the hardware can be procured COTS and has been previously demonstrated to be robust to field deployments. Project focus here will be on optimizing the data analysis tools to support measurements with low uncertainties.

This section will focus on outlining the specifications and initial testing of sensors and hardware that will be used to complete solids mass fraction measurements in the on-line monitoring platform.

7.1 SolidsMeter Ultrasonic Transducer Specifications and Bench-scale Functional Tests

The same transducer specifications in Section 6.2.3 that apply to the ultrasonic transducers for the UPE system apply to the ultrasonic transducers for the SolidsMeter system since the same slurry, piping, and environmental requirements need to be met by the transducers used in both systems. Therefore, the same types/models of transducers used for the UPE system are used for the SolidsMeter system.

The SolidsMeter DAS is also similar to the UPE DAS since an ultrasonic pulser-receiver, digitizer card, and matrix switching cards are required. The same models of transducers, digitizer card, computer, and matrix switching cards were used in the SoildsMeter DAS as were used in the UPE DAS. Consequently, the main SolidsMeter DAS looks identical to the UPE DAS (see Figure 33).

Figure 33. Photo of the UPE SolidsMeter DAS next to the UPE DAS.

The primary differences in the SolidsMeter DAS relative to the UPE DAS are (1) the use of pairs of ultrasonic transducers that operate in through-transmission (pitch-catch) mode to perform ultrasonic velocity, attenuation, and backscatter measurements across a pipe diameter, as opposed to single transducers that operate in pulse-echo mode to monitor the pipe wall/slurry interface; and (2) the use of an ultrasonic pulser/receiver model that allows for high-energy, long-duration pulsing of the transmitter transducer with either a single-frequency tone-burst or a frequency-swept “chirp” pulse that includes a range of frequencies. Consequently, the SolidsMeter DAS includes (1) two small electronic break-out boxes to split the signals to/from the ultrasonic pulser/receiver unit to the transducer pairs, one pair at a time, which the UPE DAS does not have; and (2) a larger pulser/receiver unit than the one used with the UPE DAS (short-duration, broadband spike pulse). The connection diagram of the SolidsMeter DAS is provided in

Figure 34. The signal splitters are designated as Y1 Box and Y2 Box.

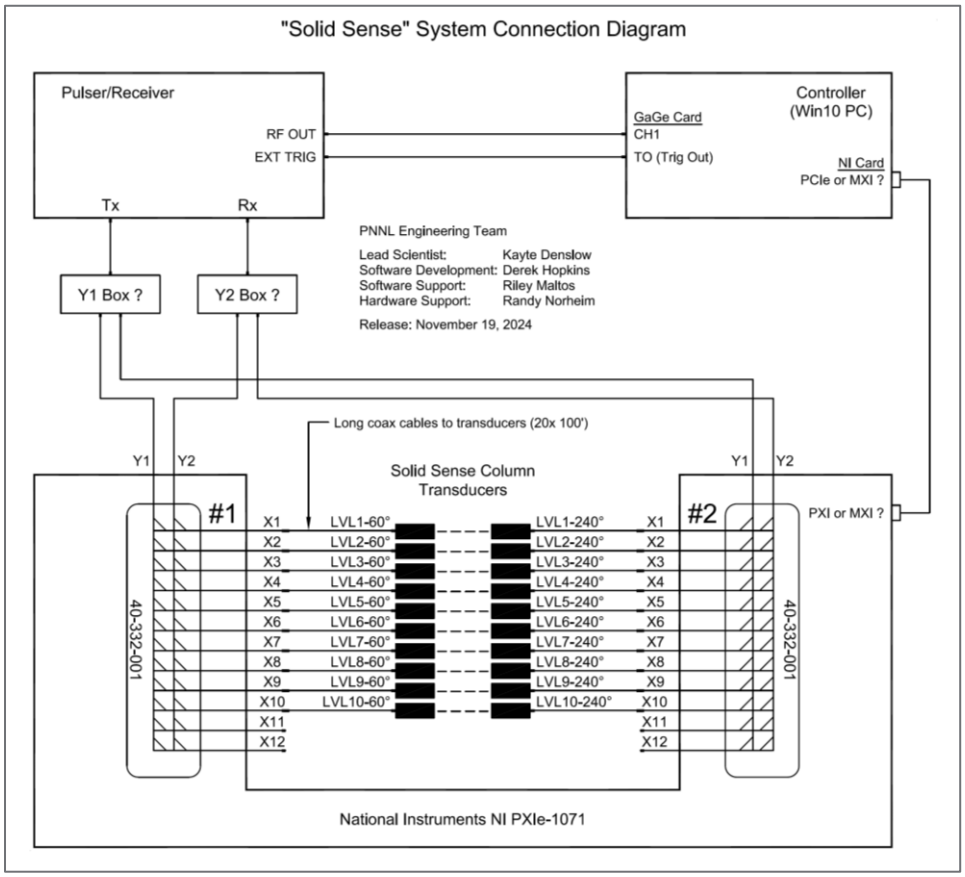

Figure 34. Connection diagram for the UPE SolidsMeter DAS.

Photos of the SolidsMeter DAS during bench-scale functional testing in February 2025 are provided in Figure 35. The more powerful ultrasonic pulser/receiver unit is the blue unit in the photos. The signal splitters are also shown.

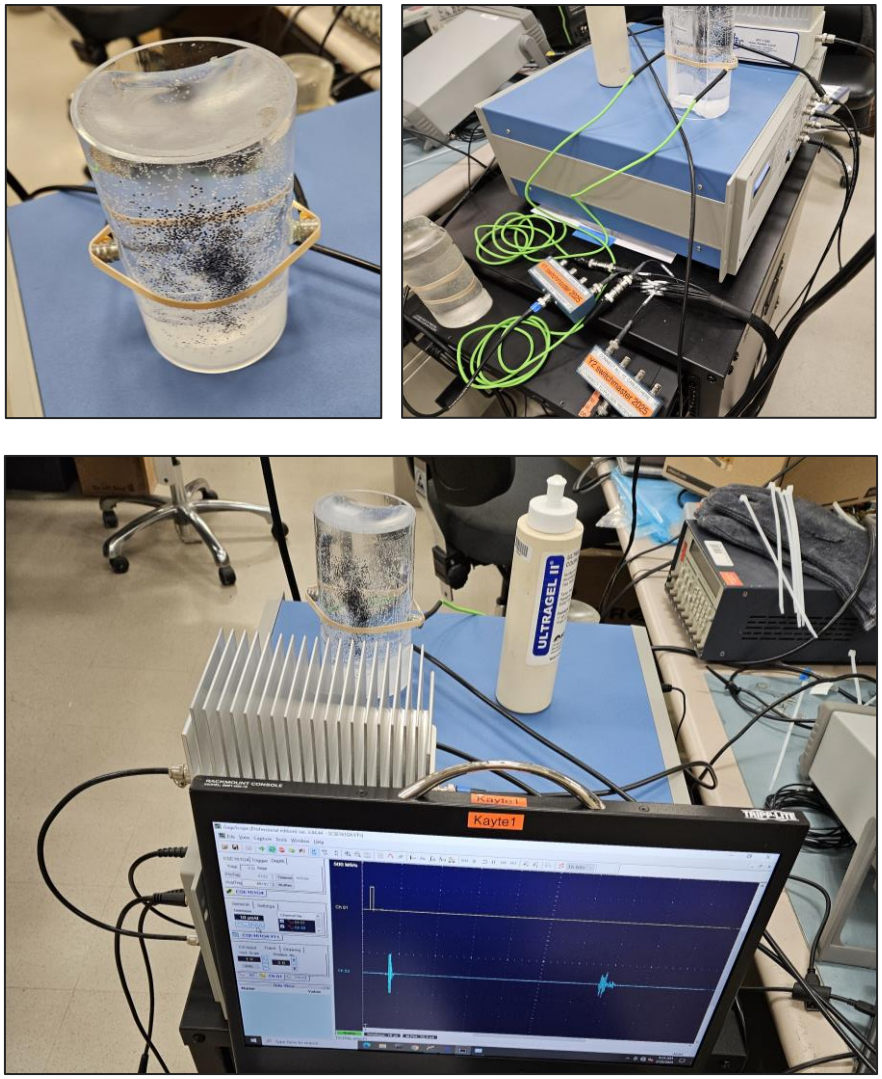

Figure 35. Photographs of the SolidsSense DAS bench-scale functional testing in February 2025. Top-left: A pair of ultrasonic transducers positioned 180 degrees apart on a mock test liquid. Top-right: SolidsMeter DAS featuring the ultrasonic pulser/receiver and signal splitters. Bottom: An ultrasonic signal displayed on the SolidsMeter DAS that passed through the mock test liquid, as transmitted by one transducer and received by the other transducer.

The long-duration, high-energy tone-burst or frequency-swept “chirp” pulses provided by the pulser/receiver unit will be necessary for the SolidsMeter transducers because (1) signals from the transmitter transducers will need to be high enough in amplitude/energy to travel across the full diameter of pipe filled with attenuative slurry and (2) there is a potential need to perform cross-correlation analysis of the pulse signal from the transmitter transducer with the through-transmission signal detected by the receiver transducer, which will require encoded chirp pulses. The long-duration, high-energy tone-burst or chirp pulses are appropriate for the SolidsMeter system because near-surface resolution at the pipe wall/slurry interface is not necessary for solids concentration measurements like for the UPE system. Instead, getting enough ultrasonic energy across the pipe diameter is the priority.

Multiple pairs of different transducer frequencies will be used to measure velocity, attenuation, and backscatter of control test slurries in Year 2 that have varying solids concentrations, PSDs, and other properties such as carrier fluid viscosity and density. The measured ultrasonic signal parameters such as time of flight, amplitude, energy decay rate, and frequency will be used with ground-truth slurry properties to train/calibrate a statistical or Machine Learning model. The reasons to collect ultrasonic velocity, attenuation, and backscatter data with multiple transducer pairs instead of one transducer pair are to (1) obtain confirmatory measurements at a given frequency, and (2) use transducer pairs of different frequencies to measure velocity/attenuation/backscatter at multiple frequencies, as permitted by slurry attenuation, to increase the confidence of the slurry concentration analysis.

The PSDs and other properties for HLW slurries began to be compiled in Year 1 of the project to support calibration slurry test matrix development. Table 11 summarizes the primary reports that are serving as information sources for this knowledge capture activity.

Table 11. A summary of reports that will serve as information sources for HLW slurry properties.

		Particle Physical Properties				Particle Chemical Properties	Physicochemical Properties of Liquids		Rheological Properties of Slurry
		PSDs	*Density*	*Shape*	*wt% UDS*		*Density*	*Viscosity*	
TOC	*SE HLW*	RPP-PLAN-51625, RPP-RPT-51652	RPP-PLAN-51625, RPP-RPT-51652	RPP-RPT-51652	e.g., PNNL-19245	PNNL-20646	RPP-PLAN-51625, RPP-RPT-51652	RPP-PLAN-51625, RPP-RPT-51652	RPP-PLAN-51625, RPP-RPT-51652,PNNL-20646
	HLW	RPP-PLAN-51625, RPP-RPT-51652	RPP-PLAN-51625, RPP-RPT-51652	RPP-RPT-51652	e.g., PNNL-19245	PNNL-20646	RPP-PLAN-51625, RPP-RPT-51652	RPP-PLAN-51625, RPP-RPT-51652	RPP-PLAN-51625, RPP-RPT-51652, PNNL-20646
	West Area	PNNL-20646	PNNL-20646	PNNL-20646	e.g., PNNL-19245	PNNL-20646	PNNL-20646	PNNL-20646	PNNL-20646
WTP	*HLW*	24590-WTP-DB-ENG-18-001	24590-WTP-DB-ENG-18-001		24590-WTP-DB-ENG-18-001	RPP-9805	RPP-9805	RPP-9805	24590-WTP-DB-ENG-18-001
	DFHLW	24590-HLW-ES-TD-24-001, Rev 0, need NDA							

7.2 Data Handling and Initial Notes About Connection to User Interface

Because hardware here is very similar to that used for UPE (Section 6.0), connections to the user interface will be similar, see Section 6.3. Year 1 work included initiating discussions between the user interface development team and the solids mass fraction sensor team to identify the data handling pathways and potential triggers for data analysis. In particular, discussion around supporting data fusion efforts to allow for cumulative solids mass fraction measurements has been initiated. This led to the identification of the need to incorporate a mathematician onto the user interface team to support programming the calculations and accurately completing error propagation.

7.3 Next Steps and Opportunities

Year 1 tests verified procured equipment is functioning and ready to support efforts into Year 2. Similar to the other sensors, tasks will include spool piece fabrication, test matrix design, full scale testing on the MTEL system at PNNL, and updating of software/data handling tools. A key aspect of work will be building machine learning or data science tools to support accurate data analysis.

8.0 Computational Fluid Dynamics Modeling to Support Testing and Integration

The team was able to initiate tasking on the development of fluid dynamics models to support spool piece design and full skid engineering plans. A significant component of work occurring in Year 1 has focused on developing models with sufficient complexity to capture the complex behavior of Hanford slurries. This involved connecting modelers with experts in slurry physical properties as well as subject matter experts in different sensing modalities. Details on model development as applied initially to the UPE spool piece are covered here.

The CFD simulations aid an optimal experimental design by providing understanding of the settling behavior and deposition of suspended solid particles in slurry flow. Transient settling and deposition of the solid particles on the pipeline wall can have a significant impact on the accuracy of the solid mass fraction measurements using optical measurement technique such as Ultrasonic sensor measurement. In this context, CFD simulations can provide the detailed insights such as critical velocity, particle deposition profile, particle concentration at various cross-sections of pipelines. Based on the simulation results, ultrasonic probe can be placed to ensure the accurate measurement. Therefore, multiphase flow simulations are conducted to conduct in STAR-CCM+[68], a robust CFD software extensively used in the many industries to solve complex flow problems. PNNL has enormous high-performance computing facilities, including thousands of cores, which can be used to predict complex phenomena of slurry flow.

The multiphase flow simulations are conducted using Granular-Eulerian Multiphase (EMP) model in STAR-CCM+. Preliminary flow simulations were conducted for Newtonian slurry flow through horizontal pipeline to develop the high-fidelity simulation framework for investigating more complex cases. The horizontal pipe has diameter of 2 in and a length of 10 ft in the initial flow simulations, though final spool piece design may have different dimensions. The computational flow domain was discretized with non-uniform mesh to efficiently capture the flow physics. It is notable that the sharp velocity gradient and particle deposition are to be expected the pipe wall. As a result, prism layer meshing (similar to boundary meshing) was applied to the region proximate to pipe wall (Figure 36Figure 36) to achieve necessary spatial resolution near the pipe wall. Furthermore, the gradient-based polyhedral mesh was used in the remaining part of the pipe where the mesh size increases away from the pipe wall.

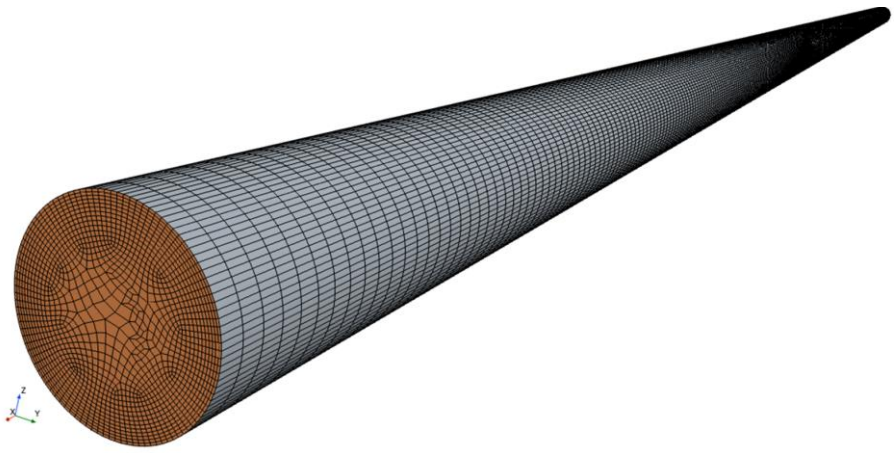

Figure 36: 3-D model of the discretized flow domain. A Prism layer and very fine meshes near the wall were created in region where particle deposition is predicted.

Benchmark cases for turbulent multiphase flow simulations were conducted based on water-sand slurry ($\rho_w = 998\, kg/m^3, \mu_w = 0.9\, mPa \cdot s,$ and $\rho_S = 5{,}000\, kg/m^3$) at various flow rates and sand particle sizes. The volumetric concentration of the sand was fixed at 10%, equivalent to 50% by weight. Figure 37 depicts the longitudinal variation of the volume fraction of the sand particles near the wall at Reynolds number (Re) of 190,000 that corresponds to $3.33\, m/s$ with the 2-inch pipe diameter. As expected, larger particle size gives rise to higher deposition of solid particle on the wall of slurry pipeline. It is evident that slurry has nearly homogeneous distributions of sand particles for the 1–10 micron sizes. With increasing particle size, sand particle begins to deposit on the pipe wall; as particle size increase, the body force due to gravity dominates over other forces acting on the particle imposed by the flow.

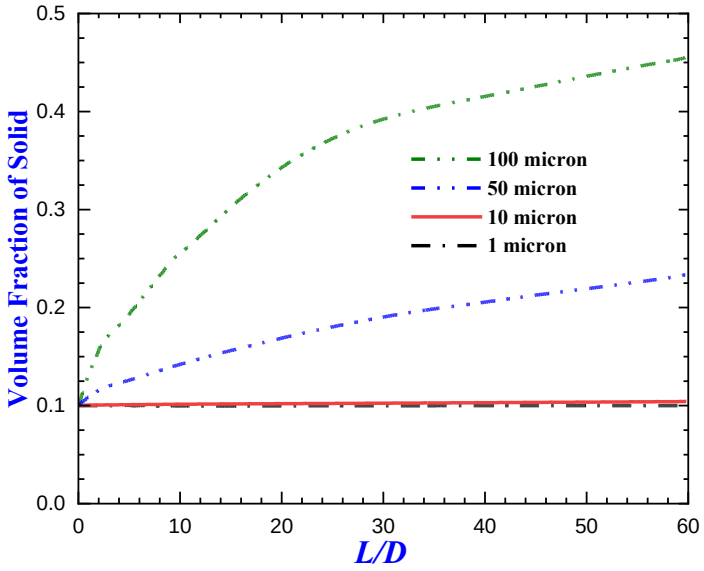

Figure 37: Longitudinal variation in the volume fraction of the sand particles near the wall with different particle sizes at Re=190,000.

This deposition behavior can be further confirmed by investigating the contour plots for volume fraction of the sand at middle and the outlet of pipe in Figure 38. It is evident that 100-micron sand particles have higher concentration at the bottom (i.e. proximate to the wall).

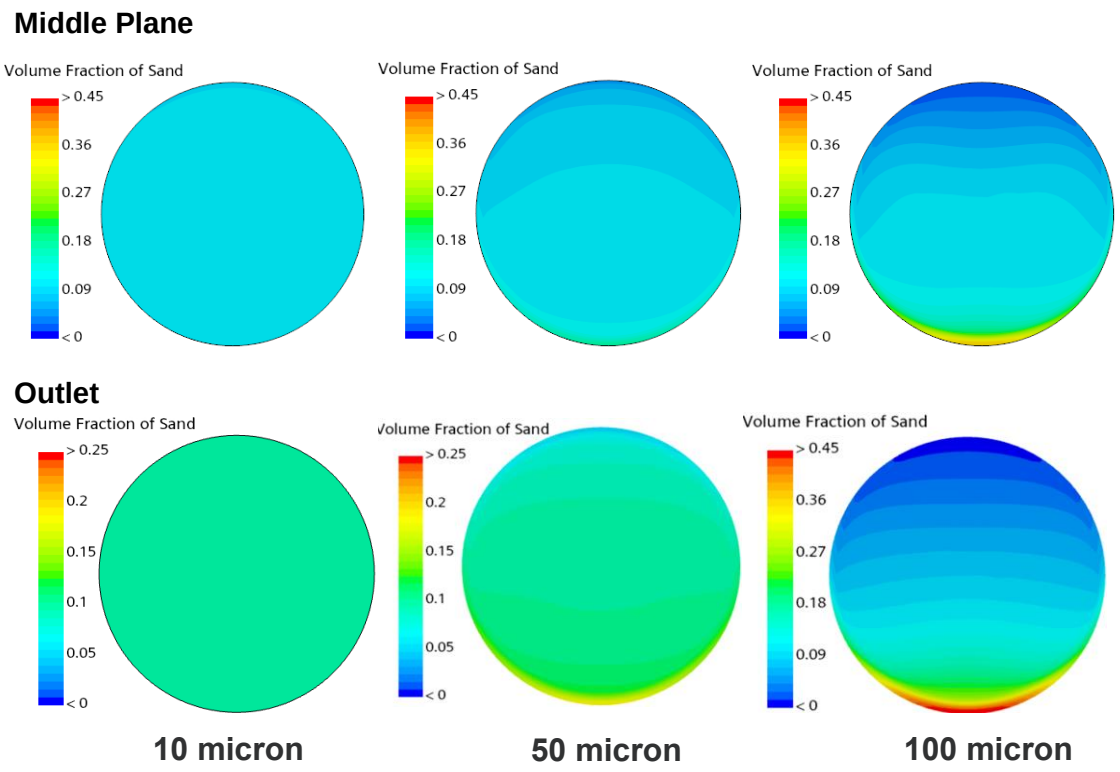

Figure 38: The contours of the volume fraction of the sand particles at the outlet of the pipe confirm the deposition behavior of different particle size.

Next, slurry flows through horizontal pipe were also investigated at two Reynolds numbers, Re=190,000 and 40,000, for larger sand particle (100 micron), representing the two different flow rates ($3.33\,m/s$ and $0.70\,m/s$ respectively with the 2-inch diameter). As expected, the larger deposition of the particle is seen at the lower Reynolds number (40,000) (see Figure 39). Specifically, the sand particles start to deposit shortly after the inlet of the pipe. With increasing Reynolds number, the increased shear force delays the particle deposition.

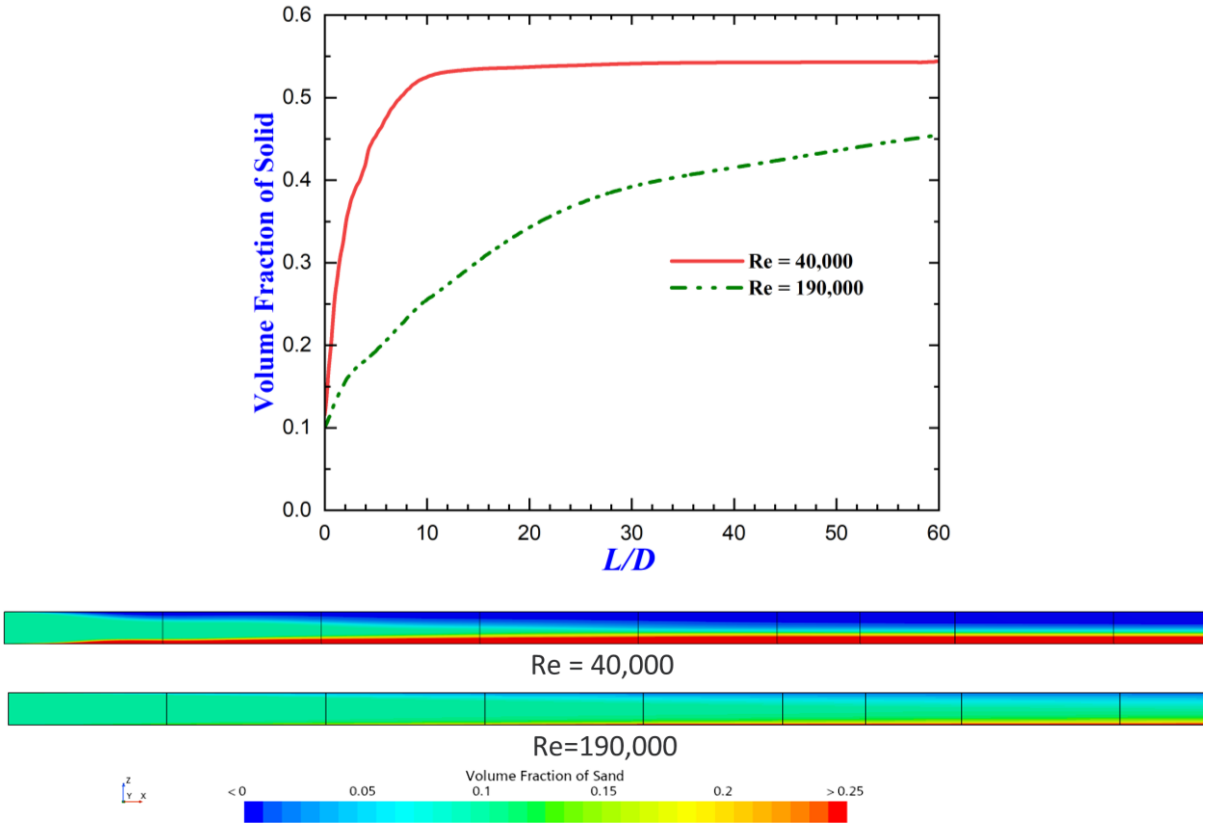

Figure 39: Longitudinal variation in the volume fraction of the sand particles (100 micron) near the wall at two slurry flow rates. The contours of the volume fraction of the sand particle in vertical longitudinal plane confirms the deposition behavior.

8.1 Next Steps and Opportunities

The CFD simulation framework will be extended to include more complex nature to realize relevant cases (e.g., slurries in West Area—see PNNL-20646 by Wells et al.[54]). The simulation will be thus performed for the representative slurries in the horizontal pipe, vertical pipe, and pipeline with elbow bend. In addition to the particle sizes/size distributions and particle densities, rheology of non-Newtonian slurry such as Bingham plastic fluids parameterized by yield stress and plastic viscosity will be implemented to properly simulate representative physicochemical characteristics of the relevant case. The CFD simulations for the non-Newtonian slurry will be validated with benchmark cases or available data in open literature, providing the accuracy and reliability of the CFD framework. This will provide foundational knowledge on solid particle deposition in the pipeline wall, which will aid in the positioning of the equipment to achieve precise measurement for complex slurries.

9.0 Notes on Collaborations

9.1 University Collaboration

University partners are exploring the applicability of machine learning to predicting critical deposition velocity based on slurry properties. This is a valuable tool to support waste processing activities as well as provide an additional avenue to verify sensor readings under future deployments. Specifically, Professor Aparna Aravelli has been leading this effort, first form Florida International University (FIU) and then from North Carolina Agriculture and Technology (NCA&T) following an opportunity to move Universities.

Developing critical deposition velocity prediction tools could be highly valuable to industrial practices for efficiency and safety but could also support goals of mission acceleration at the Hanford site. Conventional approaches mainly rely on empirical, theoretical, or simulation models, which usually have limited capability for dealing with intricate rheological behaviors both in Newtonian and Non-Newtonian liquids. Machine learning can provide a complementary data-driven technique that can capture complex relationships between experimental variables and sensor data. Recently, machine learning has been used for flow velocity model development in various applications.[69-73]

For initial efforts in Year 1, two data sets were used to formulate models for analysis. The two sets are based on the simulant types as:

- Newtonian Simulants: Tabulated critical velocities measured experimentally and by ultrasonic sensors (PulseEcho, UDV, and Attenuation).
- Non-Newtonian Simulants: Data is similar to Newtonian dataset, with the addition of yield stress as a key feature.

The data sets were previously published and included experimental measurements (RII, RIII, and Vcritical), ultrasonic sensor measurements (PulseEcho, UDV, and Attenuation), and yield stress (only applicable to non-Newtonian datasets). Figure 40shows the datasets used in this study, providing an overview of the data prior to pre-processing.

The data sets for this initial proof of principle portion of the effort were limited. In this case the pre-processing of the data sets was conducted with the goal of ensuring consistency and robustness for analysis:

- Handling Ranges: Wherever the data contained a range (e.g., 0.5–1.0), the range was converted to its average value.
- Replacing Hyphens (-): Any cells containing a hyphen (-) were identified as missing or not applicable values. These were replaced with NaN to clearly indicate the absence of data.
- Replacing NaN Values: After identifying missing values as NaN, these were replaced with -1 to facilitate processing.
- Standardizing Units: The dataset contained measurements in both meters per second (m/s) and feet per second (ft/s). For this analysis, all measurements were standardized to m/s, ensuring consistency across variables.

Synthetic data points were added to expand training sets and were generated by introducing small random noise, enhancing model robustness against overfitting.

Test Number	Simulant Type	Experimental Measurements m/s (ft/s)			Ultrasonic Sensor Measurements m/s (ft/s)		
		R II	R III	$V_{critical}$	PulseEcho	UDV	Attenuation[c]
1	Mono-dispersed (s1-d2)	n/a	n/a	0.73 (2.4)	0.73 (2.4)	0.73 (2.4)	N/A
2	Mono-dispersed (s1-d2)	0.84 (2.75)	0.81 (2.65)	0.78 (2.55)	0.81 (2.65)	0.81 (2.65)	N/A
3	Mono-dispersed (s2-d2)	1.34 (4.4)	1.31 (4.3)	1.28 (4.2)	1.25 (4.1)	1.31 (4.3)	1.52 (5.0)
4	Broad PSD	1.10 (3.6)	1.07 (3.5)	1.01 (3.3)	1.01 (3.3)	1.01 (3.3)	1.37 (4.5)
5	Broad PSD	1.28 (4.2)	1.25 (4.1)	1.22 (4.0)	1.22 (4.0)	1.25 (4.1)	1.28 (4.2)
6	Mono-dispersed (s1-d1)	1.28 (4.2)	1.25 (4.1)	1.19 (3.9)	1.19 (3.9)	1.25 (4.1)	1.25 (4.1)
7	Mono-dispersed (s1-d1)	0.88 (2.9)	0.85 (2.8)	0.76 (2.7)	0.88 (2.9)	0.76 (2.8)	0.73 (2.4)
8	Mono-dispersed (s1-d4)	0.75 (2.45)	--	0.72 (2.35)	0.72 (2.35)	0.72 (2.35)	0.64 (2.1)
9	Binary size (s1-d1(33%)/s1-d2 (67%))	1.00 (3.3)	0.97 (3.2)	0.95 (3.1)	1.04 (3.4)	0.91 (3.0)	0.91 (3.0)
10	Binary size (s1-d1 (67%)/s1-d2 (33%))	1.28 (4.2)	>1.25 (4.1)	1.25 (4.1)	1.37 (4.5)	1.25 (4.1)	1.25 (4.1)
11	Binary density (s1-d2 (67%)/s2-d2 (33%))	1.22 (4.0)	1.20 (3.9)	1.16 (3.8)	1.25 (4.1)	1.16 (3.8)	1.10 (3.6)
12	Broad PSD	~0.91 (3.0)	0.85 (2.8)	0.82 (2.7)	~0.79 ~(2.6)	>0.69& < 0.76 (>2 & <2.5)	0.79 (2.6)
13	Bi density Broad PSD	1.49 (4.9)	1.33 (4.7)	1.40 (4.6)	1.49 (4.9)	>1.22 & <1.40 (>4.0 & <4.6)	1.31 (4.3)
25	Broad PSD	1.28 (4.2)	1.22 (4.0)	1.12 (3.7)	1.22 (4.0)	1.16 – 1.19 (3.8 – 3.9)	N/A

(a). R II and R III correspond to flow velocities where focused axial motion or a pulsating (stop/go) bed, respectively, was observed at the bottom of the pipe is moving. $V_{critical}$ corresponds to the velocity at which a stationary bed was observed.

(b). N/A = No data available

(c). An average value is shown for situations where multiple indications were possible for the attenuation system.

(d). 60 wt% glycerin, Newtonian viscosity 11.7 mPa.S

Sensor measurement sensor falls within the range for R II, RIII, and $V_{critical}$

Sensor measurement sensor falls **within ±0.3 ft/s** of the range for R II, RIII, and $V_{critical}$

Sensor measurement sensor falls **outside ±0.3 ft/s** of the range for R II, RIII, and $V_{critical}$

Test #	Simulant Type	Yield Stress (Pa)	Exp. Measurements m/s (ft/s)[a,b]			Ultrasonic Sensor Measurements m/s (ft/s)		
			R II	R III	$V_{critical}$	PulseEcho	UDV	Attenuation[c]
14	Carrier fluid-Koalin	8.2	--	--	--	--	--	--
15	Mono-dispersed (Mil#8)	10.5	--	--	0.64-0.70 (2.1-2.3)	0.64 (2.1)	0.64 (2.1)	N/A
16	Mono-dispersed (Mil#8)	8.8	1.22 (4.0)	0.97 (3.2)	0.79-0.91 (2.6-3.0)	0.95 (3.1)	0.97 (3.2)	N/A
17	Broad PSD	8.5	1.28 (4.2)	--	1.10 (3.6)	1.16 (3.8)	1.10 (3.6)	1.28 (4.2)
18	Broad PSD	3.4	1.16 (3.5)	0.95 (3.1)	0.91 (3.0)	0.95 (3.1)	0.91 (3.0)	0.85 (2.8)
19	Mono-dispersed (Mil#13)	10.4	--	0.09 (0.3)	0.06 (0.2)	0.15 (0.5)	0.30 (1.0)	0.12 (0.4)
20	Mono-dispersed (Mil#13)	11.35	--	0.43 (1.4)	<0.30 (<1.0)	0.45 (1.5)	0.45 (1.5)	0.36 (1.2)
21	Duralum-Broad PSD	1.9	0.97 (3.5)	1.04 (3.4)	0.95-1.01 (3.1-3.3)	0.95 (3.1)	0.95 - 0.98 (3.1 - 3.2)	0.85 (2.8)
22	Complex simulant	2.3	1.07 (3.3)	1.04 (3.4)	0.95-1.01 (3.1-3.3)	1.01 (3.3)	1.01 (3.3)	1.01 (3.3)
23	Complex simulant	5.1	1.31 (4.3)	1.28 (4.2)	1.1-1.16 (3.6-3.8)	1.13 (3.7)	1.19 (3.9)	1.37 (4.4)
24	Complex simulant	9.7	1.52 (5.0)	1.28 (4.2)	1.25-1.43 (4.1 – 4.7)	1.31 (4.3)	1.40 (4.6)	1.34 (4.4)

(a). R II and R III correspond to flow velocities where focused axial motion (sliding bed) or a pulsating (stop/go) bed, respectively, was observed at the bottom of the pipe is moving. $V_{critical}$ corresponds to the velocity at which a stationary bed was observed.

(b). N/A = No data available

(c). An average value is shown for situations where multiple indications were possible for the attenuation system.

Sensor measurement sensor falls within the range for R II, RIII, and $V_{critical}$

Sensor measurement sensor falls **within ±0.9 m/s (0.3 ft/s)** of the range for R II, RIII, and $V_{critical}$

Sensor measurement sensor falls **outside ±0.9 m/s (0.3 ft/s)** of the range for R II, RIII, and $V_{critical}$

Figure 40: Newtonian (left) and nonnewtonian (right) datasets.[40]

The initial efforts focused on analyzing experimental and ultrasonic sensor readings from both Newtonian and Non-Newtonian datasets and various descriptive statistical measures were utilized to summarize the datasets effectively:

- Mean and Median: These metrics were calculated to identify the central tendencies in the experimental and ultrasonic measurements (e.g., RII, RIII, $V_{critical}$, PulseEcho, UDV).
- Standard Deviation and Range: These were used to quantify the variability and spread of the data, providing insights into the consistency of different simulants.
- Distribution Analysis: Histograms and density plots were generated to visualize the distribution patterns of key variables in the datasets.

Additionally, a comparative study was conducted to evaluate the relationship between experimental measurements and ultrasonic sensor readings. This included correlation analysis, scatter plots, and error analysis. Resulting heat maps are shown in Figure 41.

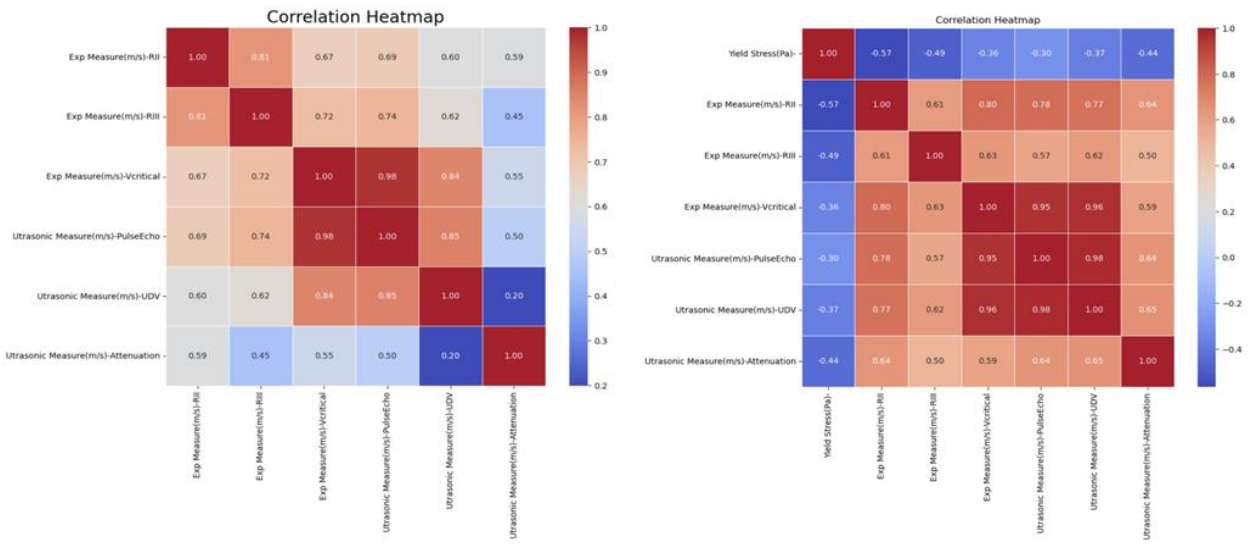

Figure 41: Correlation heatmaps for Newtonian (left) and non-Newtonian (right) datasets.

The descriptive and comparative analyses provided key insights for subsequent model development. For example, the correlations observed in the heat maps showed predictive relationships between the experimental and ultrasonic sensor data. Error analysis showed systematic biases in certain sensors (e.g., UDV), requiring feature scaling and data normalization and outlier detection.

Multiple approaches to regression were tested. Linear regression served as the baseline model for predicting critical velocity (Expt. $V_{critical}$) using experimental and ultrasonic sensor data. But additional regression approaches were also tested and applications to both experimental and synthetic data were also tested. The following steps were performed during the analysis:

The models were assessed using the following metrics:

- Mean Squared Error (MSE): Evaluates the average squared difference between predicted and actual values.
- Coefficient of Determination (R^2): Measures the proportion of variance in the dependent variable that is predictable from the independent variables.
- Feature Importance Analysis: Identifies the most influential features in the regression model for the prediction of critical velocity.

Overview of Baseline Findings:

1. *Correlation Analysis:* The relationships between Exp $V_{critical}$ and key features were explored using correlation analysis:

- Newtonian Simulants: Strong correlations were observed between Exp $V_{critical}$ and Ultra PulseEcho (0.98) and Ultra UDV (0.84). Ultra-Attenuation showed weaker correlations, indicating limited predictive influence.
- Non-Newtonian Simulants: Similar patterns were observed, with strong correlations between Exp $V_{critical}$ and Ultra PulseEcho/Ultra UDV. Yield stress initially showed weaker correlations but gained importance in later stages.

2. *Model Performance on Original Data:* Linear regression was applied to the original datasets with the following results:
   - Without Attenuation (Newtonian): High MSE and negative R^2 values were observed, indicating poor predictive power. The model struggled to generalize effectively.
   - With Attenuation (Newtonian): Including Ultra Attenuation further worsened performance, highlighting its limited contribution to predictions.
   - Without Yield Stress (Non-Newtonian): Similar to Newtonian data, the model exhibited high errors and negative R^2 values.
   - With Yield Stress (Non-Newtonian): Adding yield stress slightly improved performance but still resulted in high errors and inadequate predictions.
3. *Synthetic Data Generation:* Synthetic data augmentation was introduced to enhance the datasets:
   - Methodology: Random noise was added to original data points, creating synthetic variations to expand the dataset size. For Newtonian simulants, the dataset grew from 14 to 42 samples; for non-Newtonian, it expanded from 11 to 33 samples.
   - Correlation Stability: The relationships between Exp Vcritical and key features remained consistent, with Ultra PulseEcho and Ultra UDV retaining their strong correlations.
4. *Model Performance with Synthetic Data:* The addition of synthetic data significantly improved model performance:
   - Newtonian Simulants:
     - Without Attenuation: MSE dropped from 1.266 to 0.0146, and R^2 values increased from -23.58 to 0.78, reflecting better generalization.
     - With Attenuation: MSE further reduced to 0.0114, with R^2 scores reaching 0.834, indicating improved accuracy.
   - Non-Newtonian Simulants:
     - Without Yield Stress: MSE dropped significantly, and R^2 values stabilized around 0.90, reflecting strong generalization.
     - With Yield Stress: Including yield stress improved R^2 further to 0.91, highlighting its value in non-Newtonian predictions.
5. *Optimal Synthetic Data Quantity:* Iterative testing with different synthetic data multipliers identified the optimal dataset size (Figure 42):
   - A 5x multiplier provided the best balance between MSE reduction and stable R^2 values.
   - Beyond this multiplier, diminishing returns were observed, with additional synthetic data offering limited improvements.

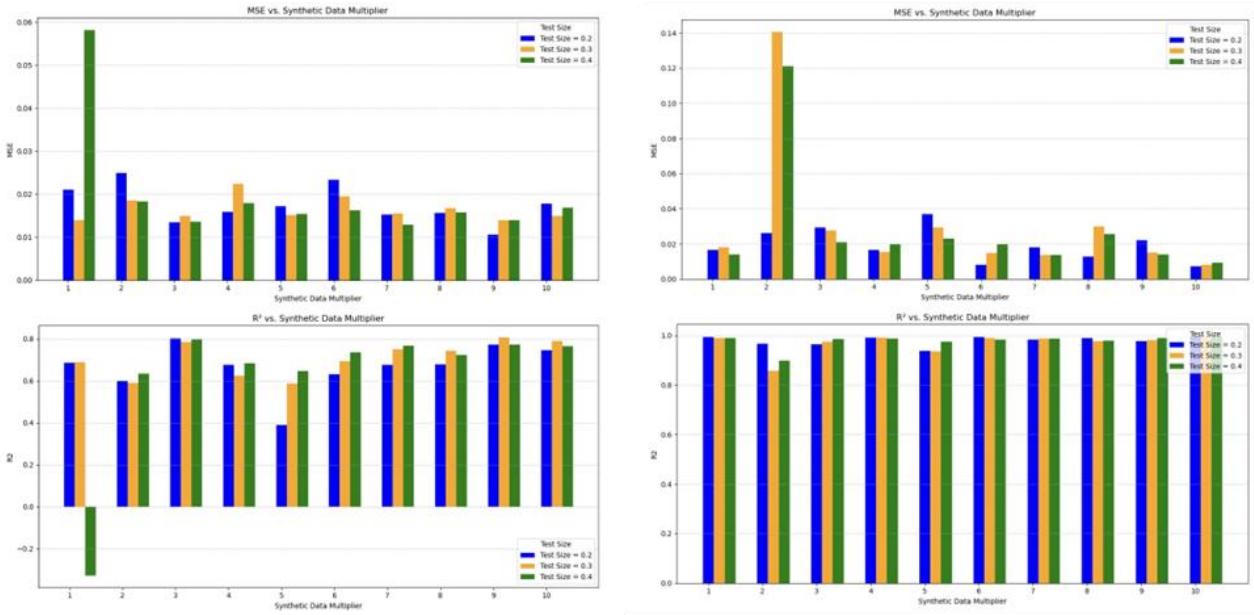

Figure 42: Impact of Synthetic Data Quantity on MSE and R^2 for Newtonian (left) and Non-Newtonian (right) Simulants. The optimal multiplier (5x) minimizes MSE and stabilizes R^2 across test sizes.

6. *Feature Importance Analysis:* Feature importance was evaluated to identify key predictors of Exp $V_{critical}$:

- Top Features: Ultra UDV consistently emerged as the strongest predictor, followed by Ultra PulseEcho. Experimental features (Exp RII, Exp RIII) had moderate contributions, while ultrasonic attenuation had a minimal impact.
- Validation: Multiple iterations confirmed the stability of feature importance rankings, ensuring robust predictor selection.

This analysis validated the effectiveness of synthetic data in improving model accuracy and generalization, with Ultra UDV and Ultra PulseEcho consistently emerging as the most critical features (Figure 43 and Figure 44). Further testing explored alternative regression models to address limitations of linear regression, as described in subsequent sections.

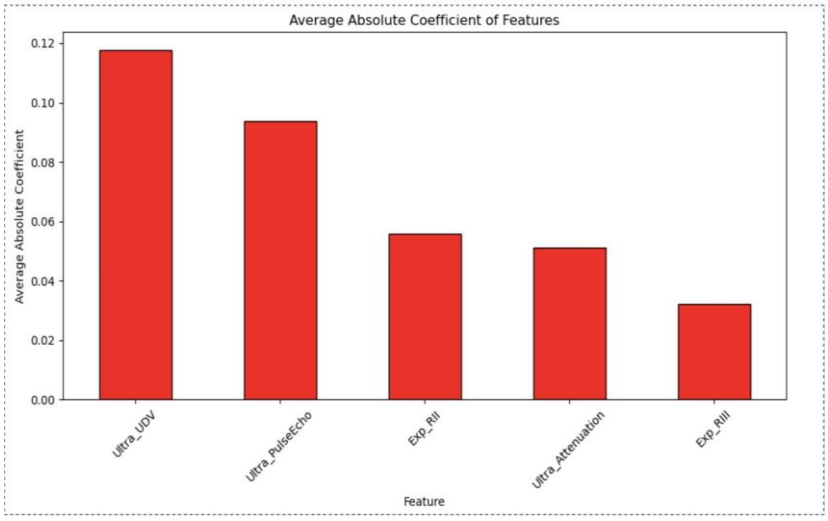

Figure 43: Feature Importance for Newtonian Simulants: Ultra UDV and Ultra PulseEcho are the most significant predictors, with moderate contributions from Exp RII and Exp RIII.

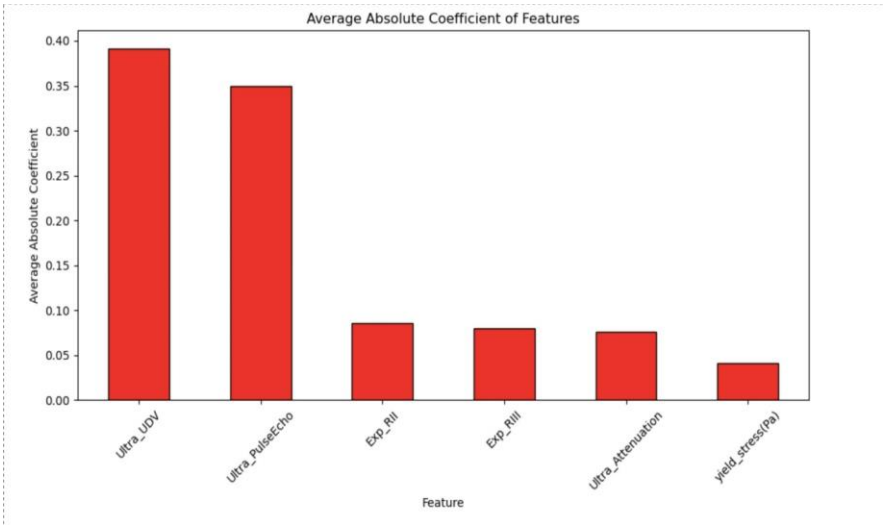

Figure 44: Feature Importance for Non-Newtonian Simulants: Ultra UDV and Ultra PulseEcho dominate.

Overview of Comparison of Regression Approaches

The performances of three regression models are tested: Linear Regression, Ridge Regression, and Support Vector Regression. Each model tested on both datasets-Newtonian and Non-Newtonian. Each model performance examined to predict critical velocity (Exp $V_{critical}$) based on various setups; using the original data, augmentation with synthetic prepared data, and key features such as yield stress, and attenuation.

1. *Performance on Newtonian Data*:

- Linear Regression was the baseline but performed poorly on the original dataset, showing high MSE and negative R^2 values. However, the inclusion of synthetic data significantly

improved its performance. With the synthetic data multiplier out of 5×, Linear Regression resulted in R^2 values above 0.75, pointing out stable and improved predictions.

- Ridge Regression introduced L2 regularization to handle overfitting and multicollinearity issues. On the Newtonian dataset, it consistently outperformed Linear Regression, even on the original data. When synthetic data was incorporated, Ridge Regression showed robust results: R^2 values at about 0.91 and lowest MSEs observed at 0.09. Besides this, the generalization of Ridge Regression across test splits (20%, 30%, and 40%) was also observed to be good since its performance remained consistent.
- Support Vector Regression (SVR) performed well in capturing non-linear relationships within the data. With synthetic data, it delivered the best overall results among all models, achieving R^2 values near 0.91 and MSE as low as 0.007. However, SVR required extensive hyperparameter tuning to optimize its predictions. Despite the computational expense, SVR's ability to model complex relationships makes it highly effective for Newtonian data.

2. *Performance on Non-Newtonian Data*:

- The inclusion of yield stress was critical for improving predictions in non-Newtonian data. Linear Regression performed poorly without this feature, showing high MSE and negative R^2 values. The addition of yield stress and synthetic data significantly enhanced its performance, achieving R^2 values exceeding 0.8 and providing more reliable predictions.
- Regression again proved to be a strong performer on non-Newtonian data. It consistently outperformed Linear Regression and achieved its best results when yield stress and synthetic data were included. The model's R2 values stabilized around 0.91, with MSE values dropping to approximately 0.07. Ridge Regression's ability to handle multicollinearity among features was especially beneficial in this dataset.
- SVR demonstrated its capability to capture the non-linear effects of yield stress, achieving excellent predictive accuracy. However, its performance lagged slightly behind the Ridge Regression, with R^2 values around 0.9 and MSE ranging from 0.11 to 0.15. Like in the Newtonian dataset, SVR's computational demands were requiring fine-tuned hyperparameters to deliver optimal performance.

Examples of results for synthetic data are presented in Figure 45 and Figure 46. These highlight the difference in key performance metrics across the regression modes studies here.

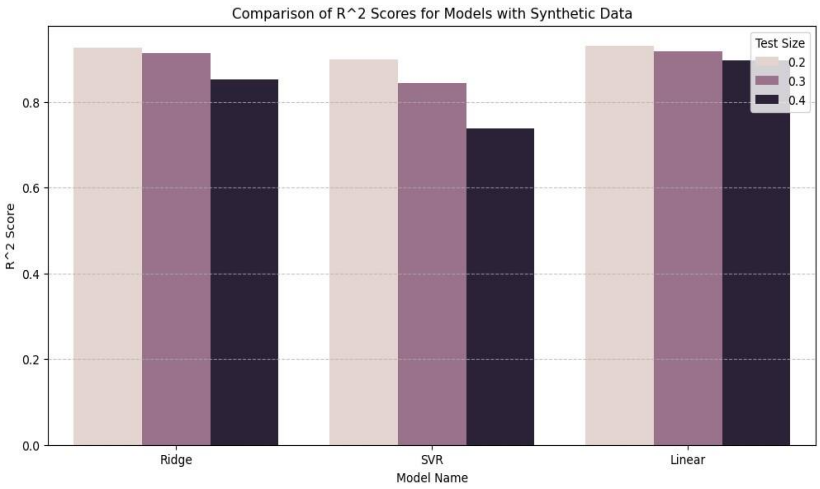

Figure 45: Comparison of R^2 Scores for Models with Synthetic Data for Non-Newtonian Simulants.

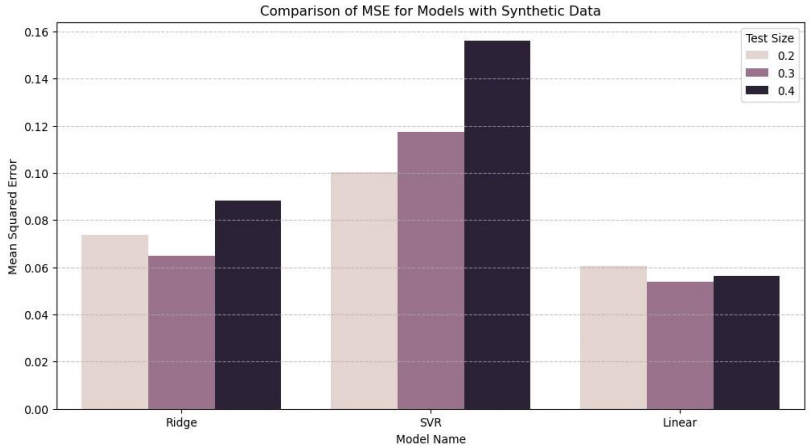

Figure 46: Comparison of MSE for Models with Synthetic Data for Non-Newtonian Simulants.

Overall, Ridge Regression emerged as the most practical model for this use case, given its ability to handle multicollinearity, its stable performance across various configurations, and its relatively low computational cost compared to SVR. While SVR achieved slightly better results in some scenarios, the further tuning required makes Ridge Regression a more feasible choice for the given dataset size and feature complexity. Synthetic data augmentation played a pivotal role in improving the performance of all three models. By introducing small variations to the original data, synthetic data expanded the dataset and enhanced model generalization. A synthetic data multiplier of 5x was identified as the optimal configuration for both Newtonian and Non-Newtonian datasets. This multiplier provided the best balance between reducing MSE and stabilizing R2 values, without introducing overfitting or diminishing returns. Beyond 5x, additional synthetic data offered limited improvements in performance, though expansion of the training sets (planned for Year 2) can support more robust model building.

Conclusions from Year 1 Results

Year 1 results suggest machine learning models have the potential to be successfully applied to predicting critical deposition velocity. Initial efforts focused on a limited training set, focusing on predicting critical velocity in Newtonian and non-Newtonian slurry flows using experimental and ultrasonic sensor data obtained from literature. Amongst the models developed, Ridge Regression proved to be the most practical and effective model, offering a balance between accuracy and computational efficiency. Support Vector Regression demonstrated excellent predictive capabilities but required significant computational resources for optimal performance.

Given the limited size of the original dataset, synthetic data augmentation played a crucial role in expanding the data and enhancing model learning. By introducing controlled variations, synthetic data not only improved model performance but also allowed for a deeper analysis of robustness and generalization. The optimal multiplier of 5x was identified as the best configuration, reducing errors while preventing overfitting.

Key features such as yield stress (for non-Newtonian data) and Ultra UDV emerged as critical predictors, significantly contributing to model accuracy. These findings emphasize the importance of combining advanced regression techniques with data augmentation to achieve robust and reliable predictions, particularly in scenarios involving complex fluid systems and limited experimental data.

Year 2 efforts will build upon these positive findings to expand training sets and begin exploring pathways to create more robust machine learning models.

9.2 Expanded Collaborations in Year 2

In addition to continuing collaborative efforts with NCA&T, efforts will expand to include a small business collaborator. The goal of the connection is to modify instrument software to be better adapted to on-line real-time data analysis and facilitate connection into the user interface. A key benefit here also includes improving pathways for tech to market options for key components of the on-line monitoring platform.

10.0 Conclusions and Look Ahead at Year 2

Project progress has met Year 1 goals of 1) developing an instrumentation plan, 2) procuring and testing chemical composition sensors, and 3) procuring and testing physical property measurement sensors. This includes Raman and LIBS systems, which will be utilized to follow both molecular species that represent precipitation, gelation, or other concerns (e.g., aluminate, phosphate, nitrate) and atomic species that represent precipitation or total waste volume concerns (e.g., fluoride and sodium), respectively. This also includes two types of flowmeters: Coriolis and electromagnetic systems, which will both be integrated in the final platform to explore robustness and accuracy of measurement under variable solids loading/chemical composition conditions. And finally, two forms of ultrasonics sensors, UPE for solids settling/critical deposition velocity and a SolidsMeter for measuring solids mass fraction, were identified as needs, procured, and tested in preparation for Year 2 efforts. In all cases, the TRL of equipment allowed for COTS procurement of components. Notably, the automated data analysis tools which will be developed/matured in Year 2 efforts represent the primary attributes of the platform that are not currently commercially available. Routes to making these tools readily available to stakeholders include licensing of technologies and can be explored in subsequent project years.

In addition to the instrument procurement and testing tasks, CFD modeling tasks were initiated to support spool piece and full platform design efforts, and the user interface development team began initial data and mathematical handling plans. Regular interaction with stakeholders was held to both ensure project direction and tasking was in line with site needs/deployment requirements and to explore any opportunities to support additional efforts or needs (e.g., supporting flow sheet maturation plans). Collaboration with Professor Aparna Aravelli was successfully transitioned from FIU to NCA&T following her move. While this did impact timelines, the university team was still able to develop initial machine learning models with the goal of expanding complexity and fidelity for predicting critical deposition velocities.

Overall, the team is well positioned to move into Year 2 where tasks will focus on calibrating sensors, developing/maturing automated data analysis tools, and fabricating/testing spool pieces. Tasking will also include continuing university collaborations to develop machine learning tools for critical deposition velocity predictions and kicking off a new collaboration with a small business partner that should help advance the tech to market plans for the optical based sensors. Engagement with stakeholders will continue and will allow efforts to remain on-track for meeting site needs and requirements. The project is on schedule to meet overall goals of integrating a comprehensive on-line monitoring test platform onto a full-scale loop for demonstration by the end of Year 3. This will both lay the design foundation for deployable units as well as provide a testbed to support future technology or flowsheet maturation efforts.

11.0 References

(1) Bohnke, C.; Duroy, H.; Fourquet, J. L. pH sensors with lithium lanthanum titanate sensitive material: applications in food industry. *Sensors and Actuators B: Chemical* **2003**, *89* (3), 240-247. DOI: https://doi.org/10.1016/S0925-4005(02)00473-2.
(2) Mohd Adli Ikram, S.; Johari, J. Water storage monitoring system with pH sensor for pharmaceutical plants. In *2016 6th International Conference on System Engineering and Technology (ICSET)*, 3-4 Oct. 2016, 2016; pp 46-52. DOI: 10.1109/ICSEngT.2016.7849621.
(3) Chung, C.-C.; Chen, H.-H.; Ting, C.-H. Grey prediction fuzzy control for pH processes in the food industry. *J Food Eng* **2010**, *96* (4), 575-582. DOI: https://doi.org/10.1016/j.jfoodeng.2009.09.004.
(4) Lines, A. M.; Tse, P.; Felmy, H. M.; Wilson, J. M.; Shafer, J.; Denslow, K. M.; Still, A. N.; King, C.; Bryan, S. A. Online, Real-Time Analysis of Highly Complex Processing Streams: Quantification of Analytes in Hanford Tank Sample. *Ind Eng Chem Res* **2019**, *58* (47), 21194-21200. DOI: 10.1021/acs.iecr.9b03636.
(5) Felmy, H. M.; Kersten, B.; Bryan, S. A.; Lines, A. M. The design and demonstration of a novel UV-vis probe for the in-situ interrogation of dark solutions. PNNL-33304, Pacific Northwest National Laboratory: Richland, Washington, 2022.
(6) Bryan, S. A.; Levitskaia, T. G.; Schlahta, S. N. Raman Based Process Monitor For Continuous Real-Time Analysis of High Level Radioactive Waste Components. In *Waste Management WM2008 Conference*, Phoenix, AZ, February 24 -28, 2008, 2008; Vol. WM2008.
(7) Bryan, S. A.; Levitskaia, T. G. Spectroscopic Based Process Monitor for Continuous Real-Time Analysis of High Level Radioactive Waste Components and Monitoring for Control and Safeguarding of Radiochemical Streams. In *Center for Process Analytical Chemistry (CPAC), University of Washington, Seattle, Washington*, 2010.
(8) Kurath, D. Pretreatment Engineering Platform: Phase 1 Final Test Report, Pacific Northwest National Laboratory, Richland, WA, PNNL-18894 WTP-RPT-197, Rev 0. 2009.
(9) Bryan, S. A.; Levitskaia, T. G.; Sinkov, S. I.; Schlahta, S. N.; Shaver, J. M. Raman based process monitor for continuous real-time analysis of high level radioactive waste components. In *232nd ACS National Meeting, San Francisco, CA*, 2006.
(10) Bryan, S. A.; Levitskaia, T. G.; Sinkov, S. I. Process Monitor Development Project Acceptance Test Report: S-109 Retrieval. Richland, Washington, Pacific Northwest National Laboratory, PNNL-15360, 2005.
(11) Edwards M.K.; Schonewill, P. P.; Shimskey, R. W.; Niver, C. M.; Bryan, S. A.; Peterson, R. A.; Smith, C. Real Time Raman Analysis of Near Tank Treatment System Process Streams. In *17th Symposium on Separation Science & Technology for Energy Applications*, Gatlinburg, Tennessee, 2011.
(12) Lines, A. M.; Bello, J. M.; Gasbarro, C.; Bryan, S. A. Combined Raman and Turbidity Probe for Real-Time Analysis of Variable Turbidity Streams. *Anal Chem* **2022**, *94*, 3652−3660. DOI: 10.1021/acs.analchem.1c05228.
(13) Gasbarro, C.; Bello, J.; Bryan, S.; Lines, A.; Levitskaia, T. Development of an Integrated Raman and Turbidity Fiber Optic Sensor for the In-Situ Analysis of High Level Nuclear Waste-13532. 2013; WM Symposia, 1628 E. Southern Avenue, Suite 9-332, Tempe, AZ 85282 (United States).
(14) Bryan, S.; Levitskaia, T.; Lines, A.; Smith, F.; Josephson, G.; Bello, J. Dual-Remote Raman Technology for In-Situ Identification of Tank Waste-13549. 2013; WM Symposia, 1628 E. Southern Avenue, Suite 9-332, Tempe, AZ 85282 (United States).
(15) Clifford, A. J.; Lackey, H. E.; Nelson, G. L.; Bryan, S. A.; Lines, A. M. Raman Spectroscopy Coupled with Chemometric Analysis for Speciation and Quantitative Analysis of Aqueous

Phosphoric Acid Systems. *Anal Chem* **2021**, *93* (14), 5890-5896. DOI: 10.1021/acs.analchem.1c00244.
(16) Lackey, H. E.; Nelson, G. L.; Lines, A. M.; Bryan, S. A. Reimagining pH Measurement: Utilizing Raman Spectroscopy for Enhanced Accuracy in Phosphoric Acid Systems. *Anal Chem* **2020**, *92* (8), 5882-5889. DOI: 10.1021/acs.analchem.9b05708.
(17) Tse, P.; Shafer, J.; Bryan, S. A.; Lines, A. M. Quantification of Raman-Interfering Polyoxoanions for Process Analysis: Comparison of Different Chemometric Models and a Demonstration on Real Hanford Waste. *Environmental Science & Technology* **2021**, *55* (19), 12943-12950. DOI: 10.1021/acs.est.1c02512.
(18) Ryan, J. V.; Parruzot, B.; Lines, A. M.; Bryan, S. A.; Seymour, L. M.; Bonnett, J. F.; Motkuri, R. K. In-situ monitoring of seeded and unseeded stage III corrosion using Raman spectroscopy. *npj Materials Degradation* **2019**, *3* (1), 34. DOI: 10.1038/s41529-019-0095-0.
(19) Parruzoti, B.; Ryan, J. V.; Lines, A. M.; Bryan, S. A.; Neeway, J. J.; Chatterjee, S.; Lukins, C. D.; Casella, A. J. Method for the in situ Measurement of pH and Alteration Extent for Aluminoborosilicate Glasses Using Raman Spectroscopy. *Anal Chem* **2018**, *90* (20), 11812-11819. DOI: 10.1021/acs.analchem.8b00960.
(20) Felmy, H. M.; Cox, R. M.; Espley, A. F.; Campbell, E. L.; Kersten, B. R.; Lackey, H. E.; Branch, S. D.; Bryan, S. A.; Lines, A. M. Quantification of Hydrogen Isotopes Utilizing Raman Spectroscopy Paired with Chemometric Analysis for Application across Multiple Systems. *Anal Chem* **2024**, *96* (18), 7220-7230. DOI: 10.1021/acs.analchem.4c00802 From NLM PubMed-not-MEDLINE.
(21) Felmy, H. M.; Lackey, H. E.; Medina, A. S.; Minette, M. J.; Bryan, S. A.; Lines, A. M. Leveraging Multiple Raman Excitation Wavelength Systems for Process Monitoring of Nuclear Waste Streams. *ACS ES&T Water* **2022**, *2* (3), 465-473. DOI: 10.1021/acsestwater.1c00408.
(22) Lines, A. M.; Tse, P.; Felmy, H. M.; Wilson, J.M. ; Shafer, J.; Denslow, K. M.; Still, A. N.; King, C.K. ; Bryan, S.A. On-line, real-time analysis of highly complex processing streams: Quantification of analytes in Hanford tank sample. *Ind. Eng. Chem. Res.* **2019**, *58* (47), 21194-21200. DOI: http://dx.doi.org/10.1021/acs.iecr.9b03636.
(23) Felmy, H. M.; Clifford, A. J.; Medina, A. S.; Cox, R. M.; Wilson, J. M.; Lines, A. M.; Bryan, S. A. On-Line Monitoring of Gas-Phase Molecular Iodine Using Raman and Fluorescence Spectroscopy Paired with Chemometric Analysis. *Environ Sci Technol* **2021**, *55* (6), 3898-3908. DOI: 10.1021/acs.est.0c06137.
(24) Bryan, S. A.; Levitskaia, T. G.; Sinkov, S. I. Chemical and Radiochemical Stability of the Process Monitor System used in the Raman Probe System Project. Pacific Northwest National Laboratory, Report #47187: Richland, Washington, 2004.
(25) Felmy, H. M.; Schafer Medina, A.; Boily, N. T. C.; Brownell, W.; Tse, P.; Bryan, S. A.; Lines, A. M. Deployment of In-Line Sampling in Tank Farms. Pacific Nothwest National Laboratory, PNNL-36616: Richland, Washington, 2024.
(26) Lackey, H. E.; Colburn, H. A.; Olarte, M. V.; Lemmon, T.; Felmy, H. M.; Bryan, S. A.; Lines, A. M. On-Line Raman Measurement of the Radiation-Enhanced Reaction of Cellobiose with Hydrogen Peroxide. *ACS Omega* **2021**, *6* (51), 35457-35466. DOI: 10.1021/acsomega.1c04852.
(27) Lackey, H. E.; Espley, A. F.; Potter, S. M.; Lamadie, F.; Miguirditchian, M.; Nelson, G. L.; Bryan, S. A.; Lines, A. M. Quantification of Lanthanides on a PMMA Microfluidic Device with Three Optical Pathlengths Using PCR of UV–Visible, NIR, and Raman Spectroscopy. *ACS Omega* **2024**, *9* (37), 38548-38556. DOI: 10.1021/acsomega.4c03857.
(28) Cremers, D. A.; Radziemski, L. J. *Handbook of laser-induced breakdown spectroscopy*; John Wiley & Sons, 2013.
(29) Dudragne, L.; Adam, P.; Amouroux, J. Time-resolved laser-induced breakdown spectroscopy: application for qualitative and quantitative detection of fluorine, chlorine, sulfur, and carbon in air. *Applied Spectroscopy* **1998**, *52* (10), 1321-1327.

(30) Schmidt, N. E.; Goode, S. R. Analysis of aqueous solutions by laser-induced breakdown spectroscopy of ion exchange membranes. *Applied spectroscopy* **2002**, *56* (3), 370-374.
(31) Gondal, M.; Hussain, T. Determination of poisonous metals in wastewater collected from paint manufacturing plant using laser-induced breakdown spectroscopy. *Talanta* **2007**, *71* (1), 73-80.
(32) Sarkar, A.; Alamelu, D.; Aggarwal, S. K. Determination of thorium and uranium in solution by laser-induced breakdown spectrometry. *Appl. Opt.* **2008**, *47*, G58-G64.
(33) Harilal, S. S.; Brumfield, B. E.; LaHaye, N. L.; Hartig, K. C.; Phillips, M. C. Optical spectroscopy of laser-produced plasmas for standoff isotopic analysis. *Applied Physics Reviews* **2018**, *5* (2), 021301. DOI: https://doi.org/10.1063/1.5016053.
(34) Eseller, K. E.; Tripathi, M. M.; Yueh, F.-Y.; Singh, J. P. Elemental analysis of slurry samples with laser induced breakdown spectroscopy. *Applied optics* **2010**, *49* (13), C21-C26.
(35) Khajehzadeh, N.; Haavisto, O.; Koresaar, L. On-stream and quantitative mineral identification of tailing slurries using LIBS technique. *Minerals Engineering* **2016**, *98*, 101-109.
(36) Onishi, Y., B. E. Wells, S. A. Hartley, C. W. Enderlin, and M. White. *Material Balance Assessment for Double-Shell Tank Waste Pipeline Transfer*; PNNL-13485; Pacific Northwest National Laboratory, Richland, Washington, 2002.
(37) Enderlin, C. W., G. Terrones, and B. Hatchell. Scaled Testing to Determine Operational Strategies for Removal of Zeolite in Savannah River Site Tank 19 Using Shrouded Axial Impeller Mixers. In *International Conference on Hydro Transport*, Banff, Canada, 2002; BHR Group Limited: Bedforshire, U.K., Vol. 1, pp 187-201.
(38) Bontha, J. R.; Adkins, H. E.; Denslow, K. M.; Jenks, J. J.; Burns, C. A.; Schonewill, P. P.; Morgen, G. P.; Greenwood, M. S.; Blanchard, J.; Peters, T. J.; et al. Test Loop Demonstration and Evaluation of Slurry Transfer Line Critical Velocity Measurement Instruments. Pacific Northwest National Laboratory, Richland, Washington., 2010.
(39) Bontha, J. R.; Adkins, H. E.; Denslow, K. M.; Jenks, J. J.; Burns, C. A.; Schonewill, P. P.; Morgen, G. P.; Greenwood, M. S.; Blanchard, J.; Peters, T. J.; et al. Supplementary Information for Test Loop Demonstration and Evaluation of Slurry Transfer Line Critical Velocity Measurement Instruments. PNNL-19560. Pacific Northwest National Laboratory, Richland, Washington, 2010.
(40) Bontha, J. R.; Denslow, K. M.; Adkins, H. E.; Jenks, J. J.; Burns, C. A.; Schonewill, P. P.; Morgen, G. P.; Greenwood, M. S. Evaluation of Three Ultrasonic Instruments for Critical Velocity Determination during Hanford Tank Waste Transfer Operations. In *Waste Management Symposia, WM2011*, Phoenix, Arizona, 2011.
(41) Denslow, K. M.; Bontha, J. R.; Burns, C. A.; Bauman, N. N.; Adkins, H. E.; Jenks, J. J.; Schonewill, P. P.; F., H. D. Hanford Tank Farms Waste Certification Flow Loop Phase IV: PulseEcho Sensor Evaluation. PNNL-20350. Pacific Northwest National Laboratory, Richland, Washington., 2011.
(42) Denslow, K. M.; Bontha, J. R.; Adkins, H. E.; Jenks, J. W. J.; Burns, C. A.; Schonewill, P. P.; Hopkins, D. F.; Thien, M. G.; Wooley, T. A. Continued Evaluation of the Pulse-Echo Ultrasonic Instrument for Critical Velocity Determination during Hanford Tank Waste Transfer Operations. In *Waste Management Symposia, WM2012*, Phoenix, Arizona, 2012.
(43) Denslow, K. M.; Bontha, J. R.; Adkins, H. E.; Jenks, J. J.; Hopkins, D. F. Hanford Tank Farms Waste Feed Flow Loop Phase VI: PulseEcho System Performance Evaluation. PNNL-22029, . Pacific Northwest National Laboratory, Richland, Washington., 2012.
(44) Denslow, K. M.; Bontha, J. R.; Adkins, H. E.; Jenks, J. W. J.; Hopkins, D. F.; Thien, M. G.; Kelly, S. E.; Wooley, T. A. System Performance Testing of the Pulse-Echo Ultrasonic Instrument for Critical Velocity Determination during Hanford Tank Waste Transfer Operations. In *Waste Management Symposia, WM2013*, Phoenix, Arizona, 2013.
(45) Wasp, E. J.; Thompson, T. L.; Aude, T. C. *A Quick Method for Making Initial cost Estimates of Slurry Pipelines*; Society for Mining, Metallurgy & Exploration, 1969.

(46) Poloski, A. P.; Adkins, H. E.; Abrefah, J.; Casella, A. M.; Hohimer, R.; Nigl, F.; Minette, M. J.; Toth, J. J.; Tingey, J. M.; Yokuda, S. M. Deposition Velocities of Non-Newtonian Slurries in Pipelines. Pacific Northwest National Laboratory, Richland, Washington., 2009.
(47) Oroskar, A. R.; Turian, R. M. The Critical Velocity in Pipeline Flow of Slurries. *Aiche J* **1980**, *26* (4), 550-558. DOI: DOI 10.1002/aic.690260405.
(48) Liddell, K. C.; Burnett, D. F. Critical Transport Velocity: A Review of Correlations and Models. CH2M HILL Hanford Group, Richland, Washington, 2000.
(49) Meacham, J. E.; Harrington, S. J.; Rodriguez, J. S.; Nguyen, V. C.; Reynolds, J. G.; Wells, B. E.; Piepel, G. F.; Cooley, S. K.; Enderlin, C. W.; Rector, D. R.; et al. One System Evaluation of Waste Transferred to the Waste Treatment Plant. Washington River Protection Solutions, Pacific Northwest National Laboratory, and URS Corporation, Richland, Washington, 2012.
(50) Thien, M. G.; Denslow, K. M.; Lee, K. P. Characterization and Delivery of Hanford High-Level Radioactive Waste Slurry. In *Hydrotransport Conference*, Golden, Colorado, 2014.
(51) Burright, J. *April 2022 Updates. Presentation made at the Oregon Hanford Cleanup Board meeting*. 2022. https://www.oregon.gov/energy/safety-resiliency/Documents/2022-05-02-OHCB-ODOE-Presentation.pdf (accessed 2024 August 03, 2024.).
(52) Blaak, T. M. System Design Description for the Replacement Cross-Site Transfer System Between 200 West and 200 East Tank Farms. Washington River Protection Solutions LLC, Richland, Washington: 2013.
(53) Brantley, W. M. Functional Design Criteria for Project W-058, Replacement of the Cross-Site Transfer System. Westinghouse Hanford Company, Richland, Washington, 1996.
(54) Wells, B. E.; Kurath, D. E.; Mahoney, L. A.; Onishi, Y.; Huckaby, J. L.; Cooley, S. K.; Burns, C. A.; Buck, E. C.; Tingey, J. M.; Daniel, R. C.; et al. Hanford Waste Physical and Rheological Properties: Data and Gaps. PNNL-20646; EMSP-RPT-006. Pacific Northwest National Laboratory, Richland, Washington., 2011.
(55) Bernards, J. K.; Hersi, G. A.; Hohl, T. M.; Jasper, R. T.; Mahoney, P. D.; Pak, N. K.; Reaksecker, S. D.; Schubick, A. J.; West, E. B.; Bergmann, L. M.; et al. River Protection Project System Plan. Washington River Protection Solutions LLC, Lucas Engineering and Management Services Inc., and FIN Consulting LLC: Richland, Washington, 2020.
(56) Bechtel National Inc., B. Interface Control Document for Waste Feed, . Bechtel National Inc.: Richland, Washington, 2014.
(57) Rathbone, B. A. Hanford External Dosimetry Technical Basis Manual: PNL-MA-842. Pacific Northwest National Laboratory: Richland, Washington, 2007.
(58) Graves, C. E. Double-Shell Tank Transfer Piping Subsystem Specification. Fluor Federal Services: Richland, Washington, 2000.
(59) Flexfire_LEDs_Inc. *What are LED IP ratings?" Online article.* 2025. https://www.flexfireleds.com/led-ip-ratings-led-flex-strip-waterproofing-explained-waterproof-v-nonwaterproof-led-strip-lights/ (accessed 2025 February 23, 2025).
(60) Efremov, V. P.; Ivanov, M. F.; Kiverin, A. D.; Yakovenko, I. S. *Shock-wave Processes Evolution in Fused Quarts under Intense Energy Action*; 2016.
(61) Merz, M. D.; Hammer, J. H.; Kjarmo, H. E. Sound Velocity and Elastic Moduli in α-Plutonium at Pressures to 50 Kbar: 5th International Conference on Plutonium and Other Actinides. Battelle-Pacific Northwest Laboratories: Richland, Washington, 1974.
(62) Rice, H. P., M. Fairweather, T. N. Hunter, B. Mahmoud, and S. Biggs. Measuring Particle Concentration in Multiphase Pipe Flow Using Acoustic Backscatter Generalization of the Dual-Frequency Inversion Method. *The Journal of the Acoustical Society of America* **2014**, *136* (1), 156-169.
(63) Shukla, A. A. P., and S. Rohani. Using Ultrasound with an Improved Model Accounting for Low-Angle Scattering. *American Institute of Chemical Engineers (AIChE) Journal* **2010**, *56* (11), 2825-2837.
(64) Povey, M. J. W. *Ultrasonic Techniques for Fluids Characterization*; Academic Press, 1997.

(65) Kytömaa, H. K. Theory of Sound Propogation in Suspensions: A Guide to Particle Size and Concentration Characterization. *Powder Technology* **1995**, *82*, 115-121.
(66) McClements, D. J. Principles of Ultrasonic Droplet Size Determination in Emulsioin. *Langmuir* **1996**, *12*, 3454-3561.
(67) Sinclair, A. N.; Chertov, A. M. Radiation endurance of piezoelectric ultrasonic transducers – A review. *Ultrasonics* **2015**, *57*, 1-10. DOI: https://doi.org/10.1016/j.ultras.2014.10.024.
(68) *Simcenter STAR-CCM+, version 2210* Siemens Product Lifecycle Management Software Inc: USA, 2022. https://thesteveportal.plm.automation.siemens.com/Home (accessed.
(69) Mirtabaie Seyed, M.; Norouzi, M.; Nazari, M.; Kim, M.; Kim Kyung, C. A Numerical Study on the Multiphase Newtonian and Non-Newtonian Displacement in a Porous Micromodel via Water–Surfactant–Polymer Flooding. *Journal of Engineering Mechanics* **2023**, *149* (9), 04023064. DOI: 10.1061/JENMDT.EMENG-7127 (acccessed 2025/03/05).
(70) Rushd, S.; Hafsa, N.; Al-Faiad, M.; Arifuzzaman, M. Modeling the Settling Velocity of a Sphere in Newtonian and Non-Newtonian Fluids with Machine-Learning Algorithms. *Symmetry* **2021**, *13* (1), 71.
(71) Tizakast, Y.; Kaddiri, M.; Lamsaadi, M.; Makayssi, T. Machine Learning based algorithms for modeling natural convection fluid flow and heat and mass transfer in rectangular cavities filled with non-Newtonian fluids. *Engineering Applications of Artificial Intelligence* **2023**, *119*, 105750. DOI: https://doi.org/10.1016/j.engappai.2022.105750.
(72) Mohammad, P.; Malekan, M.; Jalali, A. Data-driven machine learning prediction of flow curve and Newtonian to non-Newtonian flow regime transition in bulk metallic glasses within supercooled liquid region. *J Non-Cryst Solids* **2024**, *627*, 122839. DOI: https://doi.org/10.1016/j.jnoncrysol.2024.122839.
(73) Wang, D.; Thunéll, S.; Lindberg, U.; Jiang, L.; Trygg, J.; Tysklind, M.; Souihi, N. A machine learning framework to improve effluent quality control in wastewater treatment plants. *Science of The Total Environment* **2021**, *784*, 147138. DOI: https://doi.org/10.1016/j.scitotenv.2021.147138.